

Rogue waves and their patterns in the vector nonlinear Schrödinger equation

Guangxiong Zhang¹, Peng Huang¹, Bao-Feng Feng^{*2}, Chengfa Wu^{*1,3}

¹Institute for Advanced Study, Shenzhen University,
Shenzhen 518060, People's Republic of China

²School of Mathematical and Statistical Sciences,
The University of Texas Rio Grande Valley Edinburg,
Edinburg, TX 78541-2999, USA

³College of Mathematics and Statistics, Shenzhen University,
Shenzhen, 518060, People's Republic of China

December 5, 2022

Abstract

In this paper, we study the general rogue wave solutions and their patterns in the vector (or M -component) nonlinear Schrödinger (NLS) equation. By applying the Kadomtsev-Petviashvili hierarchy reduction method, we derived an explicit solution for the rogue wave expressed by τ functions that are determinants of $K \times K$ block matrices ($K = 1, 2, \dots, M$) with an index jump of $M + 1$. Patterns of the rogue waves for $M = 3, 4$ and $K = 1$ are thoroughly investigated. We find that when a specific internal parameter is large enough, the wave patterns are linked to the root structures of generalized Wronskian-Hermite polynomial hierarchy in contrast with rogue wave patterns of the scalar NLS equation, the Manakov system and many others. Moreover, the generalized Wronskian-Hermite polynomial hierarchy includes the Yablonskii-Vorob'ev polynomial hierarchy and Okamoto polynomial hierarchies as special cases, which have been used to describe the rogue wave patterns of the scalar NLS equation and the Manakov system, respectively. As a result, we extend the most recent results by Yang *et al.* for the scalar NLS equation and the Manakov system. It is noted that the case $M = 3$ displays a new feature different from the previous results. The predicted rogue wave patterns are compared with the ones of the true solutions for both cases of $M = 3, 4$. An excellent agreement is achieved.

Keywords: Kadomtsev-Petviashvili hierarchy reduction method, vector nonlinear Schrödinger equation, rogue waves, pattern formation, Wronskian-Hermite polynomials

1 Introduction

Rogue waves have been known in the maritime community as part of folklore for centuries. Notable features of such waves include sudden emergence, abnormally large amplitude, and disappearance without any trace. These characteristics indicate that rogue waves may result in tremendous impacts on their surrounding environment and have been associated with many maritime disasters [24]. Systematic studies on rogue waves started only after the first verified measurement of an extreme water wave on 1995 [31]. Remarkably, research on rogue waves has developed considerably since 2007, following the discovery of rogue waves in optical fibres [51], which has attracted much interest in both optics and hydrodynamics. Since then, there has been an explosion of studies to explore rogue waves extended to other physical systems, such as superfluid helium [29], Bose-Einstein condensates [13], capillary waves [50], and plasmas [4].

In optics and hydrodynamics, the mathematical models governing wave propagation can be derived from Maxwell's equations and the Euler equations, respectively [23]. Under further assumptions, the

*Corresponding authors. Email address: baofeng.feng@utrgv.edu (B. F. Feng), cfwu@szu.edu.cn (C. F. Wu).

nonlinear Schrödinger (NLS) equation, which describes the evolution of slowly varying wave packets in nonlinear wave systems, can be reduced from both of these two models [1]. Owing to its integrability, the NLS equation has been widely studied [8, 25, 37, 47, 54, 64] and shown to admit a number of analytic solutions. In particular, one of its rational solutions, namely the Peregrine soliton [48], is widely regarded as the prototype of rogue waves. In the past two decades, mathematical study on rogue waves has attracted much attention, and various higher-order rogue wave solutions of the NLS equation have been constructed [2, 22, 38, 30, 45]. It is worth noting that these solutions in turn have facilitated the experimental studies of rogue waves. On the other hand, explicit rogue wave solutions have been derived in various integrable equations, such as the derivative NLS equation [57], the Yajima-Oikawa equation [15, 16], the three-wave equation [59], the Manakov system [6, 19], the Sasa-Satsuma equation [27, 55], and many others. Besides, rogue waves of infinite order have been uncovered [10, 12] by making use of the Riemann-Hilbert approach [63], while rogue waves on the periodic background [17, 18, 26] have also been explored. Large-order asymptotics for solitons [9] and [11] rogue waves of the NLS equation were analyzed by using the inverse-scattering transform method.

In addition to their physical significance, rogue waves may exhibit extremely regular and symmetric patterns, which are intriguing and can provide critical information for predicting subsequent rogue waves from previous ones. For instance, circular rogue wave clusters of the NLS equation were reported in [38] by using Darboux transformation and numerical simulations. Soon after this phenomenon was confirmed analytically in [32], a systematic classification of the NLS rogue wave patterns was obtained in [39] according to the order of rogue waves and the parameter shifts involved in the Akhmediev breathers in the rogue-wave limit. Moreover, this study reveals various highly symmetric geometric structures of rogue waves under certain choices of parameters, including triangles, pentagons, heptagons, and nonagons. A even more remarkable observation is that, which was first shown in [60], the distribution of rogue waves for specific choices of parameters looks very similar to another independent object, that is, the root structure of the Yablonskii-Vorob'ev polynomial hierarchy, which is closely related to rational solutions of the Painlevé II hierarchy [21]. When specific internal parameter is large enough, the deep connection between these two objects has been established analytically in [60], which is a remarkable progress in the study of rogue waves. Following this work, it is found that [58] such patterns are universal, as rogue waves of many other integrable equations demonstrate similar patterns, such as the Boussinesq equation and the Manakov system, as long as the Schur polynomials involved in the τ functions have index jumps of two. Beyond that, Yang and Yang [62] very recently discovered that other rogue wave patterns exist when the index jumps are three, and these patterns are characterized by root structures of Okamoto polynomial hierarchies.

Inspired by the works in [60, 58, 62], some natural problems arise.

- Can we construct the rogue wave solution in M -component NLS equation?
- What about the patterns of rogue waves for $M = 3, 4$ or even the general case? Are these patterns related to some orthogonal polynomial hierarchy?

The main objective of this paper is to solve the problems listed above by considering the vector NLS equation

$$iu_{j,t} + u_{j,xx} + \left(\sum_{k=1}^M \sigma_k |u_k|^2 \right) u_j = 0, \quad j = 1, 2, \dots, M, \quad (1)$$

where M is a positive integer and $\sigma_k = \pm 1$. For $M = 2$, it is known as the Manakov system [42], which is a model that governs soliton propagation through optical fiber arrays [3, 35, 36]. Our results consist of two ingredients. First, we will apply the Kadomtsev-Petviashvili hierarchy reduction technique to derive rogue wave solutions of the vector NLS equation whose τ functions are represented by determinants of $K \times K$ block matrices ($K = 1, 2, \dots, M$) with index jumps of $M + 1$. The crucial point of this part is to solve a system of algebraic equations (see Lemma 2.1 and its proof). Then we will study the rogue wave patterns for $M = 3, 4$ and $K = 1$. We find that when a specific internal parameter is large enough, these patterns are connected to the root structure of a new orthogonal polynomial hierarchy, which is called *generalized Wronskian-Hermite polynomials* (see Section 2.2). Moreover, we notice that the Yablonskii-Vorob'ev polynomial hierarchy and Okamoto polynomial hierarchies are special cases of the generalized Wronskian-Hermite polynomials. Accordingly, our results have unified rogue wave patterns of the scalar NLS equation and the vector NLS equation (1) for $M = 2, 3, 4$. In addition, we find that the proof in the inner region for $M = 3$ is different from other cases. In the proofs of the inner region of the scalar NLS equation and the Manakov system, one can perform row and column operations to reduce the τ functions into determinants of block matrices with lower triangular matrices at the (1,1) entry whose elements on

the diagonal are all 1. Then the sizes of the determinants can be decreased; hence these waves can be approximated by possible lower-order rogue waves in the inner region. However, although the waves for $M = 3$ can also be approximated by possible lower-order rogue waves in the inner region, it turns out that in certain cases the sizes of the determinants remain unchanged after row and column operations, as the (1,1) entries of the block matrices are no longer triangular. The predicted rogue wave patterns are compared with actual ones, and excellent agreement is achieved.

The structure of this paper can now be explained. Section 2 presents some preliminary results that will be used in the subsequent discussions. We first provide explicit rogue wave solutions with index jumps of $M + 1$ of the vector NLS equation, and it is shown that these solutions are expressed by $K \times K$ block matrices ($K = 1, 2, \dots, M$). This is followed by an introduction to the generalized Wronskian-Hermite polynomials and the study of their root structures. Then rogue wave patterns for the three- and four-component NLS equations under the condition that specific parameters are large enough are stated in Section 3, which form the main results of this paper. Section 4 is devoted to comparing predicted and actual rogue wave patterns, while the proofs of the main results are provided in Section 5. We summarize the main results of this paper in Section 6. Finally, the proof of Lemma 2.1, which involves the study of multiple roots of some rational function and plays a pivotal role in this paper, and derivations of rogue wave solutions in the vector NLS equation are given in Appendices A and B respectively, while the results on root structures of the generalized Wronskian-Hermite polynomials of jump $k = 4, 5$ are proved in Appendix C.

2 Preliminaries

2.1 Rogue wave solutions of the vector nonlinear Schrödinger equation

This section presents rogue wave solutions of the vector NLS equation (1), which possesses an infinite dimensional algebra of non-commutative symmetries [40]. We note that these solutions have been studied before [7, 19, 41, 43, 49, 65]. In particular, vector Peregrine solitons were found by applying the loop group theory in [65], in which the authors proposed the problem of whether patterns of these rogue waves are related to Yablonskii-Vorob'ev polynomial hierarchy. This problem was later confirmed for the Manakov system [56], which has been taken as an example to show that universal rogue wave patterns associated with the Yablonskii-Vorob'ev polynomial hierarchy exist in integrable systems. Very recently, new patterns of another class of (degenerate) rogue waves of the Manakov system have been obtained by Yang and Yang [62] through establishing the connection between these waves and the Okamoto polynomial hierarchies. A remarkable feature of these new patterns is that, unlike previous patterns, the transformations between the locations of fundamental rogue waves and zeros of the Okamoto polynomial hierarchies are nonlinear, thereby leading to deformations of rogue patterns. Inspired by these studies, we will extend the results in [62] and solve the problem mentioned above in [65] for $M = 3, 4$ by studying patterns of degenerate rogue waves of the vector NLS equation (1). To this end, we introduce some notations and lemma that will be needed.

The Schur polynomials $S_n(\mathbf{x})$ are defined by

$$\sum_{n=0}^{\infty} S_n(\mathbf{x}) \lambda^n = \exp \left(\sum_{k=1}^{\infty} x_k \lambda^k \right),$$

where $\mathbf{x} = (x_1, x_2, \dots)$. To be more specific, we have

$$S_0(\mathbf{x}) = 1, \quad S_1(\mathbf{x}) = x_1, \quad S_2(\mathbf{x}) = \frac{1}{2}x_1^2 + x_2, \dots, \quad S_j(\mathbf{x}) = \sum_{l_1+2l_2+\dots+ml_m=j} \left(\prod_{i=1}^m \frac{x_i^{l_i}}{l_i!} \right). \quad (2)$$

Further, we define $S_j(\mathbf{x}) \equiv 0$ for $j < 0$.

Lemma 2.1. Let M be a positive integer and $\lambda_1 > 0, r_j \neq 0, k_j$ be real constants, $j = 1, 2, \dots, M$, where the k_j 's are distinct. Let $\mathcal{R}_M(z)$ be a rational function defined by

$$\mathcal{R}_M(z) = \sum_{j=1}^M \frac{r_j}{(z + k_j)^2} + 2. \quad (3)$$

Then $\mathcal{R}_M(z) = 0$ has a pair of complex conjugate roots with nonzero imaginary parts of multiplicity M

$$\lambda_1 \cos[\pi/(M+1)] - k_1 \pm i\lambda_1 \sin[\pi/(M+1)], \quad (4)$$

if the parameters $r_j, k_j, j = 2, \dots, M$, satisfy the conditions

$$k_j = k_1 + \lambda_1 (\sin[\pi/(M+1)] \cot[j\pi/(M+1)] - \cos[\pi/(M+1)]),$$

and

$$r_j = 2(-1)^{j+1} \prod_{\substack{i=1 \\ i \neq j}}^M (k_j - k_i)^{-1} \left(\lambda_1 \frac{\sin[\pi/(M+1)]}{\sin[j\pi/(M+1)]} \right)^{M+1}. \quad (5)$$

Remark 1. The equation $\mathcal{R}_M(z) = 0$ may have real roots of multiplicity M as well. For instance, the equation

$$\frac{162}{(z+2)^2} - \frac{256}{(z+3)^2} - \frac{16}{(z+1)^2} + 2 = 0$$

has a real root 1 of multiplicity 3, while the equation

$$-\frac{1024}{(z+2)^2} + \frac{3125}{(z+3)^2} - \frac{2592}{(z+4)^2} + \frac{81}{(z+1)^2} + 2 = 0$$

has a real root 2 of multiplicity 4. Nevertheless, this case will not occur in our subsequent discussions.

We will provide the proof of Lemma 2.1 in Appendix A. Next, we define the functions $\mathcal{G}_M(p)$ and $p(\kappa)$ respectively by

$$\mathcal{G}_M(p) = \sum_{j=1}^M \frac{\sigma_j \rho_j^2}{p - ik_j} + 2p, \quad (6)$$

$$\begin{aligned} \mathcal{G}_M(p(\kappa)) &= \frac{\mathcal{G}_M(p(0))}{M+1} \sum_{n=1}^{M+1} \exp\left(\exp\left(\frac{2n\pi i}{M+1}\right) \kappa\right), \\ &= \frac{\mathcal{G}_M(p(0))}{M+1} \sum_{n=1}^{M+1} \exp\left(\cos\left(\frac{2n\pi}{M+1}\right) \kappa\right) \cos\left(\sin\left(\frac{2n\pi}{M+1}\right) \kappa\right), \end{aligned} \quad (7)$$

where $\rho_j > 0, k_j$ are real constants, $j = 1, 2, \dots, M$. We may deduce from Lemma 2.1 that if σ_j, ρ_j and $k_j, j = 1, 2, \dots, M$, satisfy the constraints

$$\begin{aligned} k_j &= k_1 + \lambda_1 (\sin[\pi/(M+1)] \cot[j\pi/(M+1)] - \cos[\pi/(M+1)]), \\ \sigma_j \rho_j^2 &= 2(-1)^{j+1} \prod_{\substack{i=1 \\ i \neq j}}^M (k_j - k_i)^{-1} \left(\lambda_1 \frac{\sin[\pi/(M+1)]}{\sin[j\pi/(M+1)]} \right)^{M+1}, \end{aligned} \quad (8)$$

then the algebraic equation

$$\mathcal{G}'_M(p) = 0 \quad (9)$$

has a pair of non-imaginary roots of multiplicity M given by

$$\pm \lambda_1 \sin[\pi/(M+1)] - i\lambda_1 \cos[\pi/(M+1)] + ik_1. \quad (10)$$

Theorem 2.2. Let M be a positive integer, $\rho_j > 0, k_j$ be real constants, and $\sigma_j = 1$, where $j = 1, 2, \dots, M$. Assume ρ_j and k_j are given by (8). Let $\mathcal{G}_M(p), p(\kappa)$ be functions defined by (6) and (7)

respectively. Let $\mathbf{x}_I^\pm = (x_{1,I}^\pm, x_{2,I}^\pm, \dots)$, $I = 1, 2, \dots, M$, and $\mathbf{s} = (s_1, s_2, \dots)$ be the vectors defined by

$$x_{i,I}^+ = \alpha_i x + \beta_i i t + \sum_{j=1}^M n_j \theta_{ij} + a_{i,I}, \quad (11)$$

$$x_{i,I}^- = \alpha_i^* x - \beta_i^* i t - \sum_{j=1}^M n_j \theta_{ij}^* + a_{i,I}^*, \quad (12)$$

$$\ln \left[\frac{1}{\kappa} \left(\frac{p_0 + p_0^*}{p_1} \right) \left(\frac{p(\kappa) - p_0}{p(\kappa) + p_0^*} \right) \right] = \sum_{r=1}^{\infty} s_r \kappa^r, \quad (13)$$

where the asterisk ‘*’ represents complex conjugation, $p_0 = p(0)$, $p_1 = p'(0)$, the $a_{i,I}$ ’s are arbitrary constants, and α_i , β_i , θ_{ij} , $j = 1, 2, \dots, M$, are defined by the expansions

$$p(\kappa) - p_0 = \sum_{r=1}^{\infty} \alpha_r \kappa^r, \quad p^2(\kappa) - p_0^2 = \sum_{r=1}^{\infty} \beta_r \kappa^r, \quad \ln \frac{p(\kappa) - i k_j}{p_0 - i k_j} = \sum_{r=1}^{\infty} \theta_{rj} \kappa^r.$$

In this case, the M -component NLS equation (1) admits \mathcal{N} -th order rogue wave solutions

$$u_{j,\mathcal{N}} = \frac{g_{j,\mathcal{N}}}{f_{\mathcal{N}}} e^{i(k_j x + w_j t)}, \quad j = 1, 2, \dots, M, \quad (14)$$

where

$$w_j = \sum_{i=1}^M \sigma_i \rho_i^2 - k_j^2, \quad \mathcal{N} = (N_1, N_2, \dots, N_M), \quad (15)$$

with N_j ($j = 1, 2, \dots, M$) being nonnegative integers, and f and g_j are given by

$$f_{\mathcal{N}} = \tau_{\mathbf{n}_0}, \quad g_{j,\mathcal{N}} = \tau_{\mathbf{n}_j} \quad (16)$$

with

$$\mathbf{n}_0 = (0, 0, \dots, 0) \in \mathbb{R}^M, \quad \mathbf{n}_j = \sum_{l=1}^M \delta_{jl} \mathbf{e}_l,$$

\mathbf{e}_l being the standard unit vector in \mathbb{R}^M and δ_{jl} being the Kronecker delta. Here, $\tau_{\mathbf{n}}$ is given by the following $K \times K$ ($K = 1, 2, \dots, M$) block determinant

$$\tau_{\mathbf{n}} = \det \begin{pmatrix} \tau_{\mathbf{n}}^{[I_1, I_1]} & \tau_{\mathbf{n}}^{[I_1, I_2]} & \dots & \tau_{\mathbf{n}}^{[I_1, I_K]} \\ \tau_{\mathbf{n}}^{[I_2, I_1]} & \tau_{\mathbf{n}}^{[I_2, I_2]} & \dots & \tau_{\mathbf{n}}^{[I_2, I_K]} \\ \vdots & \vdots & \ddots & \vdots \\ \tau_{\mathbf{n}}^{[I_K, I_1]} & \tau_{\mathbf{n}}^{[I_K, I_2]} & \dots & \tau_{\mathbf{n}}^{[I_K, I_K]} \end{pmatrix}_{N \times N}, \quad (17)$$

where

$$\mathbf{n} = (n_1, n_2, \dots, n_M), \quad 1 \leq I_1 < I_2 < \dots < I_K \leq M, \quad (18)$$

$$\tau_{\mathbf{n}}^{[I, J]} = \left(m_{(M+1)i-I, (M+1)j-J}^{(\mathbf{n}, I, J)} \right)_{1 \leq i \leq N_I, 1 \leq j \leq N_J}, \quad 1 \leq I, J \leq M, \quad (19)$$

n_1, n_2, \dots, n_M are integers, I_j, N_{I_j} ($j = 1, 2, \dots, K$) are positive integers with $N_{I_1} + N_{I_2} + \dots + N_{I_K} = N$ and $N_l = 0$ for $l \in \{1, 2, \dots, M\} \setminus \{I_1, I_2, \dots, I_K\}$, and the corresponding matrix elements of (19) are defined by

$$m_{i,j}^{(\mathbf{n}, I, J)} = \sum_{v=0}^{\min(i,j)} \left[\frac{|p_1|^2}{(p_0 + p_0^*)^2} \right]^v S_{i-v}(\mathbf{x}_I^+(\mathbf{n}) + v\mathbf{s}) S_{j-v}(\mathbf{x}_J^-(\mathbf{n}) + v\mathbf{s}^*). \quad (20)$$

We provide the proof of Theorem 2.2 in Appendix B.

Remark 2. The rogue wave solutions to the vector NLS equation (1) in Theorem 2.2 are represented by τ functions which have matrix elements expressed by Schur polynomials with index jumps of $M + 1$.

These rogue waves exist only when $\mathcal{G}'_M(p) = 0$ has non-imaginary roots of order M . This indicates that the scalar NLS equation and the Manakov system have no such kind of rogue waves with index jumps of $\mathcal{J} \geq 4$. In addition, when $\mathcal{G}'_M(p) = 0$ has simple or double roots, the vector NLS equations would possess similar types of rogue waves as the scalar NLS equation or the Manakov system, where the index jumps of the corresponding Schur polynomials are 2 or 3. In such cases, the rogue wave patterns are similar to those of the scalar NLS equation [60] or the Manakov system [62] and hence we will not present these rogue waves.

Remark 3. We restrict the study of rogue wave patterns to the cases of $M = 3, 4$. Then the $p(\kappa)$ introduced in (7) can be expressed by

$$\mathcal{G}_M(p(\kappa)) = \begin{cases} \frac{\mathcal{G}_3(p(0))}{4} (e^\kappa + e^{-\kappa} + 2 \cos \kappa), & M = 3, \\ \frac{\mathcal{G}_4(p(0))}{5} \left(e^\kappa + 2e^{(-\frac{\sqrt{5}}{4} - \frac{1}{4})\kappa} \left(e^{\frac{\sqrt{5}\kappa}{2}} \cos \left(\sqrt{\frac{\sqrt{5}}{8} + \frac{5}{8}\kappa} \right) + \cos \left(\sqrt{\frac{5}{8} - \frac{\sqrt{5}}{8}\kappa} \right) \right) \right), & M = 4. \end{cases} \quad (21)$$

It is also clear that there are other parameter choices for $\mathcal{G}'_M(p) = 0$ ($M = 3, 4$) to have a pair of non-imaginary roots of order M , on account of the symmetry of the vector NLS equation (1). Let (i, j, l) be any permutation of the set $\{1, 2, 3\}$, then the condition (8) can be replaced by

$$\rho_i = \rho_j = \sqrt{2}\rho_l = 2|k_l - k_i| = 2|k_l - k_j| \neq 0, \quad k_i \neq k_j. \quad (22)$$

Similarly, assume (i, j, l, m) is any permutation of the set $\{1, 2, 3, 4\}$, then the condition (8) can be replaced by

$$2\rho_i^2 = (3 - \sqrt{5})\rho_j^2 = (3 - \sqrt{5})\rho_l^2 = 2\rho_m^2 = (6 - 2\sqrt{5})(k_j - k_i)^2 = 4(k_l - k_i)^2 = (6 + 2\sqrt{5})(k_m - k_i)^2 \neq 0. \quad (23)$$

Under these conditions, the roots are

$$p_0 = \begin{cases} \pm \frac{\rho_i}{2} + ik_l, & \text{for } M = 3, \\ \pm \frac{1}{4} \sqrt{5 + \sqrt{5}}\rho_i + i \left(k_i - \frac{1}{4} \sqrt{3 - \sqrt{5}}\rho_i \right), & \text{for } M = 4. \end{cases} \quad (24)$$

Remark 4. When $K = 1$, the τ functions are comprised of determinants of single block matrices, i.e.,

$$\tau_{\mathbf{n}} = \det_{1 \leq i, j \leq N} \left(m_{(M+1)i - I_1, (M+1)j - I_1}^{(\mathbf{n}, I_1, I_1)} \right), \quad 1 \leq I_1 \leq M,$$

where $m_{i,j}^{(\mathbf{n}, I_1, J)}$ is given by (20). In this case, we define the rogue wave solutions in Theorem 2.2 to be the I_1 -th type, $1 \leq I_1 \leq M$, and simply denote \mathbf{x}_I^\pm by \mathbf{x}^\pm by ignoring the dependence on I .

Remark 5. By rewriting $\tau_{\mathbf{n}}$ into a larger determinant similar to [45], we can show that the degrees of the polynomials $\tau_{\mathbf{n}}$ for $M = 3, 4$ with respect to x and t in Theorem 2.2 are

$$\deg(\tau_{\mathbf{n}}) = \begin{cases} 3(N_1^2 + N_2^2 + N_3^2) - 2(N_1N_2 + N_1N_3 + N_2N_3) + (3N_1 + N_2 - N_3), & M = 3, \\ 5(N_1^2 + N_2^2 + N_3^2 + N_4^2) - (N_1 + N_2 + N_3 + N_4)^2 + 4N_1 + 2N_2 - 2N_4, & M = 4, \end{cases} \quad (25)$$

where N_j ($j = 1, 2, \dots, M$) are non-negative integers such that $N_1 + N_2 + \dots + N_M = N$. We note that, when $N_I = 0$, it means that the block matrices $\tau_{\mathbf{n}}^{[I, I]}$ and $\tau_{\mathbf{n}}^{[I, I]}$ ($l = 1, 2, \dots, M$) do not appear in (17).

Remark 6. It can be calculated that

$$s_1 = s_2 = s_3 = s_5 = s_6 = s_7 = s_9 = s_{10} = s_{11} = 0, \quad \text{when } M = 3, \quad (26)$$

and

$$s_1 = s_2 = s_3 = s_4 = s_6 = s_7 = s_8 = s_9 = s_{11} = 0, \quad \text{when } M = 4, \quad (27)$$

in (13), but we do not know whether or not $s_i = 0$ holds for all $i \in \mathbb{N}$ such that $i \not\equiv 0 \pmod{M+1}$ when $M = 3, 4$. We also note that $x_{r, I}^\pm$ can be removed from the solution when $r \equiv 0 \pmod{M+1}$, by using the technique developed in [60].

2.2 Generalized Wronskian-Hermite polynomials

Hermite polynomials are a sequence of classical orthogonal polynomials, and they arise in many areas of mathematics, such as probability, combinatorics, random matrix theory, etc. Like other orthogonal polynomials, Hermite polynomials can be defined from various viewpoints. It is also worth noting that there are two different standardizations in common use. However, it turns out neither of them is convenient for the analysis of wave patterns. Instead, we will introduce a slightly different definition [61]. Let $p_j(z)$ be Schur polynomials defined by

$$\sum_{j=0}^{\infty} p_j(z) \epsilon^j = \exp(z\epsilon + \epsilon^2), \quad (28)$$

with $p_j(z) \equiv 0$ for $j < 0$. Then it can be shown that the polynomials $p_j(z)$ are related to Hermite polynomials via certain rescaling.

Next, we introduce Wronskian-Hermite polynomials, which have appeared in the study of certain monodromy-free Schrödinger operators [44]. Let N be a positive integer and $\Lambda = (n_1, n_2, \dots, n_N)$, where $\{n_i\}$ are distinct positive integers such that $n_1 < n_2 < \dots < n_N$, then the Wronskian-Hermite polynomial $W_\Lambda(z)$ is defined as

$$W_\Lambda(z) = \begin{vmatrix} p_{n_1}(z) & p_{n_1-1}(z) & \cdots & p_{n_1-N+1}(z) \\ p_{n_2}(z) & p_{n_2-1}(z) & \cdots & p_{n_2-N+1}(z) \\ \vdots & \vdots & \ddots & \vdots \\ p_{n_N}(z) & p_{n_N-1}(z) & \cdots & p_{n_N-N+1}(z) \end{vmatrix}. \quad (29)$$

Note from (31) that $p'_{k+1}(z) = p_k(z)$. This implies that the Wronskian-Hermite polynomial $W_\Lambda(z)$ can be rewritten as

$$W_\Lambda(z) = \text{Wronskian}[p_{n_1}(z), p_{n_2}(z), \dots, p_{n_N}(z)]. \quad (30)$$

In particular, when the indices (n_1, n_2, \dots, n_N) are consecutive, these polynomials are called generalized Hermite polynomials, which are closely related to rational solutions of the fourth Painlevé equation [21].

The Yablonskii-Vorob'ev polynomials [56, 53] and Okamoto polynomials [46] are another two important classes of special polynomials, and as shown in [21, 62], they can be generalized to hierarchies that have close connections with rogue wave patterns of certain integrable systems [58, 62]. It turns out that the Wronskian-Hermite polynomials can be generalized in a similar way. Let $p_j^{[m]}(z)$, where $m > 1$ is a positive integer, be Schur polynomials defined by

$$\sum_{j=0}^{\infty} p_j^{[m]}(z) \epsilon^j = \exp(z\epsilon + \epsilon^m), \quad (31)$$

with $p_j^{[m]}(z) \equiv 0$ for $j < 0$. Then the generalized Wronskian-Hermite polynomials are defined by

$$W_\Lambda^{[m]}(z) = \begin{vmatrix} p_{n_1}^{[m]}(z) & p_{n_1-1}^{[m]}(z) & \cdots & p_{n_1-N+1}^{[m]}(z) \\ p_{n_2}^{[m]}(z) & p_{n_2-1}^{[m]}(z) & \cdots & p_{n_2-N+1}^{[m]}(z) \\ \vdots & \vdots & \ddots & \vdots \\ p_{n_N}^{[m]}(z) & p_{n_N-1}^{[m]}(z) & \cdots & p_{n_N-N+1}^{[m]}(z) \end{vmatrix}. \quad (32)$$

In particular, these polynomials are called generalized Wronskian-Hermite polynomials of jump $k > 0$ if $n_{j+1} - n_j = k$, $j = 1, 2, \dots, N-1$. Further, when $n_1 = l$, where $1 \leq l < k$, we denote the generalized Wronskian-Hermite polynomial of jump $k > 0$ by $W_N^{[m,k,l]}(z)$, i.e.,

$$W_N^{[m,k,l]}(z) = c_N^{[m,k,l]} \begin{vmatrix} p_l^{[m]}(z) & p_{l-1}^{[m]}(z) & \cdots & p_{l-N+1}^{[m]}(z) \\ p_{l+k}^{[m]}(z) & p_{l+k-1}^{[m]}(z) & \cdots & p_{l+k-N+1}^{[m]}(z) \\ \vdots & \vdots & \ddots & \vdots \\ p_{l+k(N-1)}^{[m]}(z) & p_{l+k(N-1)-1}^{[m]}(z) & \cdots & p_{l+k(N-1)-N+1}^{[m]}(z) \end{vmatrix}, \quad (33)$$

where

$$c_N^{[m,k,l]} = \left(\prod_{n=1}^N \gamma_n! \right) / \left[\prod_{1 \leq i < j \leq N} (\gamma_j - \gamma_i) \right], \quad (34)$$

$$\gamma_n = l + (n-1)k, \quad 1 \leq n \leq N. \quad (35)$$

For the convenience of later use, we have multiplied a constant $c_N^{[m,k,l]}$ in (33), which makes $W_N^{[m,k,l]}(z)$ a monic polynomial.

Since we can deduce from (31) that $(p_{j+1}^{[m]})'(z) = p_j^{[m]}(z)$, $W_N^{[m,k,l]}(z)$ can be rewritten as

$$W_N^{[m,k,l]}(z) = \text{Wronskian} [p_l(z), p_{l+k}(z), \dots, p_{l+k(N-1)}(z)]. \quad (36)$$

If we take $m = 2, k = 4$, then the first few $W_N^{[2,4,l]}(z)$ ($N, l = 1, 2, 3$) are

$$\begin{aligned} W_1^{[2,4,1]}(z) &= z, \\ W_2^{[2,4,1]}(z) &= z^3 (z^2 + 10), \\ W_3^{[2,4,1]}(z) &= z^6 (z^6 + 42z^4 + 540z^2 + 2520), \\ W_1^{[2,4,2]}(z) &= z^2 + 2, \\ W_2^{[2,4,2]}(z) &= z (z^6 + 18z^4 + 60z^2 + 120), \\ W_3^{[2,4,2]}(z) &= z^3 (z^{12} + 60z^{10} + 1260z^8 + 12000z^6 + 54000z^4 + 181440z^2 + 302400), \\ W_1^{[2,4,3]}(z) &= z(z^2 + 6), \\ W_2^{[2,4,3]}(z) &= z^3 (z^6 + 30z^4 + 252z^2 + 840), \\ W_3^{[2,4,3]}(z) &= z^6 (z^{12} + 84z^{10} + 2700z^8 + 43680z^6 + 388080z^4 + 1995840z^2 + 4656960). \end{aligned}$$

We remark that, when $k = 2$, the generalized Wronskian-Hermite polynomials $W_N^{[2m+1,2,1]}(z)$ are related to the Yablonskii-Vorob'ev polynomials through some rescaling. In addition, $W_N^{[m,3,1]}(z)$ and $W_N^{[m,3,2]}(z)$ are multiples of the Okamoto polynomial hierarchies of $Q_N^{[m]}(z)$ and $R_N^{[m]}(z)$ respectively [62]. In other words, the Yablonskii-Vorob'ev polynomial hierarchy and the Okamoto polynomial hierarchies are special cases of the generalized Wronskian-Hermite polynomials.

As we will see in the subsequent sections, rogue wave patterns of the vector NLS equation (1) are asymptotically determined by the distribution of zeros of the generalized Wronskian-Hermite polynomials. Root structures of certain special cases of the generalized Wronskian-Hermite polynomials have been obtained in previous studies, such as the Yablonskii-Vorob'ev polynomial hierarchy [21, 5, 28, 52, 14] and the Okamoto polynomials hierarchies [20, 34, 28]. For instance, it has been shown that all nonzero roots of the Yablonskii-Vorob'ev polynomials and the Okamoto polynomials $Q_N^{[1]}(z)$ and $R_N^{[1]}(z)$ are simple [28, 34]. Despite that, as far as we know, root structures for higher members of generalized Wronskian-Hermite polynomials have not been studied yet.

Now we discuss root structures of the generalized Wronskian-Hermite polynomials of jump 4 and 5, which will be used in later studies on rogue wave patterns. Let N_0 be the remainder of N divided by m , i.e.,

$$N_0 \equiv N \pmod{m} \quad \text{or} \quad N = km + N_0,$$

where k is a nonnegative integer, and we denote $[a]$ by the largest integer less than or equal to a real number a . Then our results can be summarized as follows.

Theorem 2.3. The generalized Wronskian-Hermite polynomials $W_N^{[m,4,l]}$ of jump 4 are monic with degree $N(3N - 3 + 2l)/2$, and has the form

$$W_N^{[m,4,l]} = z^\Gamma w_N^{[m,4,l]}(\zeta), \quad \zeta = z^m, \quad (37)$$

where $w_N^{[m,4,l]}(\zeta)$ is a monic polynomial with real coefficients, $w_N^{[m,4,l]}(0) \neq 0$, and Γ is the multiplicity of the zero root given by

$$\Gamma = \frac{3}{2} (N_1^2 + N_2^2 + N_3^2) - (N_1 N_2 + N_1 N_3 + N_2 N_3) + \frac{1}{2} (3N_1 + N_2 - N_3) \quad (38)$$

with the values of N_1, N_2 and N_3 characterized as follows.

- When $m \equiv 1 \pmod{4}$, we have

$$\begin{aligned}
l = 3 : (N_1, N_2, N_3) &= \begin{cases} (N_0, 0, 0), & 0 \leq N_0 \leq \lfloor \frac{m}{4} \rfloor \\ (\lfloor \frac{m}{4} \rfloor, N_0 - \lfloor \frac{m}{4} \rfloor, 0), & \lfloor \frac{m}{4} \rfloor + 1 \leq N_0 \leq 2 \lfloor \frac{m}{4} \rfloor \\ (\lfloor \frac{m}{4} \rfloor, \lfloor \frac{m}{4} \rfloor, N_0 - 2 \lfloor \frac{m}{4} \rfloor), & 2 \lfloor \frac{m}{4} \rfloor + 1 \leq N_0 \leq 3 \lfloor \frac{m}{4} \rfloor \\ (m - 1 - N_0, m - 1 - N_0, m - 1 - N_0), & 3 \lfloor \frac{m}{4} \rfloor + 1 \leq N_0 \leq m - 1 \end{cases} \\
l = 2 : (N_1, N_2, N_3) &= \begin{cases} (0, N_0, 0), & 0 \leq N_0 \leq \lfloor \frac{m}{4} \rfloor \\ (0, \lfloor \frac{m}{4} \rfloor, N_0 - \lfloor \frac{m}{4} \rfloor), & \lfloor \frac{m}{4} \rfloor + 1 \leq N_0 \leq 2 \lfloor \frac{m}{4} \rfloor \\ (\lfloor \frac{m}{4} \rfloor - 1, \lfloor \frac{m}{4} \rfloor - 1, N_0 - 2 \lfloor \frac{m}{4} \rfloor - 1), & 2 \lfloor \frac{m}{4} \rfloor + 1 \leq N_0 \leq 3 \lfloor \frac{m}{4} \rfloor \\ (m - 1 - N_0, m - 1 - N_0, m - 1 - N_0), & 3 \lfloor \frac{m}{4} \rfloor + 1 \leq N_0 \leq m - 1 \end{cases} \\
l = 1 : (N_1, N_2, N_3) &= \begin{cases} (0, 0, N_0), & 0 \leq N_0 \leq \lfloor \frac{m}{4} \rfloor \\ (\lfloor \frac{m}{4} \rfloor - 1, N_0 - \lfloor \frac{m}{4} \rfloor - 1, 0), & \lfloor \frac{m}{4} \rfloor + 1 \leq N_0 \leq 2 \lfloor \frac{m}{4} \rfloor + 1 \\ (\lfloor \frac{m}{4} \rfloor - 1, \lfloor \frac{m}{4} \rfloor, N_0 - 2 \lfloor \frac{m}{4} \rfloor - 1), & 2 \lfloor \frac{m}{4} \rfloor + 2 \leq N_0 \leq 3 \lfloor \frac{m}{4} \rfloor + 1 \\ (m - 1 - N_0, m - N_0, m - N_0), & 3 \lfloor \frac{m}{4} \rfloor + 2 \leq N_0 \leq m - 1. \end{cases}
\end{aligned}$$

- When $m \equiv 2 \pmod{4}$, we have

$$\begin{aligned}
l = 3 : (N_1, N_2, N_3) &= \begin{cases} (\frac{km}{2} + N_0, 0, \frac{km}{2}), & 0 \leq N_0 \leq \lfloor \frac{m}{4} \rfloor \\ (\frac{km}{2} + \lfloor \frac{m}{4} \rfloor, 0, \frac{km}{2} + N_0 - \lfloor \frac{m}{4} \rfloor), & \lfloor \frac{m}{4} \rfloor + 1 \leq N_0 \leq 3 \lfloor \frac{m}{4} \rfloor + 1 \\ (\frac{km}{2} + N_0 - 2 \lfloor \frac{m}{4} \rfloor - 1, 0, \frac{km}{2} + 2 \lfloor \frac{m}{4} \rfloor + 1), & 3 \lfloor \frac{m}{4} \rfloor + 2 \leq N_0 \leq m - 1 \end{cases} \\
l = 2 : (N_1, N_2, N_3) &= \begin{cases} (\frac{km}{2} - 1, 0, \frac{km}{2} + N_0), & 0 \leq N_0 \leq \lfloor \frac{m}{4} \rfloor \\ (\frac{km}{2} + N_0 - 1 - \lfloor \frac{m}{4} \rfloor, 0, \frac{km}{2} + \lfloor \frac{m}{4} \rfloor), & \lfloor \frac{m}{4} \rfloor + 1 \leq N_0 \leq 3 \lfloor \frac{m}{4} \rfloor + 1 \\ (\frac{km}{2} + 2 \lfloor \frac{m}{4} \rfloor, 0, \frac{km}{2} + N_0 - 2 \lfloor \frac{m}{4} \rfloor - 1), & 3 \lfloor \frac{m}{4} \rfloor + 2 \leq N_0 \leq m - 1 \end{cases} \\
l = 1 : (N_1, N_2, N_3) &= \begin{cases} (\frac{km}{2}, 0, \frac{km}{2} + N_0), & 0 \leq N_0 \leq \lfloor \frac{m}{4} \rfloor + 1 \\ (\frac{km}{2} + N_0 - \lfloor \frac{m}{4} \rfloor - 1, 0, \frac{km}{2} + \lfloor \frac{m}{4} \rfloor + 1), & \lfloor \frac{m}{4} \rfloor + 2 \leq N_0 \leq 3 \lfloor \frac{m}{4} \rfloor + 2 \\ (\frac{km}{2} + 2 \lfloor \frac{m}{4} \rfloor + 1, 0, \frac{km}{2} + N_0 - 2 \lfloor \frac{m}{4} \rfloor - 1), & 3 \lfloor \frac{m}{4} \rfloor + 3 \leq N_0 \leq m - 1. \end{cases}
\end{aligned}$$

- When $m \equiv 3 \pmod{4}$, we have

$$\begin{aligned}
l = 3 : (N_1, N_2, N_3) &= \begin{cases} (N_0, 0, 0), & 0 \leq N_0 \leq \lfloor \frac{m}{4} \rfloor \\ (N_0 - 1 - \lfloor \frac{m}{4} \rfloor, \lfloor \frac{m}{4} \rfloor, 0), & \lfloor \frac{m}{4} \rfloor + 1 \leq N_0 \leq 2 \lfloor \frac{m}{4} \rfloor + 1 \\ (N_0 - 2 \lfloor \frac{m}{4} \rfloor - 2, \lfloor \frac{m}{4} \rfloor, \lfloor \frac{m}{4} \rfloor), & 2 \lfloor \frac{m}{4} \rfloor + 2 \leq N_0 \leq 3 \lfloor \frac{m}{4} \rfloor + 2 \\ (m - 1 - N_0, m - 1 - N_0, m - 1 - N_0), & 3 \lfloor \frac{m}{4} \rfloor + 3 \leq N_0 \leq m - 1 \end{cases} \\
l = 2 : (N_1, N_2, N_3) &= \begin{cases} (0, N_0, 0), & 0 \leq N_0 \leq \lfloor \frac{m}{4} \rfloor + 1 \\ (N_0 - \lfloor \frac{m}{4} \rfloor - 1, \lfloor \frac{m}{4} \rfloor + 1, 0), & \lfloor \frac{m}{4} \rfloor + 2 \leq N_0 \leq 2 \lfloor \frac{m}{4} \rfloor + 1 \\ (N_0 - 2 \lfloor \frac{m}{4} \rfloor - 2, \lfloor \frac{m}{4} \rfloor, \lfloor \frac{m}{4} \rfloor + 1), & 2 \lfloor \frac{m}{4} \rfloor + 2 \leq N_0 \leq 3 \lfloor \frac{m}{4} \rfloor + 2 \\ (m - 1 - N_0, m - 1 - N_0, m - N_0), & 3 \lfloor \frac{m}{4} \rfloor + 3 \leq N_0 \leq m - 1 \end{cases} \\
l = 1 : (N_1, N_2, N_3) &= \begin{cases} (0, 0, N_0), & 0 \leq N_0 \leq \lfloor \frac{m}{4} \rfloor + 1 \\ (0, N_0 - \lfloor \frac{m}{4} \rfloor - 1, \lfloor \frac{m}{4} \rfloor + 1), & \lfloor \frac{m}{4} \rfloor + 2 \leq N_0 \leq 2 \lfloor \frac{m}{4} \rfloor + 2 \\ (N_0 - 2 \lfloor \frac{m}{4} \rfloor - 2, \lfloor \frac{m}{4} \rfloor + 1, \lfloor \frac{m}{4} \rfloor + 1), & 2 \lfloor \frac{m}{4} \rfloor + 3 \leq N_0 \leq 3 \lfloor \frac{m}{4} \rfloor + 2 \\ (m - 1 - N_0, m - 1 - N_0, m - N_0), & 3 \lfloor \frac{m}{4} \rfloor + 3 \leq N_0 \leq m - 1. \end{cases}
\end{aligned}$$

Theorem 2.4. The generalized Wronskian-Hermite polynomials $W_N^{[m,5,l]}$ of jump 5 are monic with degree $N(2N - 2 + l)$, and has the form

$$W_N^{[m,5,l]} = z^\Gamma w_N^{[m,5,l]}(\zeta), \quad \zeta = z^m, \quad (39)$$

where $w_N^{[m,5,l]}(\zeta)$ is a monic polynomial with real coefficients, $w_N^{[m,5,l]}(0) \neq 0$, and Γ is the multiplicity of the zero root given by

$$\Gamma = \frac{5}{2} (N_1^2 + N_2^2 + N_3^2 + N_4^2) - \frac{1}{2} (N_1 + N_2 + N_3 + N_4)^2 + 2N_1 + N_2 - N_4. \quad (40)$$

The values of N_1, N_2, N_3, N_4 can be characterized in a similar way as Theorem 2.3 (the details are provided in Lemma 6.1 of Appendix C).

We provide the proofs of Theorems 2.3 and 2.4 in Appendix C.

Remark 7. We note that Theorems 2.3 and 2.4 provide the multiplicities of the zero root of the generalized Wronskian-Hermite polynomials $W_N^{[m,4,l]}$ and $W_N^{[m,5,l]}$ respectively, and as we will see subsequently, these multiplicities are essential in the analysis of rogue wave patterns in the inner region when specific parameters are very large (see Theorems 3.1 and 3.2). It is also clear that the roots of $W_N^{[m,4,l]}$ are distributed symmetrically on some circles in the sense that if z_0 is a root of $W_N^{[m,4,l]}$, then so is $z_0 \exp(2k\pi i/m)$, where $k = 0, 1, \dots, m-1$.

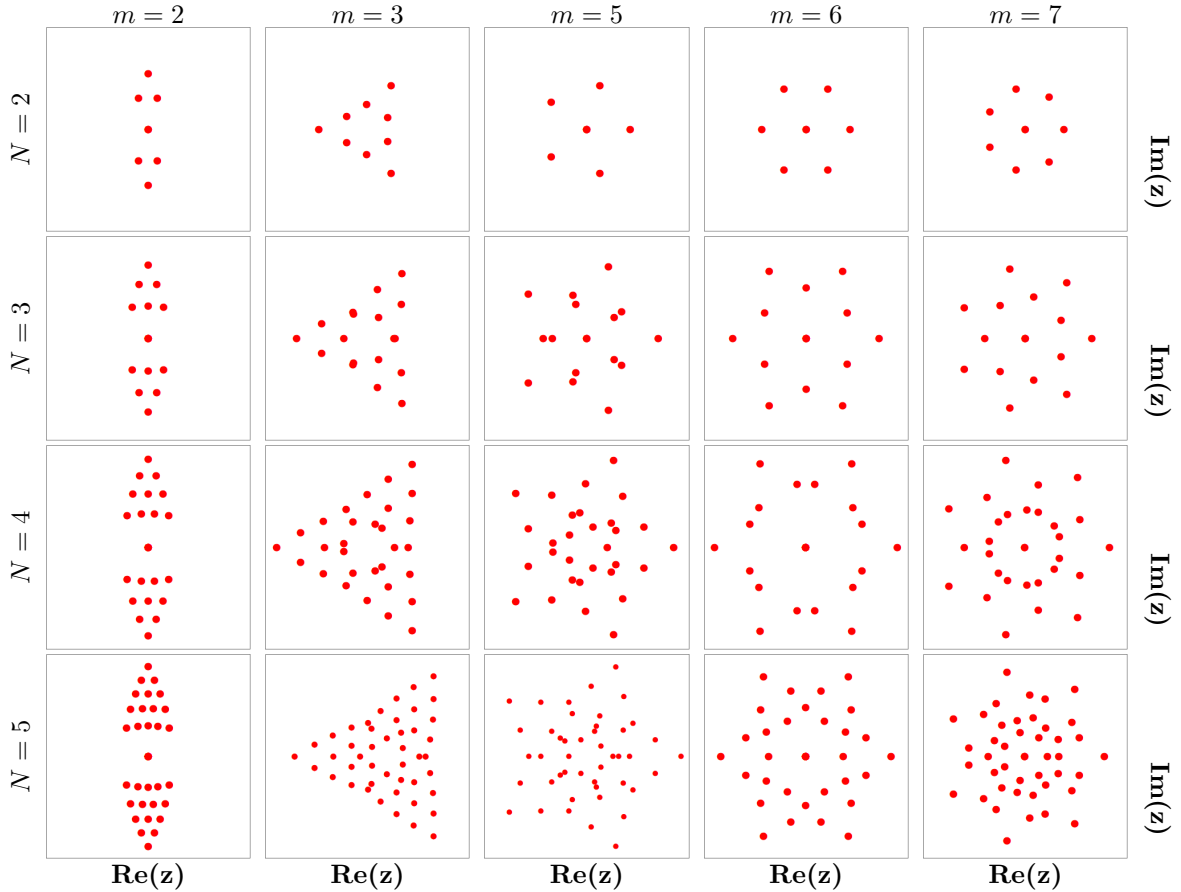


Figure 1: Plots of the roots of the polynomials $W_N^{[m,4,3]}(z)$ for $2 \leq N \leq 5$ and $m = 2, 3, 5, 6, 7$.

In the analytical study of rogue wave patterns, a crucial assumption is that all the nonzero roots of the corresponding generalized Wronskian-Hermite polynomials $W_N^{[m,k,l]}$ are simple [60, 58, 62]. This assumption has been proved for Yablonskii-Vorob'ev polynomials $W_N^{[3,2,1]}(z)$ and Okamoto polynomials $W_N^{[2,3,1]}(z)$ [28] and $W_N^{[2,3,2]}(z)$ [28, 34]. Nevertheless, this assumption has not been verified for the general case. Since our results will also rely on this assumption, we propose a conjecture similar to those in [60, 58, 62].

Conjecture. All nonzero roots of the generalized Wronskian-Hermite polynomials $W_N^{[m,k,l]}$ are simple for any integers $N \geq 1, m \geq 1, k \geq 2, 1 \leq l \leq k-1$.

Although we are not able to prove this conjecture, we have verified it numerically for a variety of special cases which include all the particular generalized Wronskian-Hermite polynomials $W_N^{[m,k,l]}$ that will be involved in this paper.

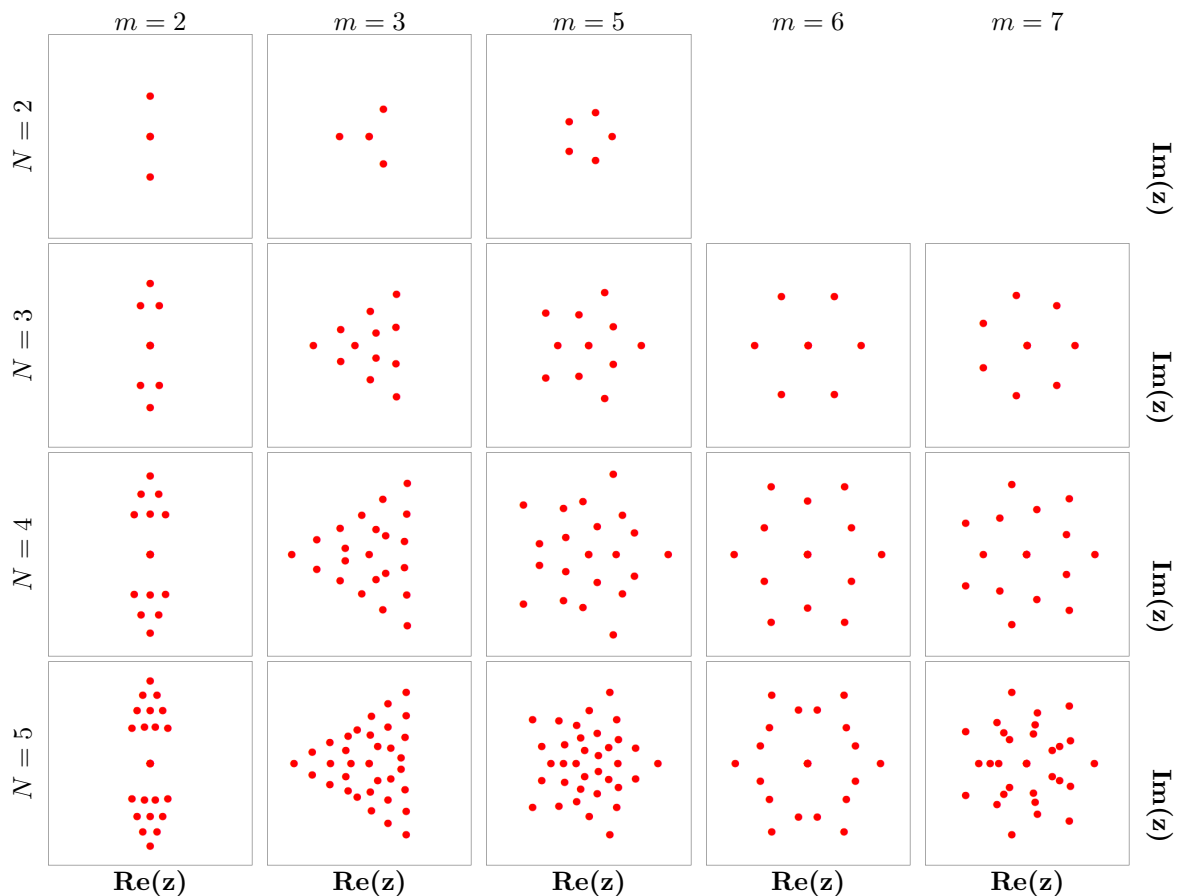


Figure 2: Plots of the roots of the polynomials $W_N^{[m,4,1]}(z)$ for $2 \leq N \leq 5$ and $m = 2, 3, 5, 6, 7$.

The distribution of roots of the Yablonskii-Vorob'ev polynomial hierarchies and Okamoto polynomial hierarchies demonstrates highly regular and symmetric structures [21, 20]. The original Yablonskii-Vorob'ev polynomials form approximately equilateral triangles, while the higher members of the Yablonskii-Vorob'ev polynomial hierarchy form various shapes, such as pentagons, septagons, nonagons and undecagons, etc., depending on the values of m [62]. The roots of Okamoto polynomials exhibit completely different structures compared with Yablonskii-Vorob'ev polynomials. Both of the $W_N^{[2,3,1]}(z)$ and $W_N^{[2,3,2]}(z)$ have similar root structures as these roots are located on two “triangles” except that $W_N^{[2,3,1]}(z)$ has an extra row of roots on a straight line between these two triangles. Here, we use “triangles” because the edges of these triangles are curved rather than straight lines. A natural question is what characteristics the root structures of the generalized Wronskian-Hermite polynomials would exhibit. To this end, we plot the roots of $W_N^{[m,4,l]}(z)$ and $W_N^{[m,5,l]}(z)$ in Figs. 1-2 and 3, respectively.

3 Rogue wave patterns of the three- and four-component nonlinear Schrödinger equation

Theorem 3.1. Let $p_0, p_1, \theta_{1n}, \rho_n, k_n, w_n$ ($n = 1, 2, 3$) be the same as in Theorem 2.2. Assume that $|a_m| \gg 1$ and all other parameters are $O(1)$ in the i -th type \mathcal{N}_i -th order rogue waves ($i = 1, 2, 3$)

$$u_{1,\mathcal{N}_i}(x, t), \quad u_{2,\mathcal{N}_i}(x, t), \quad u_{3,\mathcal{N}_i}(x, t), \quad (41)$$

of the three-component nonlinear Schrödinger equation, where

$$\mathcal{N}_i = N \sum_{j=1}^3 \delta_{ij} e_j,$$

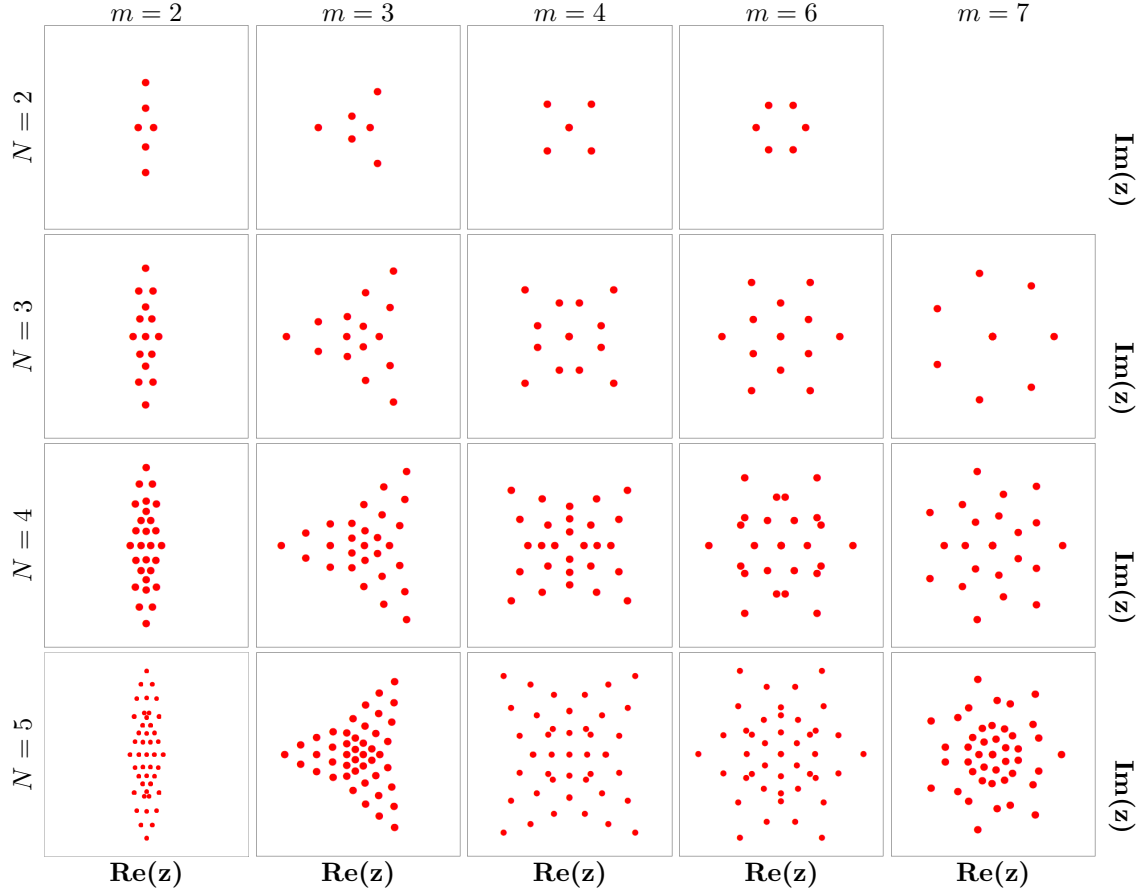


Figure 3: Plots of the roots of the polynomials $W_N^{[m,5,1]}(z)$ for $2 \leq N \leq 5$ and $m = 2, 3, 5, 6, 7$.

N is a positive integer, e_j is the standard unit vector in \mathbb{R}^3 and δ_{ij} is the Kronecker delta. We also assume that all non-zero roots of the generalized Wronskian-Hermite polynomials $W_N^{[m,4,4-i]}$ of jump 4 are simple. Then, we have the following results concerning the asymptotics of the rogue waves (41).

- (1) In the outer region on the (x, t) plane, when $\sqrt{x^2 + t^2} = O(|a_m|^{1/m})$, the \mathcal{N}_i -th order rogue waves separate into $N(3N + 5 - 2i)/2 - \Gamma$ fundamental rogue waves, where Γ is given in (37). These fundamental rogue waves are

$$\hat{u}_1(x, t) = \rho_1 e^{i(k_1 x + \omega_1 t)} \frac{[p_1 x + 2p_0 p_1(it) + \theta_{11}] [p_1^* x - 2p_0^* p_1^*(it) - \theta_{11}^*] + |h_0|^2}{|p_1 x + 2p_0 p_1(it)|^2 + |h_0|^2}, \quad (42)$$

$$\hat{u}_2(x, t) = \rho_2 e^{i(k_2 x + \omega_2 t)} \frac{[p_1 x + 2p_0 p_1(it) + \theta_{12}] [p_1^* x - 2p_0^* p_1^*(it) - \theta_{12}^*] + |h_0|^2}{|p_1 x + 2p_0 p_1(it)|^2 + |h_0|^2}, \quad (43)$$

$$\hat{u}_3(x, t) = \rho_3 e^{i(k_3 x + \omega_3 t)} \frac{[p_1 x + 2p_0 p_1(it) + \theta_{13}] [p_1^* x - 2p_0^* p_1^*(it) - \theta_{13}^*] + |h_0|^2}{|p_1 x + 2p_0 p_1(it)|^2 + |h_0|^2}, \quad (44)$$

where $|h_0|^2 = |p_1|^2 / (p_0 + p_0^*)^2$, and their positions (\hat{x}_0, \hat{t}_0) are given by

$$\hat{x}_0 = \frac{1}{\Re(p_0)} \Re \left[\frac{p_0^*}{p_1} \left(z_0 a_m^{1/m} - \Delta_i \right) \right], \quad \hat{t}_0 = \frac{1}{2\Re(p_0)} \Im \left[\frac{1}{p_1} \left(z_0 a_m^{1/m} - \Delta_i \right) \right], \quad (45)$$

where z_0 is any one of the non-zero simple roots of $W_N^{[m,4,4-i]}(z)$, Δ_i is a z_0 -dependent $O(1)$ quantity, and (\Re, \Im) refer to the real and imaginary parts of a complex number, respectively. The approximation error here is $O(|a_m|^{-1/m})$. In other words, when $|a_m| \gg 1$ and $(x - \hat{x}_0)^2 + (t - \hat{t}_0)^2 = O(1)$, we have the following asymptotics

$$u_{n, \mathcal{N}_i}(x, t) = \hat{u}_n(x - \hat{x}_0, t - \hat{t}_0) + O(|a_m|^{-1/m}), \quad n = 1, 2, 3. \quad (46)$$

- (2) In the inner region, where $x^2 + t^2 = O(1)$, if zero is a root of the generalized Wronskian-Hermite polynomials $W_N^{[m,4,4-i]}(z)$, then $[u_{1,\mathcal{N}_i}(x,t), u_{2,\mathcal{N}_i}(x,t), u_{3,\mathcal{N}_i}(x,t)]$ is approximately a lower $\widehat{\mathcal{N}}_i$ -th order rogue wave

$$u_{1,\widehat{\mathcal{N}}_i}(x,t), \quad u_{2,\widehat{\mathcal{N}}_i}(x,t), \quad u_{3,\widehat{\mathcal{N}}_i}(x,t)$$

where $\widehat{\mathcal{N}}_i = \sum_{j=1}^3 N_{j,4-i} \mathbf{e}_j$ and $N_{j,l}$ refers to the value of N_j against $l \in \{1, 2, 3\}$ given in Theorem

2.3. Moreover, the internal parameters

$$(\hat{a}_{1,n}, \hat{a}_{2,n}, \hat{a}_{3,n}, \hat{a}_{5,n}, \hat{a}_{6,n} \dots, \hat{a}_{4N_{n,4-i}-n,n}), \quad n = 1, 2, 3,$$

in this lower-order rogue waves are related to those in the original rogue wave as follows.

– For $m \equiv 1$ or $3 \pmod{4}$, we have

$$\hat{a}_{j,1} = \hat{a}_{j,2} = \hat{a}_{j,3} = a_j + \left(N - \sum_{n=1}^3 N_{n,4-i} \right) s_j, \quad j = 1, 2, 3, 5, 6, 7 \dots$$

– For $m \equiv 2 \pmod{4}$, we have

$$\hat{a}_{j,1} = \hat{a}_{j,3} = \begin{cases} a_j + \left(N - \sum_{n=1}^3 N_{n,4-i} \right) s_j, & \text{if } j = 1, 2, 3, 5, \dots, m-1, m+1, \dots, \\ \left(N - \sum_{n=1}^3 N_{n,4-i} \right) s_j, & \text{if } j = m. \end{cases}$$

Here, s_j is defined in Theorem 2.2. The approximation error of this lower-order rogue wave is $O(|a_m|^{-1})$. In other words, when $|a_m| \gg 1$ and $x^2 + t^2 = O(1)$, we have

$$\begin{aligned} & u_{n,\mathcal{N}_i}(x,t; a_2, a_3, a_5, a_6, \dots) \\ &= u_{n,\widehat{\mathcal{N}}_i}(x,t; \hat{a}_{j,1}, \hat{a}_{j,2}, \hat{a}_{j,3}, j = 1, 2, 3, 5, 6 \dots) + O(|a_m|^{-1}), \quad n = 1, 2, 3. \end{aligned}$$

If zero is not a root of $W_N^{[m,4,4-i]}(z)$, the solution

$$[u_{1,\mathcal{N}_i}(x,t), \quad u_{2,\mathcal{N}_i}(x,t), \quad u_{3,\mathcal{N}_i}(x,t)]$$

is approximately the constant background

$$\left[\rho_1 e^{i(k_1 x + \omega_1 t)}, \quad \rho_2 e^{i(k_3 x + \omega_2 t)}, \quad \rho_3 e^{i(k_3 x + \omega_3 t)} \right].$$

Theorem 3.2. Let $p_0, p_1, \theta_{1n}, \rho_n, k_n, w_n$ ($n = 1, 2, 3, 4$) be the same as in Theorem 2.2. Assume that $|a_m| \gg 1$ and all other parameters are $O(1)$ in the i -th type \mathcal{N}_i -th order rogue waves ($i = 1, 2, 3, 4$)

$$u_{1,\mathcal{N}_i}(x,t), \quad u_{2,\mathcal{N}_i}(x,t), \quad u_{3,\mathcal{N}_i}(x,t), \quad u_{4,\mathcal{N}_i}(x,t) \quad (47)$$

of the four-component nonlinear Schrödinger equation, where

$$\mathcal{N}_i = N \sum_{j=1}^4 \delta_{ij} \mathbf{e}_j,$$

N is a positive integer, \mathbf{e}_j is the standard unit vector in \mathbb{R}^4 and δ_{ij} is the Kronecker delta. We also assume that all non-zero roots of the generalized Wronskian-Hermite polynomials $W_N^{[m,5,5-i]}$ of jump 5 are simple. Then, we have the following results concerning the asymptotics of the rogue waves (47).

- (1) In the outer region on the (x,t) plane, when $\sqrt{x^2 + t^2} = O(|a_m|^{1/m})$, the N -th order rogue waves separate into $N(2N + 3 - i) - \Gamma$ fundamental rogue waves, where Γ is given in (39). These

fundamental rogue waves are

$$\bar{u}_1(x, t) = \rho_1 e^{i(k_1 x + \omega_1 t)} \frac{[p_1 x + 2p_0 p_1(it) + \theta_{11}] [p_1^* x - 2p_0^* p_1^*(it) - \theta_{11}^*] + |h_0|^2}{|p_1 x + 2p_0 p_1(it)|^2 + |h_0|^2}, \quad (48)$$

$$\bar{u}_2(x, t) = \rho_2 e^{i(k_2 x + \omega_2 t)} \frac{[p_1 x + 2p_0 p_1(it) + \theta_{12}] [p_1^* x - 2p_0^* p_1^*(it) - \theta_{12}^*] + |h_0|^2}{|p_1 x + 2p_0 p_1(it)|^2 + |h_0|^2}, \quad (49)$$

$$\bar{u}_3(x, t) = \rho_3 e^{i(k_3 x + \omega_3 t)} \frac{[p_1 x + 2p_0 p_1(it) + \theta_{13}] [p_1^* x - 2p_0^* p_1^*(it) - \theta_{13}^*] + |h_0|^2}{|p_1 x + 2p_0 p_1(it)|^2 + |h_0|^2}, \quad (50)$$

$$\bar{u}_4(x, t) = \rho_4 e^{i(k_4 x + \omega_4 t)} \frac{[p_1 x + 2p_0 p_1(it) + \theta_{14}] [p_1^* x - 2p_0^* p_1^*(it) - \theta_{14}^*] + |h_0|^2}{|p_1 x + 2p_0 p_1(it)|^2 + |h_0|^2}, \quad (51)$$

where $|h_0|^2 = |p_1|^2 / (p_0 + p_0^*)^2$, and their positions (\bar{x}_0, \bar{t}_0) are given by

$$\bar{x}_0 = \frac{1}{\Re(p_0)} \Re \left[\frac{p_0^*}{p_1} \left(z_0 a_m^{1/m} - \bar{\Delta}_i \right) \right], \quad \bar{t}_0 = \frac{1}{2\Re(p_0)} \Im \left[\frac{1}{p_1} \left(z_0 a_m^{1/m} - \bar{\Delta}_i \right) \right], \quad (52)$$

where z_0 is any one of the non-zero simple roots of $W_N^{[m, 5, 5-i]}(z)$, $\bar{\Delta}_i$ is a z_0 -dependent $O(1)$ quantity. The approximation error here is $O(|a_m|^{-1/m})$. In other words, when $|a_m| \gg 1$ and $(x - \bar{x}_0)^2 + (t - \bar{t}_0)^2 = O(1)$, we have the following asymptotics

$$u_{n, \mathcal{N}_i}(x, t) = \bar{u}_n(x - \bar{x}_0, t - \bar{t}_0) + O(|a_m|^{-1/m}), \quad n = 1, 2, 3, 4. \quad (53)$$

- (2) In the inner region, where $x^2 + t^2 = O(1)$, if zero is a root of the generalized Wronskian-Hermite polynomials $W_N^{[m, 5, 5-i]}(z)$, then $[u_{1, \mathcal{N}_i}(x, t), u_{2, \mathcal{N}_i}(x, t), u_{3, \mathcal{N}_i}(x, t), u_{4, \mathcal{N}_i}(x, t)]$ is approximately a lower $\bar{\mathcal{N}}_i$ -th order rogue wave

$$u_{1, \bar{\mathcal{N}}_i}(x, t), u_{2, \bar{\mathcal{N}}_i}(x, t), u_{3, \bar{\mathcal{N}}_i}(x, t), u_{4, \bar{\mathcal{N}}_i}(x, t)$$

where $\bar{\mathcal{N}}_i = \sum_{j=1}^4 N_{j, 5-i} e_j$ and $N_{j, l}$ refers to the value of N_j against $l \in \{1, 2, 3, 4\}$ are given in Theorem 2.4. Moreover, the internal parameters

$$(\bar{a}_{1, n}, \bar{a}_{2, n}, \bar{a}_{3, n}, \bar{a}_{4, n}, \bar{a}_{6, n} \dots, \bar{a}_{5N_{n, 5-i-n}, n}), \quad n = 1, 2, 3, 4,$$

in this lower-order rogue waves are related to those in the original rogue wave by

$$\bar{a}_{j, 1} = \bar{a}_{j, 2} = \bar{a}_{j, 3} = \bar{a}_{j, 4} = a_j + \left(N - \sum_{n=1}^4 N_{n, 5-i} \right) s_j, \quad j = 1, 2, 3, 4, 6, 7 \dots,$$

where s_j is defined in Theorem 2.2. The approximation error of this lower-order rogue wave is $O(|a_m|^{-1})$. In other words, when $|a_m| \gg 1$ and $x^2 + t^2 = O(1)$, we have

$$\begin{aligned} & u_{n, \mathcal{N}_i}(x, t; a_2, a_3, a_4, a_6, \dots) \\ &= u_{n, \bar{\mathcal{N}}_i}(x, t; \bar{a}_{j, 1}, \bar{a}_{j, 2}, \bar{a}_{j, 3}, \bar{a}_{j, 4}, j = 1, 2, 3, 4, 6, 7 \dots) + O(|a_m|^{-1}), \quad n = 1, 2, 3, 4. \end{aligned}$$

If zero is not a root of $W_N^{[m, 5, 5-i]}(z)$, the solution

$$[u_{1, \mathcal{N}_i}(x, t), u_{2, \mathcal{N}_i}(x, t), u_{3, \mathcal{N}_i}(x, t), u_{4, \mathcal{N}_i}(x, t)]$$

is approximately the constant background

$$\left[\rho_1 e^{i(k_1 x + \omega_1 t)}, \quad \rho_2 e^{i(k_2 x + \omega_2 t)}, \quad \rho_3 e^{i(k_3 x + \omega_3 t)}, \quad \rho_4 e^{i(k_4 x + \omega_4 t)} \right].$$

4 Comparison between predicted and true rogue wave patterns

4.1 Comparison in the three-component NLS equation

In this subsection, we compare our predictions of rogue wave patterns in Theorem 3.1 with true rogue waves of the three-component NLS equation. It is noted that the predicted i -th type $|u_{n,\mathcal{N}_i}(x,t)|$, $n = 1, 2, 3$, from Theorem 3.1 can be divided into a simple form

$$|u_{n,\mathcal{N}_i}(x,t)| = |u_{n,\widehat{\mathcal{N}}_i}(x,t)| + \sum_{j=1}^{N_p} \left(|\hat{u}_n(x - \hat{x}_0^{(j)}, t - \hat{t}_0^{(j)})| - \rho_n \right), \quad n = 1, 2, 3, \quad (54)$$

where $u_{n,\widehat{\mathcal{N}}_i}(x,t)$ is a lower-order rogue wave of the three-component NLS equation with all its internal parameters set to 0, $\widehat{\mathcal{N}}_i = (N_1, N_2, N_3)$ is given by Theorems 3.1 and 2.3, $\hat{u}_n(x,t)$, $n = 1, 2, 3$, is the fundamental rogue wave of the three-component NLS equation, whose predicted location $(\hat{x}_0^{(j)}, \hat{t}_0^{(j)})$ can be obtained from (45), and N_p is the number of fundamental rogue waves given in Theorem 3.1. To analyze the triple root case, we choose the background wavenumbers $k_2 = -k_1 = 1$ and $k_3 = 0$, which gives $\rho_1 = \rho_2 = \rho_3^2 = 2$ by (22). Further, we select $p_0 = 1$, $p_1 = -1/\sqrt[4]{3}$ and $p_2 = 1/\sqrt{3}$ for the subsequent analysis.

4.1.1 First-type rogue waves of the three-component NLS equation

We start with $(2, 0, 0)$ -th order rogue wave solutions. Moreover, we let one of the internal parameters $(a_2, a_3, a_5, a_6, a_7)$ be large and set others to 0. We note that a_1 can be set to 0 by normalization, and a_4 is a parameter that can be removed. Then, the very large parameter is one of

$$a_2 = 30, \quad a_3 = 100, \quad a_5 = 1200, \quad a_6 = 3000, \quad a_7 = 7000. \quad (55)$$

According to Theorem 3.1, the position (\hat{x}_0, \hat{t}_0) of each fundamental rogue wave corresponding to

$$u_{1,\mathcal{N}_1}(x,t), \quad u_{2,\mathcal{N}_1}(x,t), \quad u_{3,\mathcal{N}_1}(x,t)$$

can be predicted by equation (45). The lower (N_1, N_2, N_3) -th order rogue wave would appear in the inner region, and the value of (N_1, N_2, N_3) can be obtained from Theorems 3.1 and 2.3. In our prediction, the (N_1, N_2, N_3) values for these five rogue solutions are

$$(N_1, N_2, N_3) = (1, 0, 1), \quad (0, 0, 0), \quad (1, 1, 0), \quad (1, 0, 1), \quad (0, 1, 0),$$

respectively. Note that $(0, 0, 0)$ means no lower-order rogue wave exists in the inner region. Because of our choice of parameters a_m and the value of s_j shown in Remark 6, the internal parameters in these predicted lower (N_1, N_2, N_3) -th order rogue waves of the inner region are all zero.

For $[u_{1,\mathcal{N}_1}(x,t), u_{2,\mathcal{N}_1}(x,t), u_{3,\mathcal{N}_1}(x,t)]$, their corresponding predicted rogue wave patterns are illustrated in the last three rows of Fig. 4, with the first row being the locations of predicted rogue waves. These predicted rogue waves are generated in the following way. We first replace each non-center dot, which is the non-zero root, in the first row of Fig. 4 by a fundamental rogue wave according to (42)-(44). Then the center dot is replaced by a lower (N_1, N_2, N_3) -th order rogue wave with all internal parameters set to zero.

It can be seen from Fig. 4 that the large- a_2 solution displays a skewed double-triangle, corresponding to the double-triangle root structure of $W_2^{[2,4,3]}(z)$. The large- a_3 solution exhibits a skewed triple-triangle, corresponding to the triple-triangle root structure of $W_2^{[3,4,3]}(z)$. The large- a_5 solution displays a deformed pentagon, corresponding to the pentagon-shaped root structure of $W_2^{[5,4,3]}(z)$. The large- a_6 solution exhibits a deformed hexagon, corresponding to the hexagon-shaped root structure of $W_2^{[6,4,3]}(z)$. The large- a_7 solution displays a deformed heptagon, corresponding to the heptagon-shaped root structure of $W_2^{[7,4,3]}(z)$. It seems that triple-triangle is a new type of pattern compared with those of the NLS equation [59] and Manakov system [61].

By comparison of the true rogue waves to the predicted ones (see Figs. 4 and 5), we can observe that each of the rogue waves matches perfectly in terms of position and rogue wave shape. Notice that the predicted pattern looks very different from the root structure of $W_2^{[m,4,3]}(z)$. This is due to the term Δ_1 leading to a nonlinear transformation from the root structure. When $|a_m|$ is set to be very large, the

term Δ_1 can be neglected, and the patterns become much closer to certain linear transformations of the root structure of $W_2^{[m,4,3]}(z)$.

Apart from the above observations, we can also qualitatively compare the differences between predicted and true rogue waves. To illustrate this, we choose the 1st type $(2, 0, 0)$ -th order rogue waves, then select various large real values of a_3 to analyze errors in the outer region and various large real values of a_5 to analyze errors in the inner region. Referring to the work of Yang and Yang [60], we define

$$\text{error of Peregrine location} = \sqrt{(\hat{x}_0 - x_0)^2 + (\hat{t}_0 - t_0)^2}, \quad (56)$$

and

$$\text{error of inner region} = \left| u_{1, \mathcal{N}_1}(x, t) - \hat{u}_{1, \hat{\mathcal{N}}_1}(x, t) \right|_{x=t=0}, \quad (57)$$

where (x_0, t_0) is the location where each rogue wave reaches maximum modulus value and (\hat{x}_0, \hat{t}_0) is the predicted location of each fundamental rogue wave. These errors and decay rate of $|a_3|^{-1/3}$ and $|a_5|^{-1}$ for large- a_3 and large- a_5 solutions are plotted in Fig. 6. As can be seen, the results of the numerical analysis also match very well.

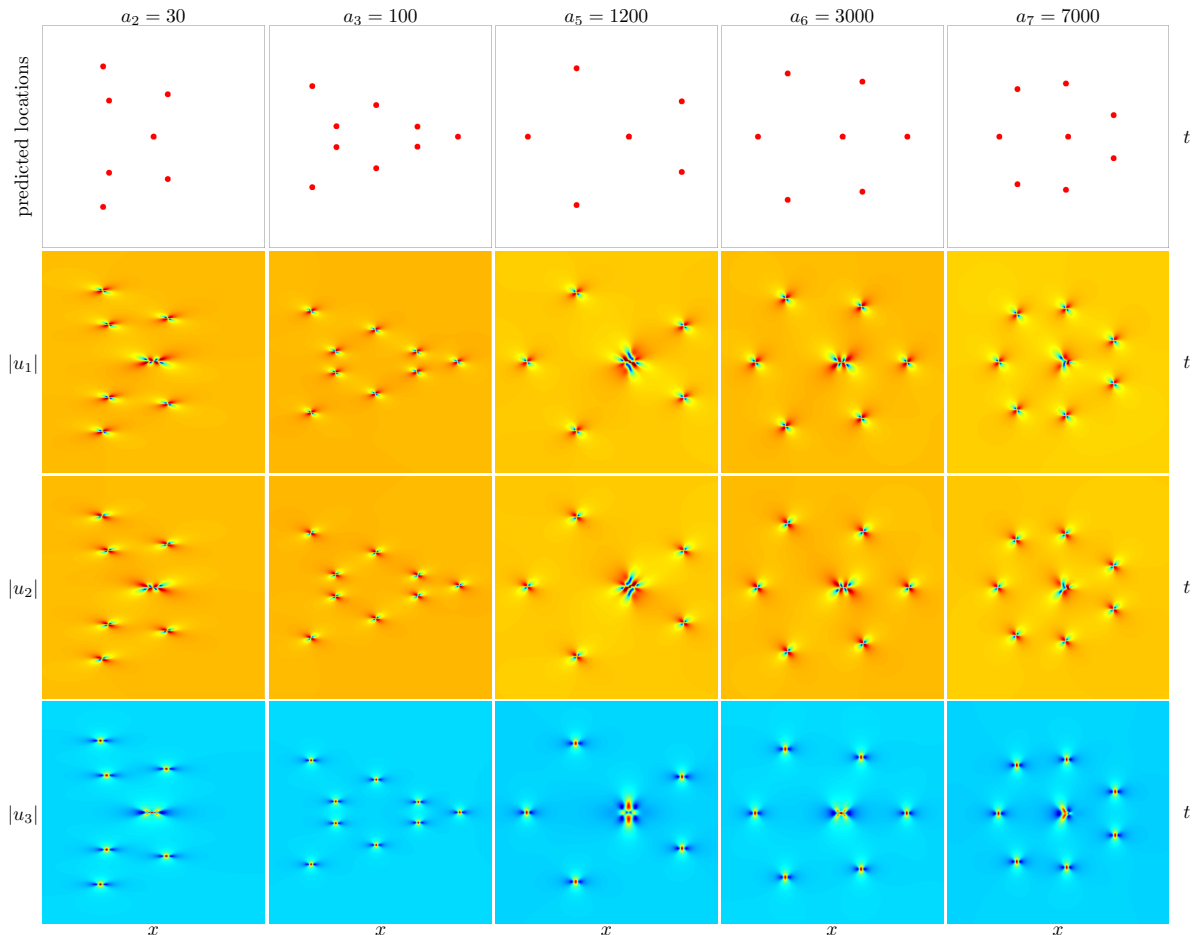


Figure 4: Predicted 1st type $(2, 0, 0)$ -th order rogue waves of the three-component NLS from Theorem 3.1. Each column depicts rogue waves with a single large parameter a_m , whose value is indicated on top, and all other internal parameters are set to zero. Top row: predicted (\hat{x}_0, \hat{t}_0) locations by formulae (45). Second row: predicted $|u_1(x, t)|$. Third row: predicted $|u_2(x, t)|$. Bottom row: predicted $|u_3(x, t)|$. First column: the (x, t) intervals are $-21 \leq x \leq 21$, $-25 \leq t \leq 25$. Second column: the (x, t) intervals are $-30 \leq x \leq 30$, $-25 \leq t \leq 25$. Third column: the (x, t) intervals are $-30 \leq x \leq 20$, $-16 \leq t \leq 16$. Fourth column: the (x, t) intervals are $-30 \leq x \leq 25$, $-15 \leq t \leq 15$. Fifth column: the (x, t) intervals are $-30 \leq x \leq 25$, $-15 \leq t \leq 15$.

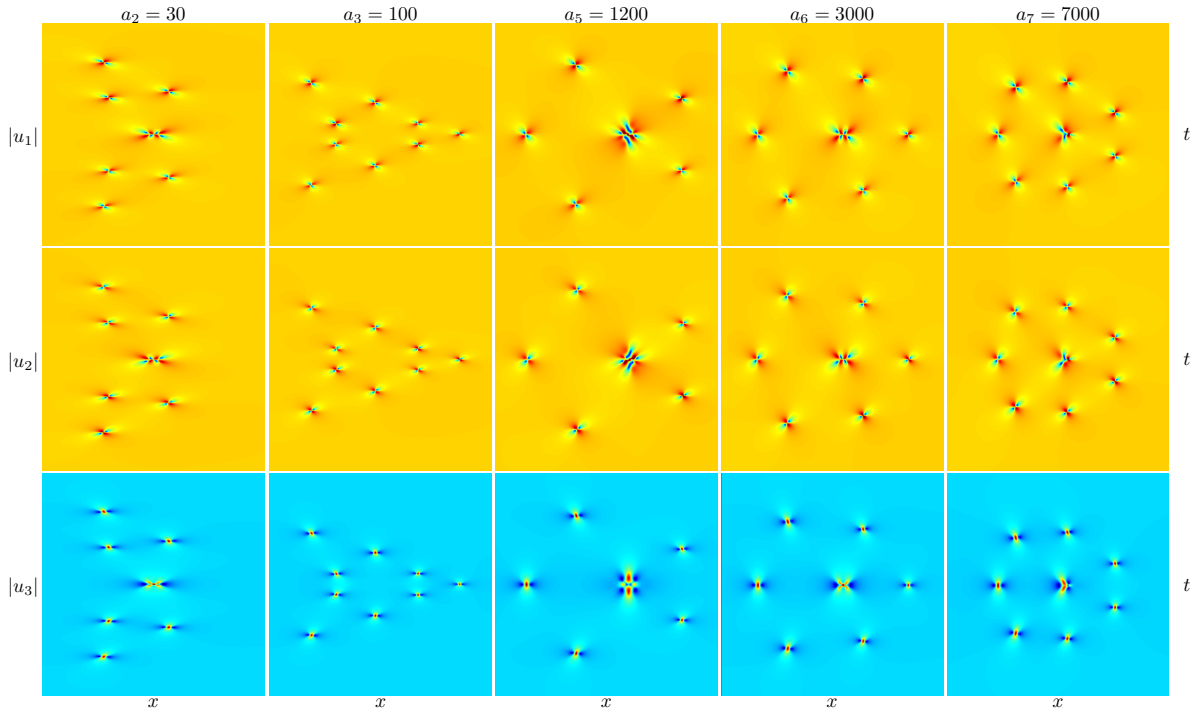


Figure 5: True 1st type $(2, 0, 0)$ -th order rogue waves of the three-component NLS with the same parameters as Fig. 4. The (x, t) interval for each column is the same as the corresponding column in Fig. 4.

4.1.2 Second-type rogue waves of the three-component NLS equation

In this case, we mainly carry out the second-type rogue waves in detail by taking $N_2 = 3$, i.e., $(N_1, N_2, N_3) = (0, 3, 0)$. For brevity, we only let one of the internal parameters $(a_2, a_3, a_5, a_6, a_7)$ be large, and the others are set to 0. The very large parameter is one of

$$a_2 = 30, \quad a_3 = 400, \quad a_5 = 4800, \quad a_6 = 3000, \quad a_7 = 7000. \quad (58)$$

According to Theorem 3.1, the position (\hat{x}_0, \hat{t}_0) of each fundamental rogue wave

$$u_{1, \mathcal{N}_2}(x, t), \quad u_{2, \mathcal{N}_2}(x, t), \quad u_{3, \mathcal{N}_2}(x, t)$$

can be predicted by equation (45). The lower (N_1, N_2, N_3) -th order rogue wave would appear in the inner region. The values of (N_1, N_2, N_3) can be deduced by Theorems 3.1 and 2.3. In our prediction, the (N_1, N_2, N_3) values for these five rogue solutions are

$$(N_1, N_2, N_3) = (1, 0, 1), \quad (0, 0, 0), \quad (0, 0, 0), \quad (1, 0, 1), \quad (1, 2, 0),$$

respectively. Note that $(0, 0, 0)$ means no lower-order rogue wave exists in the inner region. On account of our choice of parameters a_m and the value of s_j shown in Remark 6, the internal parameters in these predicted lower (N_1, N_2, N_3) -th order rogue waves of the inner region are all chosen to be zero.

For $[u_{1, \mathcal{N}_2}(x, t), u_{2, \mathcal{N}_2}(x, t), u_{3, \mathcal{N}_2}(x, t)]$, their corresponding lower-order rogue wave patterns are shown in the last three rows of Fig. 7, with the first row being the predicted locations of the rogue waves. As seen in Fig. 7, solutions in the first column are skewed double-triangles, while solutions from the second to the fifth columns are skewed triple-triangles, pentagons, hexagons and heptagons respectively.

Comparing the true rogue waves with predicted ones (see Figs. 7 and 8), we can observe that each of the rogue waves strikingly matches in position and rogue wave shape. Not only that, but it is also numerically demonstrated that the actual and predicted results match very well. Since they are very similar to the previous error analysis, we omit the details.

4.1.3 Third-type rogue waves of the three-component NLS equation

In this case, we choose $(0, 0, 4)$ -th order rogue wave solutions. We only set one of the internal parameters $(a_2, a_3, a_5, a_6, a_7)$ to be large, and the remaining parameters are set to 0. The very large parameter is

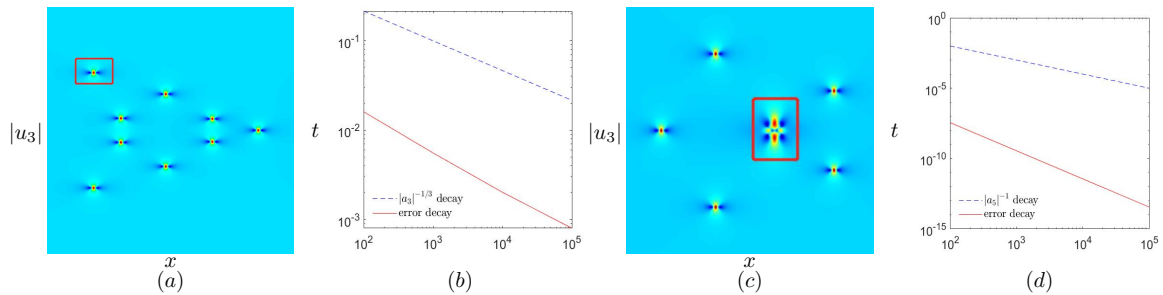


Figure 6: Decay of errors in our predictions of Theorem 3.1 for the outer and inner regions of the 1st type $(2, 0, 0)$ -th order rogue waves in the three-component NLS with various large real values of a_3 or a_5 , while other internal parameters are set to zero. (a) $|u_3(x, t)|$ of the true rogue wave with $a_3 = 100$. (b) Decay of error versus a_3 for the outer fundamental rogue wave marked by the red box, together with the $|a_3|^{-1/3}$ decay for comparison. (c) $|u_3(x, t)|$ of the true rogue wave with $a_5 = 1000$. (d) Decay of error versus a_5 for the lower order rogue wave marked by the red box, together with the $|a_5|^{-1}$ decay for comparison.

one of

$$a_2 = 100, \quad a_3 = 200, \quad a_5 = 1500, \quad a_6 = 5000, \quad a_7 = 10000. \quad (59)$$

According to Theorem 3.1, the position (\hat{x}_0, \hat{t}_0) of each fundamental rogue wave

$$u_{1, \mathcal{N}_3}(x, t), \quad u_{2, \mathcal{N}_3}(x, t), \quad u_{3, \mathcal{N}_3}(x, t)$$

can be predicted by equation (45). The lower (N_1, N_2, N_3) -th order rogue wave would appear in the inner region. The value of (N_1, N_2, N_3) can be obtained from Theorems 3.1 and 2.3. In our prediction, the (N_1, N_2, N_3) values for these five rogue wave solutions are

$$(N_1, N_2, N_3) = (2, 0, 2), \quad (0, 0, 1), \quad (0, 1, 1), \quad (2, 0, 2), \quad (0, 2, 2),$$

respectively. We remark that $(0, 0, 1)$ means there is only a fundamental rogue wave in the inner region. The internal parameters in these predicted lower (N_1, N_2, N_3) -th order rogue waves of the inner region are all zero, due to our choice of parameters a_m and the value of s_j shown in Remark 6.

For $[u_{1, \mathcal{N}_3}(x, t), u_{2, \mathcal{N}_3}(x, t), u_{3, \mathcal{N}_3}(x, t)]$, their corresponding predicted rogue wave patterns are shown in the last three rows of Fig. 9, with the first row being the locations of the rogue waves. It can be seen from Fig. 9 that the large- a_3 solution exhibits a skewed triple-triangle, corresponding to the triple-triangle root structure of $W_4^{[3,4,1]}(z)$. The large- a_5 solution displays a deformed pentagon, corresponding to the pentagon-shaped root structure of $W_4^{[5,4,1]}(z)$. The large- a_6 solution exhibits a deformed hexagon, corresponding to the hexagon-shaped root structure of $W_4^{[6,4,1]}(z)$. The large- a_7 solution exhibits a deformed heptagon, corresponding to the heptagon-shaped root structure of $W_4^{[7,4,1]}(z)$.

Comparing the actual rogue waves with the predicted ones (see Figs. 9 and 10), we can observe that each of the rogue waves matches perfectly in position and rogue wave shape. Moreover, one can further compare them numerically. The results also support our prediction, and since they are very similar to previous analysis, the details are omitted.

4.1.4 Effect of parameters on the rogue wave shapes

We first represent the complex parameter a_m as $a_m = |a_m| \exp(i\vartheta_m)$. In what follows, we will discuss the effects of the modulus $|a_m|$ and the argument ϑ_m on the shapes of rogue waves.

To illustrate the effect of the changes of ϑ_m , we consider the 2nd type $(0, 3, 0)$ -th order rogue waves of the three-component NLS equation and set $|a_3| = 300$ while the remaining parameters a_m are set to 0. Here we simply choose four values of a_3 , namely,

$$(300 \exp(-\pi i/3), \quad 300, \quad 300 \exp(\pi i/3), \quad 300 \exp(\pi i)),$$

then the corresponding predicted and true rogue wave patterns are shown in Fig. 11. It can be seen that the orientation of the rogue wave pattern is changed when we vary the values of ϑ_3 . In fact, this can be seen from Theorem 3.1 as well. In addition, we find that the orientation of the rogue wave pattern is obtained by rotating angle $\arg(-a_m)/m$ of the root structure of $W_3^{[3,4,2]}(z)$, where ‘‘arg’’ represents the

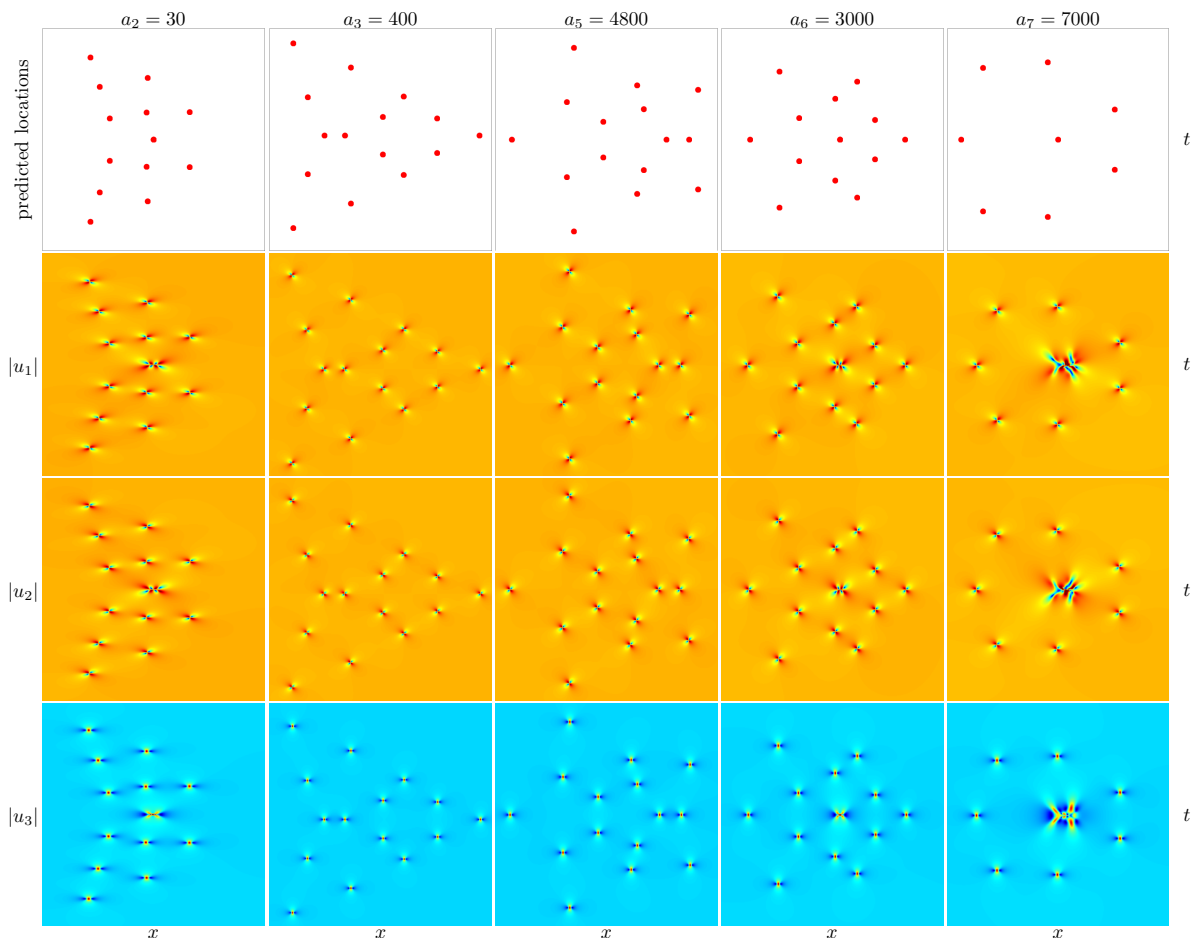


Figure 7: Predicted 2nd type $(0, 3, 0)$ -th order rogue waves of the three-component NLS from Theorem 3.1. Each column depicts rogue waves with a single large parameter a_m , whose value is indicated on top, and all other internal parameters are set to zero. Top row: predicted (\hat{x}_0, \hat{t}_0) locations by formulae (45). Second row: predicted $|u_1(x, t)|$. Third row: predicted $|u_2(x, t)|$. Bottom row: predicted $|u_3(x, t)|$. First column: the (x, t) intervals are $-25 \leq x \leq 25$, $-26 \leq t \leq 26$. Second column: the (x, t) intervals are $-45 \leq x \leq 51$, $-29 \leq t \leq 27$. Third column: the (x, t) intervals are $-47 \leq x \leq 31$, $-22 \leq t \leq 22$. Fourth column: the (x, t) intervals are $-40 \leq x \leq 35$, $-20 \leq t \leq 20$. Fifth column: the (x, t) intervals are $-35 \leq x \leq 30$, $-20 \leq t \leq 20$.

argument of a complex number.

To study the effect of changes in $|a_m|$ on rogue wave patterns, we choose 2nd type $(0, 3, 0)$ -th order rogue waves. Set the argument of a_2 to 0 while the remaining parameters a_m are chosen to be 0. The corresponding predicted and true rogue wave patterns are depicted in Fig. 12. It can be observed that the shape of the rogue wave pattern becomes closer and closer to the linear transformation of the roots of $W_3^{[2,4,2]}(z)$ when the modulus of a_2 gets larger. Specifically, when $a_2 = 20$, both predicted and true rogue wave patterns look very irregular, especially those located on the negative x -axis. However, further increasing the value of a_2 , the distortion will gradually be weakened. For $a_2 = 500$, the shape of rogue waves is very close to a linear transformation of the roots of $W_3^{[2,4,2]}(z)$. The reason is that Δ_2 is a z_0 -dependent $O(1)$ quantity. Specifically, when a_2 takes a very large value, the value of Δ_2 in (45) can be ignored and the predicted rogue wave can be obtained approximately by some linear transformation from the root structure of $W_3^{[2,4,2]}(z)$.

4.2 Comparison in the four-component NLS equation

In this subsection, we compare our predicted rogue wave patterns in Theorem 3.2 with true rogue waves of the four-component NLS equation. For the quadruple root case, we choose background wavenumbers $k_1 = -k_4 = (\sqrt{5} - 1)/4$ and $k_2 = -k_3 = -(\sqrt{5} + 1)^2/8$, which implies $\rho_1 = \rho_4 = \sqrt{2}$ and $\rho_2 = \rho_3 = \sqrt{\sqrt{5} + 3}$ according to (23). In this circumstance, we select $p_0 = \sqrt{(\sqrt{5} + 5)/2}/2$ and $p_1 = \sqrt[10]{(11\sqrt{5} + 25)/4608}$.

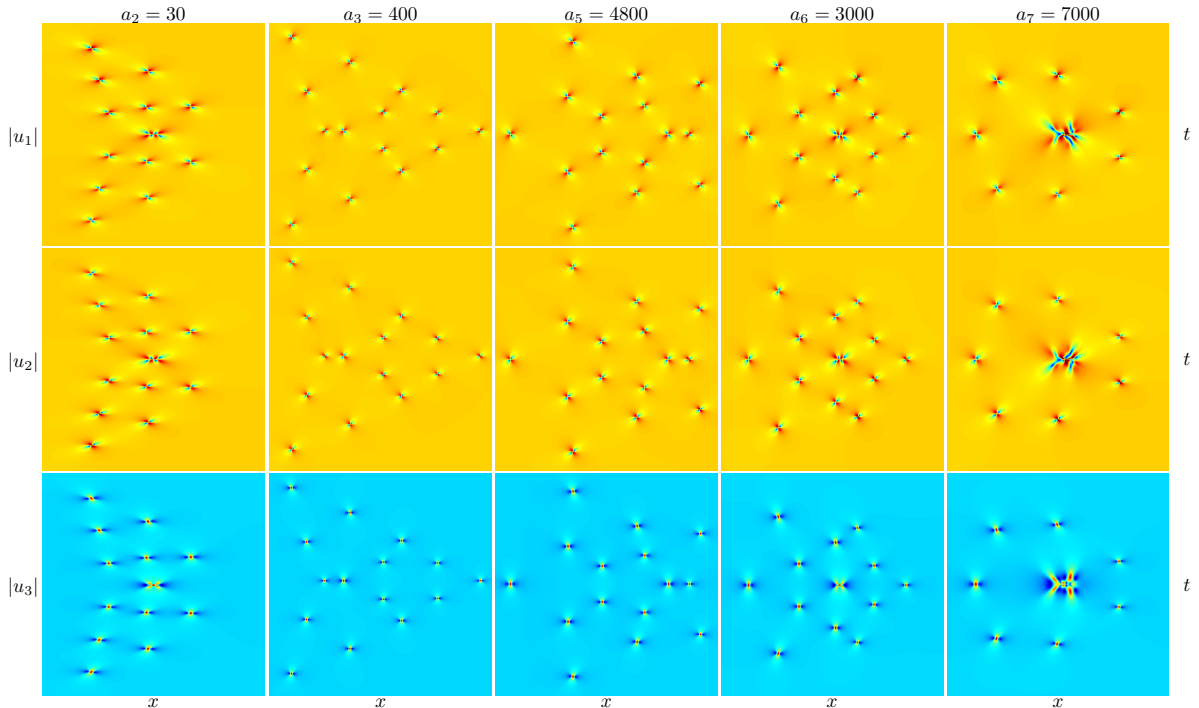


Figure 8: True 2nd type $(0, 3, 0)$ -th order rogue waves of the three-component NLS with the same parameters as Fig. 7. The (x, t) interval for each column is the same as the corresponding column in Fig. 7.

4.2.1 Third-type rogue waves of the four-component NLS equation

In this case, we focus on $(0, 0, 2, 0)$ -th order rogue wave solution. For brevity, we only consider the first four irreducible parameters (a_2, a_3, a_4, a_6) , and set the rest of the parameters to 0. Then, for the internal parameters (a_2, a_3, a_4, a_6) , we let one of them be large and set the others to 0. The very large parameter is one of

$$a_2 = 50, \quad a_3 = 200, \quad a_4 = 500, \quad a_6 = 5000. \quad (60)$$

According to Theorem 3.2, the position (\bar{x}_0, \bar{t}_0) of each fundamental rogue wave

$$u_{1, \mathcal{N}_1}(x, t), \quad u_{2, \mathcal{N}_1}(x, t), \quad u_{3, \mathcal{N}_1}(x, t), \quad u_{4, \mathcal{N}_1}(x, t)$$

can be predicted by (52). The (N_1, N_2, N_3, N_4) -th order rogue wave would appear in the inner region, and the (N_1, N_2, N_3, N_4) values for these five rogue wave solutions are obtained from Theorems 3.2 and 2.4 as

$$(N_1, N_2, N_3, N_4) = (0, 0, 0, 0), \quad (0, 0, 1, 1), \quad (0, 1, 1, 0), \quad (0, 0, 1, 1),$$

Note that $(0, 0, 0, 0)$ means no lower-order rogue wave exists in the center region. Owing to our choice of parameters a_m and the value of s_j shown in Remark 6, the internal parameters in these predicted lower (N_1, N_2, N_3, N_4) -th order rogue waves of the center region are all chosen to be zero.

For $[u_{1, \mathcal{N}_1}(x, t), u_{2, \mathcal{N}_1}(x, t), u_{3, \mathcal{N}_1}(x, t), u_{4, \mathcal{N}_1}(x, t)]$, their corresponding predicted rogue wave patterns are shown in the last four rows of Fig. 13, with the first row being the locations of the rogue waves. Each column is separated when one of the parameters (a_2, a_3, a_4, a_6) is large.

As depicted in Fig. 13, the large- a_2 solution exhibits a skewed double-triangle, corresponding to the double-triangle root structure of $W_2^{[2,5,2]}(z)$. The large- a_3 solution exhibits a skewed triple-triangle, corresponding to the triple-triangle root structure of $W_2^{[3,5,2]}(z)$. The large- a_4 solution exhibits a deformed rectangle, corresponding to the rectangle-shaped root structure of $W_2^{[4,5,2]}(z)$. The large- a_6 solution exhibits a deformed hexagon, corresponding to the hexagon-shaped root structure of $W_2^{[6,5,2]}(z)$.

Comparing the actual rogue waves with the predicted rogue waves (see Figs. 13 and 14), we can observe that each of the rogue waves matches perfectly in terms of position and rogue wave shape. Notice that the predicted pattern looks very different from the root structure of $W_2^{[m,5,2]}(z)$. This is caused by $\bar{\Delta}_3$, which leads to a nonlinear transformation from the root structure. When we take $|a_m|$ very large, the term $\bar{\Delta}_3$ can be neglected, and our pattern becomes more similar to a certain linear

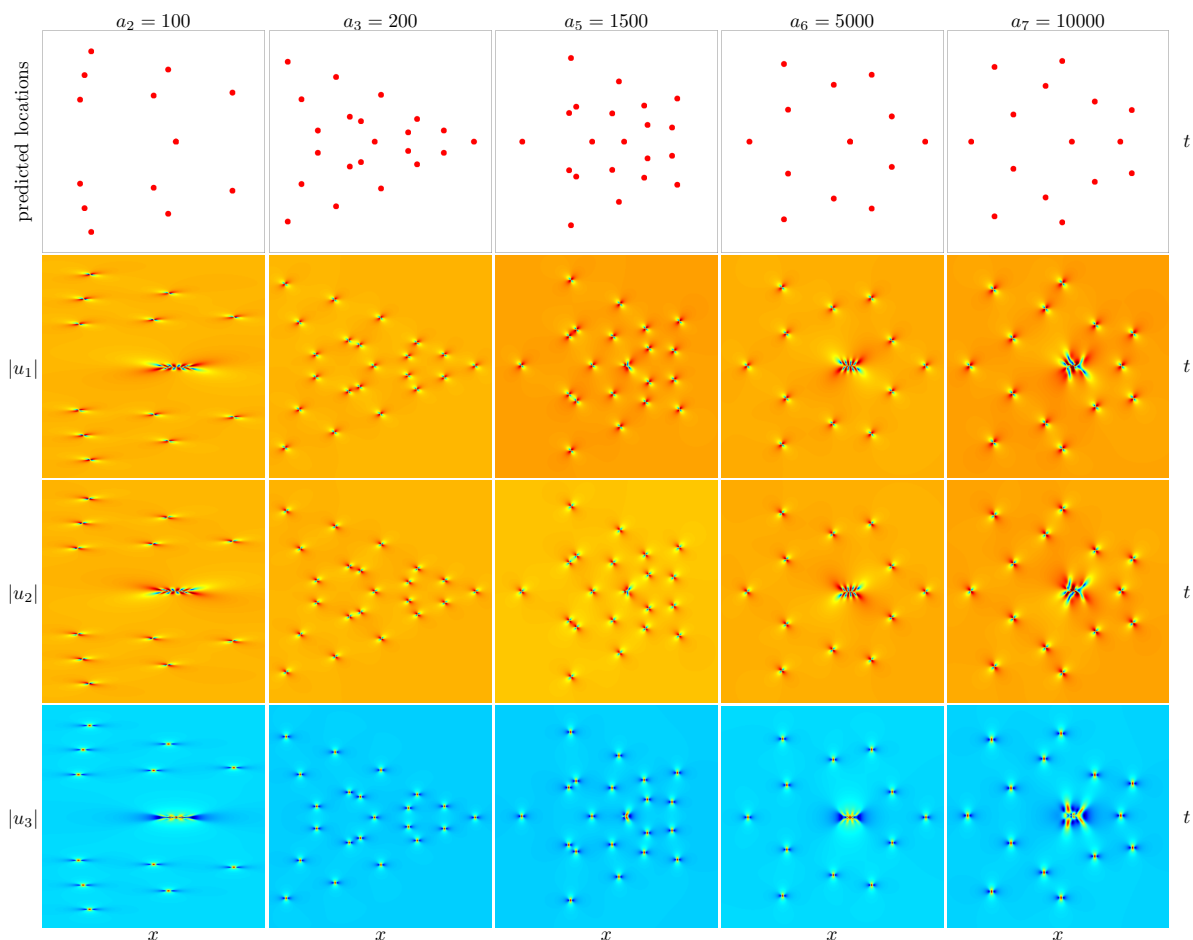


Figure 9: Predicted 3rd type $(0, 0, 4)$ -th order rogue waves of the three-component NLS from Theorem 3.1. Each column corresponds to rogue waves with a single large parameter a_m , whose value is indicated on top, and all other internal parameters are set to zero. Top row: predicted (\hat{x}_0, \hat{t}_0) locations by formulae (45). Second row: predicted $|u_1(x, t)|$. Third row: predicted $|u_2(x, t)|$. Bottom row: predicted $|u_3(x, t)|$. First column: the (x, t) intervals are $-30 \leq x \leq 20$, $-50 \leq t \leq 50$. Second column: the (x, t) intervals are $-45 \leq x \leq 50$, $-32 \leq t \leq 32$. Third column: the (x, t) intervals are $-55 \leq x \leq 40$, $-25 \leq t \leq 25$. Fourth column: the (x, t) intervals are $-55 \leq x \leq 40$, $-25 \leq t \leq 25$. Fifth column: the (x, t) intervals are $-45 \leq x \leq 35$, $-40 \leq t \leq 20$.

transformation of the root structure of $W_2^{[m, 5, 2]}(z)$. The numerical results also match very well, and as they are very similar to the previous error analysis, we omit the details.

4.2.2 Fourth-type four-component NLS equation rogue wave solution

In this circumstance, we consider $(0, 0, 0, 2)$ -th order rogue waves. For brevity, we only let one of the internal parameters (a_2, a_3, a_4, a_6) be large and the others are set to 0. The very large parameter is one of

$$a_2 = 50, \quad a_3 = 200, \quad a_4 = 500, \quad a_5 = 5000. \quad (61)$$

According to Theorem 3.2, the position (\bar{x}_0, \bar{t}_0) of each fundamental rogue wave

$$u_{1, \mathcal{N}_4}(x, t), \quad u_{2, \mathcal{N}_4}(x, t), \quad u_{3, \mathcal{N}_4}(x, t), \quad u_{4, \mathcal{N}_4}(x, t)$$

can be predicted by (52). The possible (N_1, N_2, N_3, N_4) -th order rogue wave would appear in the inner region, and the (N_1, N_2, N_3, N_4) values for these five rogue wave solutions are obtained from Theorems 3.2 and 2.4 as

$$(N_1, N_2, N_3, N_4) = (0, 0, 0, 0), \quad (0, 0, 0, 0), \quad (0, 0, 1, 1), \quad (0, 0, 0, 0),$$

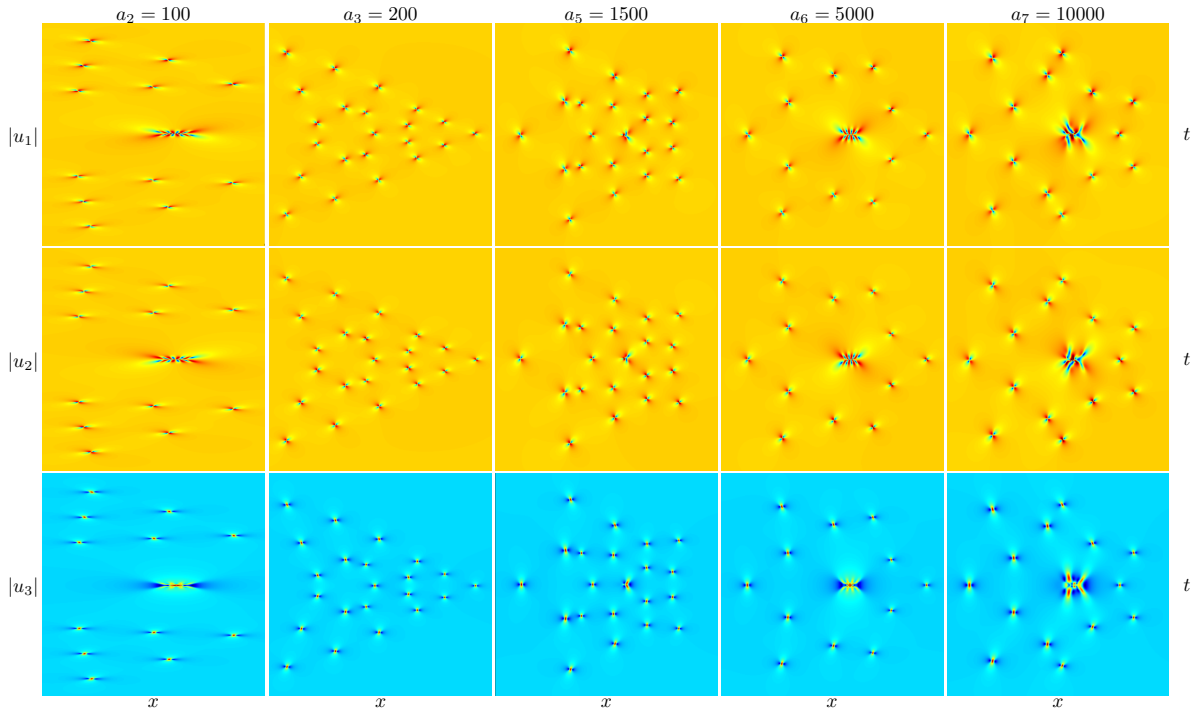


Figure 10: True 3rd type $(0, 0, 4)$ -th order rogue waves of the three-component NLS with the same parameters as Fig. 9. The (x, t) interval for each column is the same as the corresponding column in Fig. 9.

respectively. Note that $(0, 0, 0, 0)$ means that there are no lower-order rogue waves in the center region. For the same reason as previous cases, the internal parameters in these predicted lower (N_1, N_2, N_3, N_4) -th order rogue waves of the center region are all taken to be zero.

For $[u_{1, \mathcal{N}_2}(x, t), u_{2, \mathcal{N}_2}(x, t), u_{3, \mathcal{N}_2}(x, t)]$, their corresponding predicted rogue wave patterns are shown in the last three rows of Fig. 15, with the first row being the predicted locations of the rogue waves. It can be seen from Fig. 15 that the first to fourth columns are skewed double-triangles, skewed triple-triangles, rectangles and hexagons, respectively.

Comparing the true rogue waves with predicted ones (see Figs. 15 and 16), we can observe that each of the rogue waves matches perfectly in terms of position and rogue wave shape. The results of the numerical analysis also match very well, but we omit the details because they are very similar to the previous error analysis.

5 Proof of the main results

Proof of Theorem 3.1. We will only provide the proof for $i = 1$ as the proofs are similar in other cases. Assume $|a_m|$ is large and the rest parameters are $O(1)$ in the 1st type rogue wave solutions of the three-component NLS equation. We first consider the case when (x, t) is far away from the origin and $(x^2 + t^2)^{1/2} = O(|a_m|^{1/m})$. In this circumstance, we have

$$S_j(\mathbf{x}^+(\mathbf{n}) + \nu \mathbf{s}) = S_j(x_1^+, x_2^+, x_3^+, \nu s_4, x_5^+, x_6^+, x_7^+, \nu s_8, \dots, x_m^+ + \nu s_m, \dots) \sim S_j(\mathbf{v}), \quad (62)$$

where

$$\mathbf{v} = (p_0 x + 2p_0 p_1 i t, 0, \dots, 0, a_m, 0, \dots).$$

According to Remark 6, we have $s_1 = s_2 = s_3 = s_5 = s_6 = s_7 = 0$. By the definition of Schur polynomials, we have the relation

$$S_j(\mathbf{v}) = a_m^{j/m} p_j^{[m]}(z), \quad (63)$$

where

$$z = a_m^{-1/m} (\alpha_1 x + \beta_1 i t) = a_m^{-1/m} (p_0 x + 2p_0 p_1 i t). \quad (64)$$

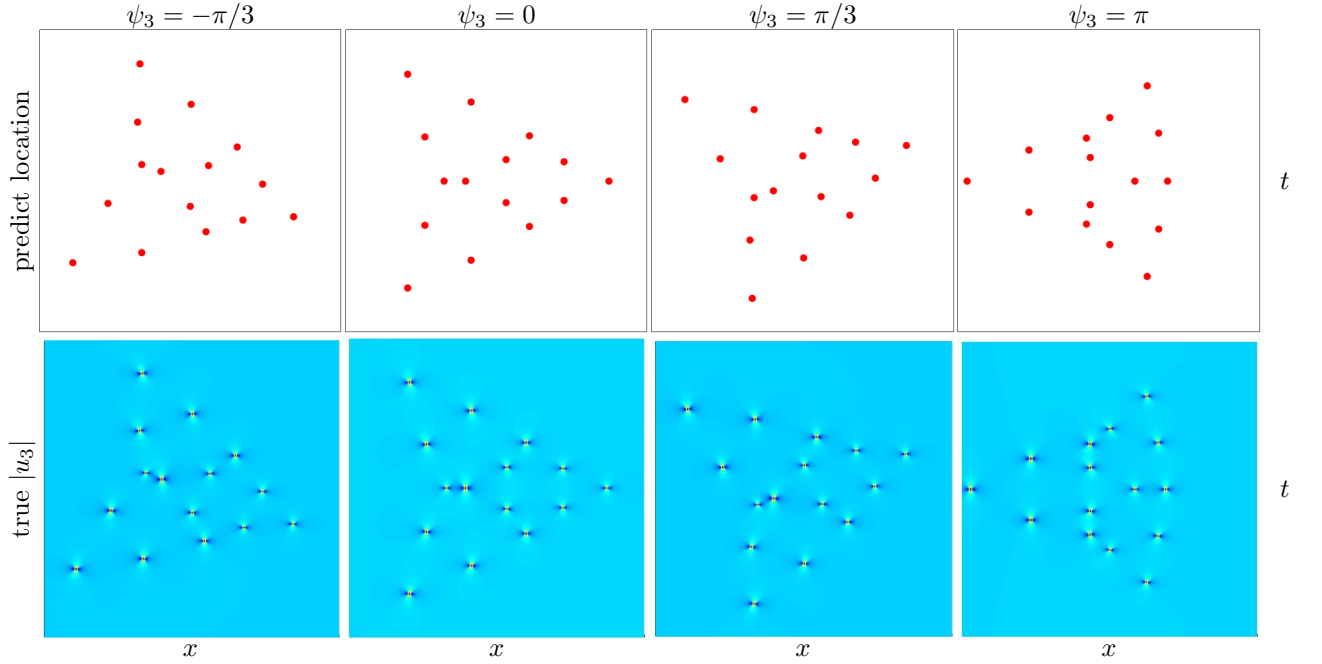


Figure 11: Effect of the argument in a_3 on orientations of the 2nd type $(0, 3, 0)$ -th order rogue waves of the three-component NLS equation. Each column represents a rogue wave with a different value of a_3 with the same modulus 300 but a different argument, and all other internal parameters are set to zero. The (x, t) intervals are $-55 \leq x \leq 55$ and $-30 \leq t \leq 30$.

Then it follows that

$$\det_{1 \leq i, j \leq N} [S_{4i-j}(\mathbf{x}^+(\mathbf{n}) + \nu_j \mathbf{s})] \sim (c_N^{[m,4,3]})^{-1} a_m^{3N(N+1)/2m} W_N^{[m,4,3]}(z) \quad (65)$$

and

$$\det_{1 \leq i, j \leq N} [S_{4i-j}(\mathbf{x}^-(\mathbf{n}) + \nu_j \mathbf{s}^*)] \sim (c_N^{[m,4,3]})^{-1} (a_m^*)^{3N(N+1)/2m} W_N^{[m,4,3]}(z^*). \quad (66)$$

Here, $S_j \equiv 0$ when $j < 0$.

Next, we rewrite the function $\tau_{\mathbf{n}}$ into the following form by Laplace expansion

$$\begin{aligned} \tau_{\mathbf{n}} = & \sum_{0 \leq \nu_1 < \nu_2 < \dots < \nu_N \leq 4N-1} \det_{1 \leq i, j \leq N} [(h_0)^{\nu_j} S_{4i-1-\nu_j}(\mathbf{x}^+(\mathbf{n}) + \nu_j \mathbf{s})] \\ & \times \det_{1 \leq i, j \leq N} [(h_0^*)^{\nu_j} S_{4i-1-\nu_j}(\mathbf{x}^-(\mathbf{n}) + \nu_j \mathbf{s}^*)], \end{aligned} \quad (67)$$

where $h_0 = p_1 / (p_0 + p_0^*)$.

It is clear that the highest order term in a_m in this $\tau_{\mathbf{n}}$ comes from the index choices of $\nu_j = j - 1$. Therefore, we have

$$\tau_{\mathbf{n}} \sim |\alpha|^2 |a_m|^{3N(N+1)/m} \left| W_N^{[m,4,3]}(z) \right|^2, \quad (68)$$

where $\alpha = h_0^{N(N-1)/2} (c_N^{[m,4,3]})^{-1}$. From the asymptotic analysis above, we conclude that the leading-order term of $\tau_{\mathbf{n}}$ is independent of \mathbf{n} . Consequently, when (x, t) is not close to $(\check{x}_0, \check{t}_0)$, which is related to the roots of $W_N^{[m,4,3]}(z)$ by

$$z_0 = a_m^{-1/m} (p_0 \check{x}_0 + 2p_0 p_1 i \check{t}_0),$$

we have

$$\frac{\tau_{\mathbf{n}_1}}{\tau_{\mathbf{n}_0}} \sim 1, \quad \frac{\tau_{\mathbf{n}_2}}{\tau_{\mathbf{n}_0}} \sim 1, \quad \frac{\tau_{\mathbf{n}_3}}{\tau_{\mathbf{n}_0}} \sim 1, \quad |a_m| \gg 1. \quad (69)$$

However, when (x, t) is close to $(\check{x}_0, \check{t}_0)$, the coefficient of the term with highest order in a_m vanishes. To deal with this case, we have to consider lower order terms in a_m , which require more precise

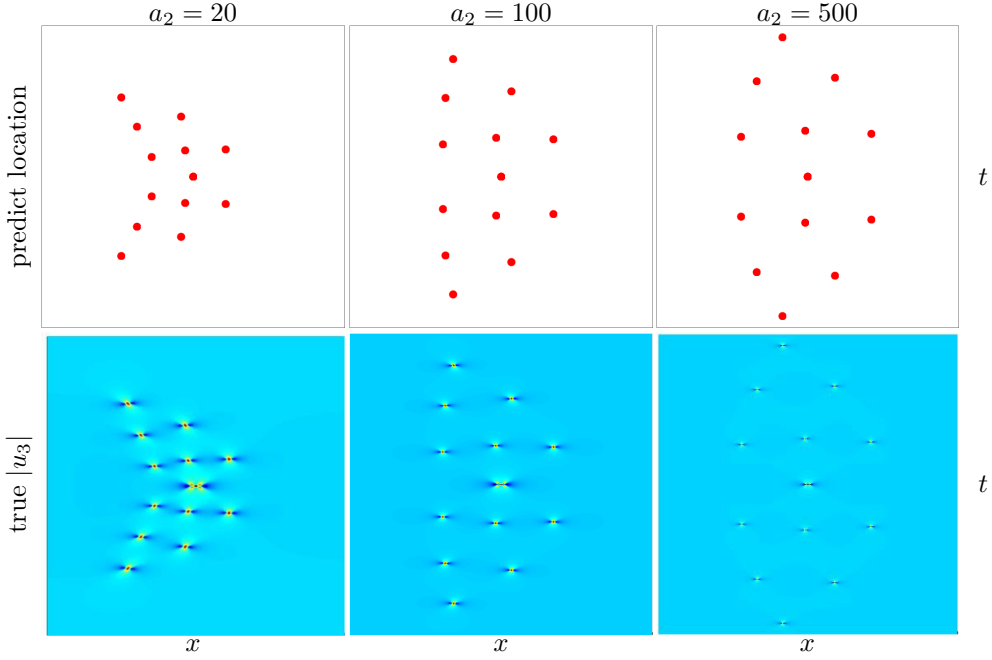


Figure 12: Effect of the size a_2 on shapes of the 2nd type $(0, 3, 0)$ -th order rogue waves of the three-component NLS equation. Each column represents a rogue wave with different values of a_2 indicated on top, and all other internal parameters are set to zero. Top row: prediction location of $|u_3(x, t)|$. Bottom row: true $|u_3(x, t)|$. First column: the (x, t) intervals are $-30 \leq x, t \leq 30$. Second column: the (x, t) intervals are $-45 \leq x, t \leq 45$. Third column: the (x, t) intervals are $-85 \leq x, t \leq 85$.

asymptotics. In this circumstance, i.e., (x, t) is near $(\check{x}_0, \check{t}_0)$, we find that

$$\begin{aligned}
& S_j(\mathbf{x}^+(\mathbf{n}) + \nu \mathbf{s}) \\
&= S_j(x_1^+, x_2^+, x_3^+, \nu s_4, x_5^+, x_6^+, x_7^+, \nu s_8, \dots, x_m^+ + \nu s_m, \dots) \\
&= [S_j(\hat{\mathbf{v}}) + \hat{x}_2^+(\check{x}_0, \check{t}_0) S_{j-2}(\hat{\mathbf{v}})] \left[1 + O\left(a_m^{-2/m}\right) \right], \quad |a_m| \gg 1,
\end{aligned}$$

where

$$\begin{aligned}
\hat{\mathbf{v}} &= (p_0 x + 2p_0 p_1 i t + n_1 \theta_{11} + n_2 \theta_{12} + n_3 \theta_{13}, 0, \dots, 0, a_m, 0, \dots), \\
\hat{x}_2^+(x, t) &= p_2 x + (2p_0 p_2 + p_1^2)(it),
\end{aligned}$$

$p_2 = p_1^2$ and a_1 in x_1^+ is set to 0. Similar to (63), we can get

$$S_j(\hat{\mathbf{v}}) = a_m^{j/m} p_j^{[m]}(\hat{z}), \quad (70)$$

where

$$\hat{z} = a_m^{-1/m} (p_0 x + 2p_0 p_1 i t + n_1 \theta_{11} + n_2 \theta_{12} + n_3 \theta_{13}). \quad (71)$$

In this case, there are two index choices of ν_j that will produce leading-order terms in a_m for $\tau_{\mathbf{n}}$. One of them is $\nu = (0, 1, \dots, N-1)$ while the other is $\nu = (0, 1, \dots, N-2, N)$.

(1) For the first choice of index, i.e., $\nu_j = j-1$, there are two parts that will provide leading-order terms. The first part stems from $S_j(\hat{\mathbf{v}})$, and we find that the dominant term involving $\mathbf{x}^+(\mathbf{n})$ is expressed as

$$\alpha a_m^{\frac{3N(N+1)}{2m}} W_N^{[m,4,3]}(\hat{z}) \left[1 + O\left(a_m^{-2/m}\right) \right]. \quad (72)$$

Then, we expand $W_N^{[m,4,3]}(\hat{z})$ around z_0 , and noting $W_N^{[m,4,3]}(z_0) = 0$, we obtain

$$W_N^{[m,4,3]}(\hat{z}) = a_m^{-1/m} [p_0(x - \check{x}_0) + 2p_0 p_1 i(t - \check{t}_0) + n_1 \theta_{11} + n_2 \theta_{12} + n_3 \theta_{13}] \left[W_N^{[m,4,3]} \right]'(z_0) \left[1 + O\left(a_m^{-1/m}\right) \right]. \quad (73)$$

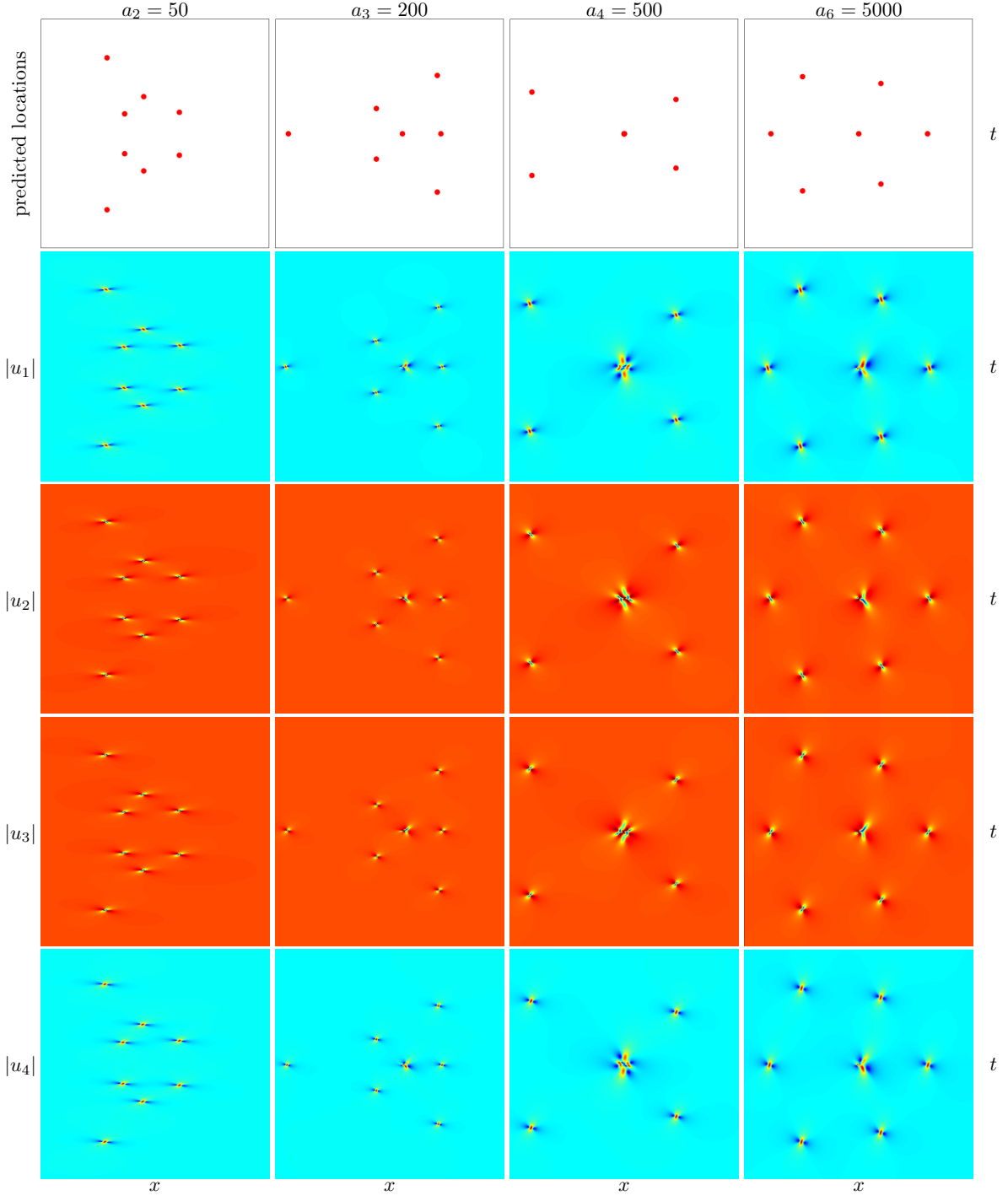


Figure 13: Predicted 3rd type $(0,0,2,0)$ -th order rogue waves of the four-component NLS equation from Theorem 3.2. Each column corresponds to a rogue wave with a single large parameter a_m , whose value is indicated on top, and all other internal parameters are set to zero. Top row: predicted (\bar{x}_0, \bar{t}_0) locations by formulae (52). Second row: predicted $|u_1(x, t)|$. Third row: predicted $|u_2(x, t)|$. Fourth row: predicted $|u_3(x, t)|$. Bottom row: predicted $|u_4(x, t)|$. First column: the (x, t) intervals are $-25 \leq x \leq 25$, $-40 \leq t \leq 40$. Second column: the (x, t) intervals are $-50 \leq x \leq 40$, $-35 \leq t \leq 35$. Third column: the (x, t) intervals are $-30 \leq x \leq 30$, $-20 \leq t \leq 20$. Fourth column: the (x, t) intervals are $-30 \leq x \leq 30$, $-15 \leq t \leq 15$.

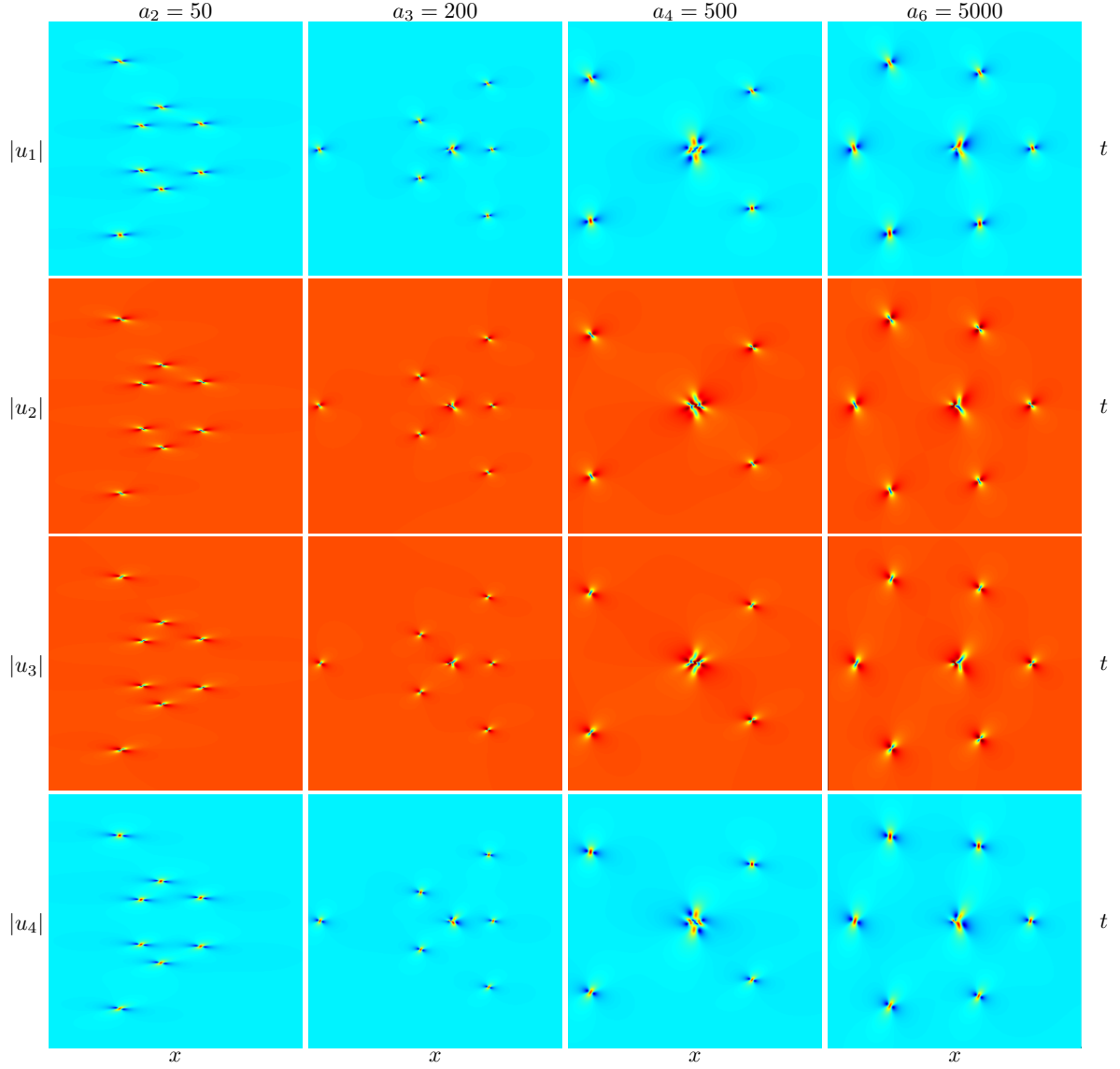


Figure 14: True 3rd type $(0, 0, 2, 0)$ -th order rogue waves of the four-component NLS equation with the same parameters as Fig. 13. The (x, t) interval for each column is the same as the corresponding column in Fig. 13.

As a result, the corresponding leading-order term in a_m is

$$\alpha a_m^{\frac{3N(N+1)-2}{2m}} \left[p_0(x - \check{x}_0) + 2p_0 p_1 i(t - \check{t}_0) + n_1 \theta_{11} + n_2 \theta_{12} + n_3 \theta_{13} \right] \left[W_N^{[m,4,3]} \right]'(z_0) \left[1 + O\left(a_m^{-1/m}\right) \right]. \quad (74)$$

The other leading-order term results from the determinants containing $\hat{x}_2^+(\check{x}_0, \check{t}_0) S_{j-2}$, that is,

$$\hat{x}_2^+(\check{x}_0, \check{t}_0) h_0^{N(N-1)/2} \sum_{j=1}^N \det_{1 \leq i \leq N} [S_{4i-1}(\hat{\mathbf{v}}), \dots, S_{4i-(j-1)}(\hat{\mathbf{v}}), S_{4i-j-2}(\hat{\mathbf{v}}), S_{4i-(j+1)}(\hat{\mathbf{v}}), \dots, S_{4i-N}(\hat{\mathbf{v}})] \times \left[1 + O\left(a_m^{-1/m}\right) \right]. \quad (75)$$

Combing (74) and (75) yields the leading-order term in a_m [62] of the first determinant in (67) containing $\mathbf{x}^+(\mathbf{n})$ corresponding to the index choice $\nu_j = j - 1$, that is,

$$\alpha a_m^{[3N(N+1)-2]/2m} \left[p_0(x - \check{x}_0) + 2p_0 p_1 i(t - \check{t}_0) + n_1 \theta_{11} + n_2 \theta_{12} + n_3 \theta_{13} + \Delta_1 \right] \left[W_N^{[m,4,3]} \right]'(z_0) \left[1 + O\left(a_m^{-1/m}\right) \right]$$

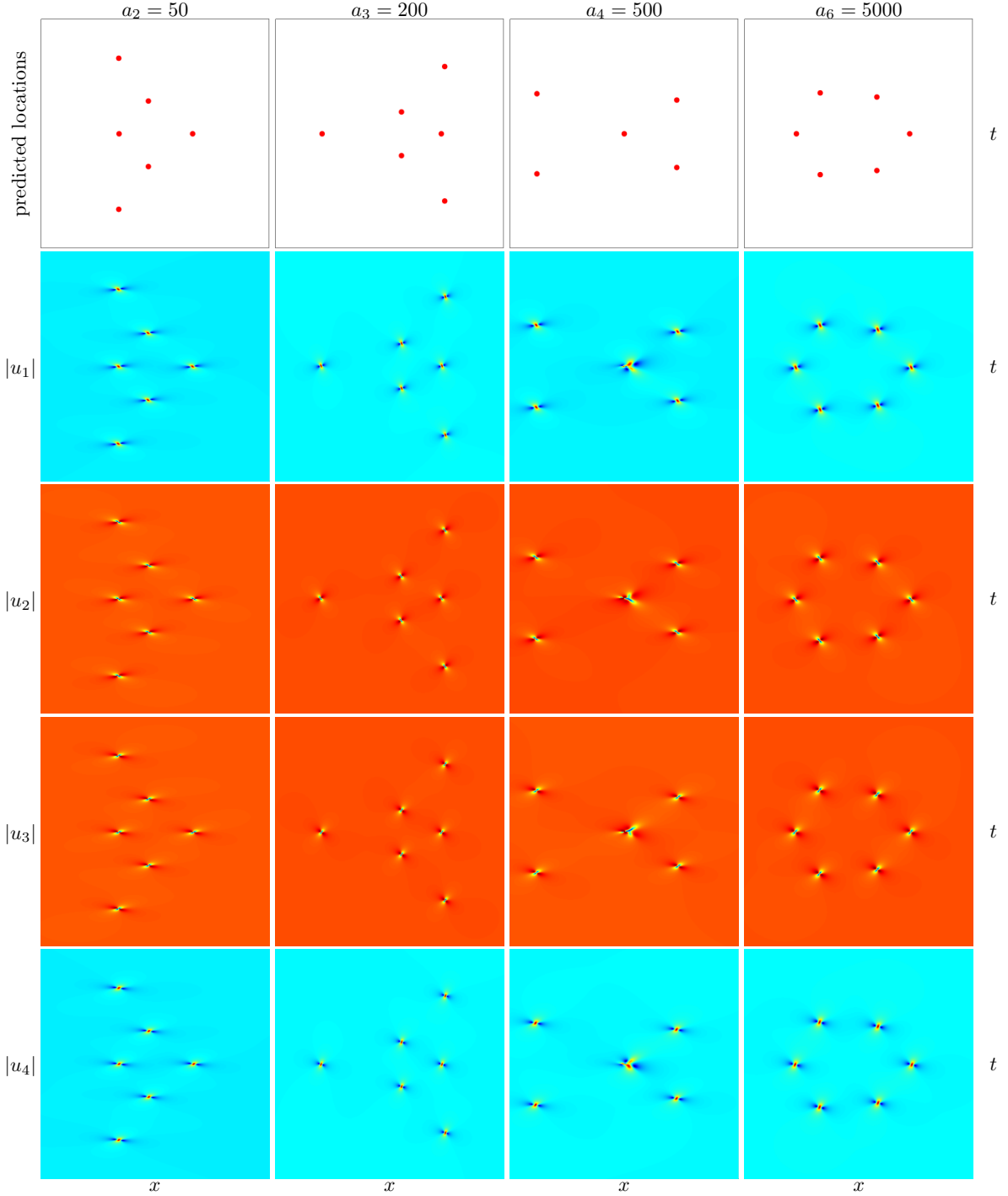


Figure 15: Predicted 4th type $(0,0,0,2)$ -th order rogue waves of the four-component NLS equation from Theorem 3.2. Each column corresponds to rogue waves with a single large parameter a_m , whose value is indicated on top, and all other internal parameters are set to zero. Top row: predicted (\bar{x}_0, \bar{t}_0) locations by formulae (52). Second row: predicted $|u_1(x, t)|$. Third row: predicted $|u_2(x, t)|$. Fourth row: predicted $|u_3(x, t)|$. Bottom row: predicted $|u_4(x, t)|$. First column: the (x, t) intervals are $-25 \leq x \leq 25$, $-35 \leq t \leq 35$. Second column: the (x, t) intervals are $-55 \leq x \leq 35$, $-25 \leq t \leq 25$. Third column: the (x, t) intervals are $-25 \leq x \leq 25$, $-25 \leq t \leq 25$. Fourth column: the (x, t) intervals are $-30 \leq x \leq 30$, $-20 \leq t \leq 20$.

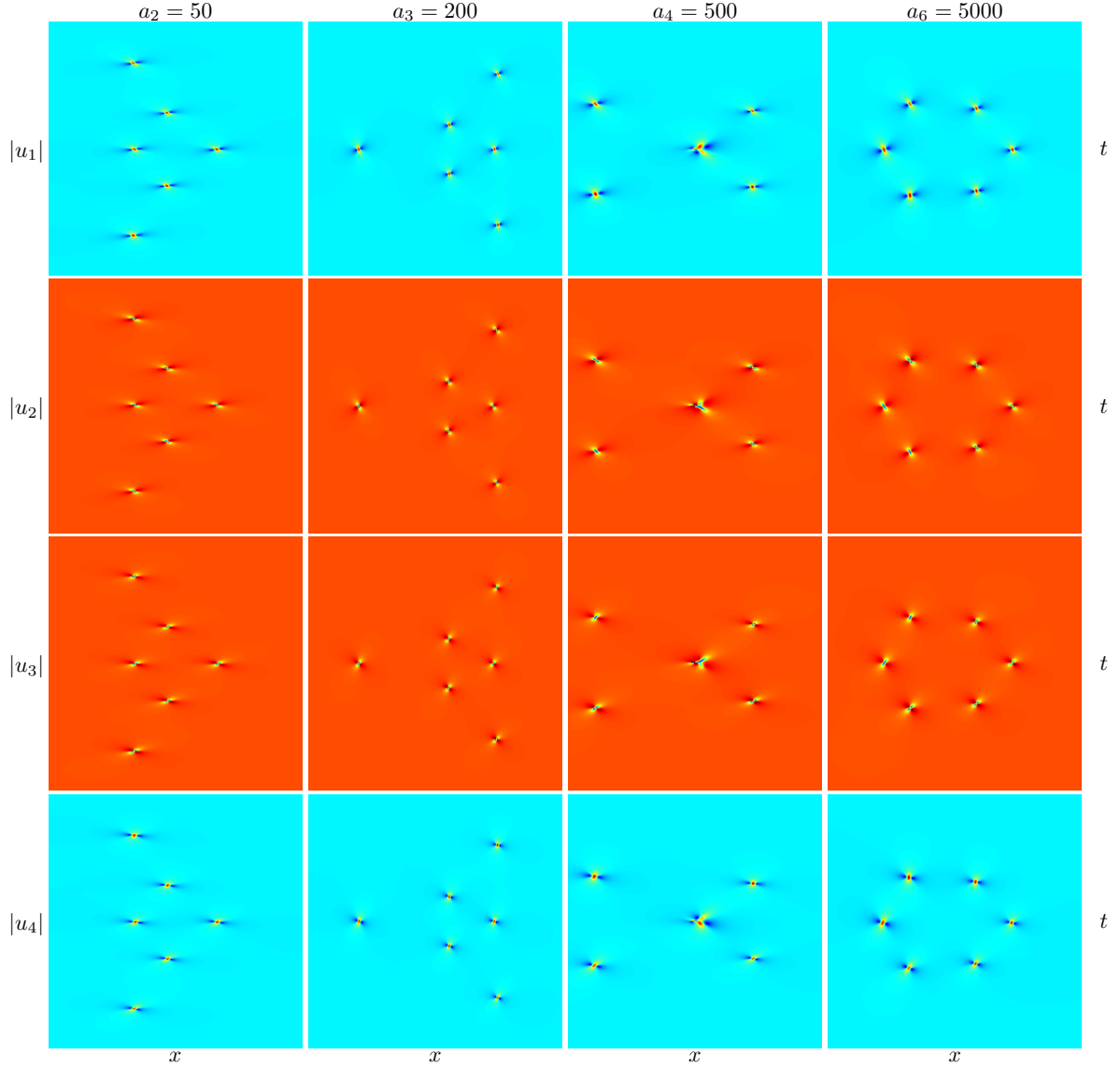


Figure 16: True 4th type $(0, 0, 0, 2)$ -th order rogue waves of the four-component NLS equation with the same parameters as Fig. 15. The (x, t) interval for each column is the same as the corresponding column in Fig. 15.

where

$$\Delta_1 = \frac{\hat{x}_2^+(\hat{x}_0, \hat{t}_0) \sum_{j=1}^N \det_{1 \leq i \leq N} \left[p_{4i-1}^{[m]}(z_0), \dots, p_{4i-j+1}^{[m]}(z_0), p_{4i-j-2}^{[m]}(z_0), p_{4i-j-1}^{[m]}(z_0), \dots, p_{4i-N}^{[m]}(z_0) \right]}{a_m^{1/m} \left[W_N^{[m,4,3]} \right]'(z_0)} \quad (76)$$

and $\Delta_1 = O(1)$ as

$$\hat{x}_2^+(\hat{x}_0, \hat{t}_0) = p_2 \hat{x}_0 + (2p_0 p_2 + p_1^2) (i \hat{t}_0) = O(|a_m^{1/m}|).$$

Further, we can absorb the Δ_1 into (\hat{x}_0, \hat{t}_0) [62] and obtain

$$\alpha a_m^{\frac{3N(N+1)-2}{2m}} \left[p_0 (x - \hat{x}_0) + 2p_0 p_1 i (t - \hat{t}_0) + n_1 \theta_{11} + n_2 \theta_{12} + n_3 \theta_{13} \right] \left[W_N^{[m,4,3]} \right]'(z_0) \left[1 + O\left(a_m^{-1/m}\right) \right]. \quad (77)$$

where \hat{x}_0 and \hat{t}_0 are given in (45).

Similarly, the second determinant in (67) containing $\mathbf{x}^-(\mathbf{n})$ corresponding to the index choice $\nu_j = j-1$

contributes the term

$$\alpha^*(a_m^*)^{\frac{3N(N+1)-2}{2m}} \left[p_0^*(x - \hat{x}_0) - 2p_0^*p_1^*(t - \hat{t}_0) - n_1\theta_{11}^* - n_2\theta_{12}^* - n_3\theta_{13}^* \right] \left[W_N^{[m,4,3]} \right]'(z_0^*) \left[1 + O\left(a_m^{-1/m}\right) \right]. \quad (78)$$

(2) For the second choice of index, i.e., $\nu = (0, 1, \dots, N-2, N)$, the dominant term in a_m can be calculated in a similar way as (65), that is,

$$h_0^{\frac{N(N-1)+2}{2}} a_m^{\frac{3N(N+1)-2}{2m}} \det_{1 \leq i \leq N} \left[p_{4i-1}^{[m]}(z_0), p_{4i-2}^{[m]}(z_0), \dots, p_{4i-(N-1)}^{[m]}(z_0), p_{4i-N-1}^{[m]}(z_0) \right] \left[1 + O\left(a_m^{-1/m}\right) \right]. \quad (79)$$

Since $p_{j-1}^{[m]}(z) = \left[p_j^{[m]} \right]'(z)$, the above term can be expressed as

$$h_0 \alpha a_m^{\frac{3N(N+1)-2}{2m}} \left[W_N^{[m,4,3]} \right]'(z_0) \left[1 + O\left(a_m^{-1/m}\right) \right].$$

Similarly, its conjugate counterpart reads

$$h_0^* \alpha^* (a_m^*)^{\frac{3N(N+1)-2}{2m}} \left[W_N^{[m,4,3]} \right]'(z_0^*) \left[1 + O\left(a_m^{-1/m}\right) \right].$$

Summarizing the above two contributions, we conclude that

$$\begin{aligned} \tau_{\mathbf{n}}(x, t) &= |\alpha|^2 \left| \left[W_N^{[m,4,3]} \right]'(z_0) \right|^2 |a_m|^{[3N(N+1)-2]/m} \times \left(\left[p_1(x - \hat{x}_0) + 2ip_0p_1(t - \hat{t}_0) + n_1\theta_{11} + n_2\theta_{12} + n_3\theta_{13} \right] \right. \\ &\quad \left. \left[p_1^*(x - \hat{x}_0) - 2ip_0^*p_1^*(t - \hat{t}_0) - n_1\theta_{11}^* - n_2\theta_{12}^* - n_3\theta_{13}^* \right] + |h_0|^2 \right) \\ &\quad \times \left[1 + O\left(a_m^{-1/m}\right) \right]. \end{aligned} \quad (80)$$

Finally, under the assumption that all nonzero roots of the generalized Wronskian-Hermite polynomials $W_N^{[m,k,l]}$ are simple, the above leading-order term in a_m for $\tau_{\mathbf{n}}(x, t)$ is non-zero. Hence, using (80), we conclude that, near (\hat{x}_0, \hat{t}_0) , the N -th order rogue wave is approximated by a fundamental rogue wave of the three-component NLS equation given in Theorem 3.1 with error $O(|a_m|^{-1/m})$.

In order to study the patterns of the 1st type rogue waves of the three-component NLS rogue waves under the condition $|a_m| \gg 1$ in the inner region with $x^2 + t^2 = O(1)$, we first use similar method as that in [45] to rewrite the determinant $\tau_{\mathbf{n}}$ as a $5N \times 5N$ determinant

$$\tau_{\mathbf{n}} = \begin{vmatrix} \mathbf{O}_{N \times N} & \Phi_{N \times 4N} \\ -\Psi_{4N \times N} & \mathbf{I}_{4N \times 4N} \end{vmatrix}, \quad (81)$$

where

$$\Phi_{i,j} = \left(\frac{p_1}{p_0 + p_0^*} \right)^{j-1} S_{4i-j}[\mathbf{x}^+(\mathbf{n}) + (j-1)\mathbf{s}], \quad \Psi_{i,j} = \left(\frac{p_1^*}{p_0 + p_0^*} \right)^{i-1} S_{4j-i}[\mathbf{x}^-(\mathbf{n}) + (i-1)\mathbf{s}^*].$$

It is clear that each element in (81) is a polynomial in a_m . To express these polynomials explicitly, we define \mathbf{y}^{\pm} to be the vector \mathbf{x}^{\pm} without the a_m term, i.e.,

$$\mathbf{x}^+ = \mathbf{y}^+ + (0, \dots, 0, a_m, 0, \dots), \quad \mathbf{x}^- = \mathbf{y}^- + (0, \dots, 0, a_m^*, 0, \dots). \quad (82)$$

Then we can expand the Schur polynomials $S_j(\mathbf{x}^{\pm} + \nu\mathbf{s})$ by

$$S_j(\mathbf{x}^+ + \nu\mathbf{s}) = \sum_{l=0}^{[j/m]} \frac{a_m^l}{l!} S_{j-lm}(\mathbf{y}^+ + \nu\mathbf{s}), \quad S_j(\mathbf{x}^- + \nu\mathbf{s}^*) = \sum_{l=0}^{[j/m]} \frac{(a_m^*)^l}{l!} S_{j-lm}(\mathbf{y}^- + \nu\mathbf{s}^*), \quad (83)$$

where $[a]$ refers to the largest inter less than or equal to a . To determine the highest order term in a_m of $\tau_{\mathbf{n}}$, a straightforward way is to keep only the highest order of a_m in each element. However, it turns out the resulting determinant will vanish. To tackle this issue, we can use similar argument as that in [60] to perform row and column operations. Notice that we have totally three cases to consider, i.e., $m \equiv j \pmod{4}$, $j = 1, 2, 3$. Since the proof for $j = 2$ is different from those in the NLS equation [59] and the Manakov system [60], we first focus on the proof of this case. As the proofs for the cases $j = 1$ and 3 are

similar to [60], we only provide a brief proof for $j = 1$.

For $m \equiv 2 \pmod{4}$, i.e., $m = 4r + 2$ ($r \geq 0$), according to the block structure of the determinant $\tau_{\mathbf{n}}$, we can perform row operations on the matrix $\Phi_{N \times 4N}$. For convenience, we define $\hat{S}_j = S_j(\mathbf{y}^+ + \nu \mathbf{s})$ and omit $(p_1/(p_0 + p_0^*))^{j-1}$ in the following representation because they are the same in each column and have no affect on the row operations. Then, we can substitute (83) into $\Phi_{N \times 4N}$ and rewrite it into the form

$$\Phi_{N \times 4N} \sim \begin{bmatrix} & \hat{S}_3 & & \hat{S}_2 & & \cdots \\ & \hat{S}_7 & & \hat{S}_6 & & \cdots \\ & \vdots & & \vdots & & \ddots \\ & \hat{S}_{m-3} & & \hat{S}_{m-4} & & \cdots \\ a_m \hat{S}_1 + \hat{S}_{m+1} & & & a_m \hat{S}_0 + \hat{S}_m & & \cdots \\ a_m \hat{S}_5 + \hat{S}_{m+5} & & & a_m \hat{S}_4 + \hat{S}_{m+4} & & \cdots \\ & \vdots & & \vdots & & \ddots \\ a_m \hat{S}_{m-1} + \hat{S}_{2m-1} & & & a_m \hat{S}_{m-2} + \hat{S}_{2m-2} & & \cdots \\ \frac{a_m^2}{2!} \hat{S}_3 + a_m \hat{S}_{m+3} + \hat{S}_{2m+3} & & & \frac{a_m^2}{2!} \hat{S}_2 + a_m \hat{S}_{m+2} + \hat{S}_{2m+2} & & \cdots \\ & \vdots & & \vdots & & \ddots \\ \frac{a_m^2}{2!} \hat{S}_{m-3} + a_m \hat{S}_{2m-3} + \hat{S}_{3m-3} & & & \frac{a_m^2}{2!} \hat{S}_{m-4} + a_m \hat{S}_{2m-4} + \hat{S}_{3m-4} & & \cdots \\ \frac{a_m^3}{3!} \hat{S}_1 + \frac{a_m^2}{2!} \hat{S}_{m+1} + O(a_m) & & & \frac{a_m^3}{3!} \hat{S}_0 + \frac{a_m^2}{2!} \hat{S}_m + O(a_m) & & \cdots \\ & \vdots & & \vdots & & \ddots \\ \frac{a_m^3}{3!} \hat{S}_{m-1} + \frac{a_m^2}{2!} \hat{S}_{2m-1} + O(a_m) & & & \frac{a_m^3}{3!} \hat{S}_{m-2} + \frac{a_m^2}{2!} \hat{S}_{2m-2} + O(a_m) & & \cdots \\ \frac{a_m^4}{4!} \hat{S}_3 + \frac{a_m^3}{3!} \hat{S}_{m+3} + \frac{a_m^2}{2!} \hat{S}_{2m+3} + O(a_m) & & & \frac{a_m^4}{4!} \hat{S}_2 + \frac{a_m^3}{3!} \hat{S}_{m+2} + \frac{a_m^2}{2!} \hat{S}_{2m+2} + O(a_m) & & \cdots \\ & \vdots & & \vdots & & \ddots \\ \frac{a_m^4}{4!} \hat{S}_{m-3} + \frac{a_m^3}{3!} \hat{S}_{2m-3} + \frac{a_m^2}{2!} \hat{S}_{3m-3} + O(a_m) & & & \frac{a_m^4}{4!} \hat{S}_{m-4} + \frac{a_m^3}{3!} \hat{S}_{2m-4} + \frac{a_m^2}{2!} \hat{S}_{3m-4} + O(a_m) & & \cdots \\ & \vdots & & \vdots & & \ddots \end{bmatrix}.$$

In this case, we can notice that the coefficients of the highest a_m power terms in the first column are proportional to

$$\hat{S}_3, \hat{S}_7, \dots, \hat{S}_{m-3}; \hat{S}_1, \hat{S}_5, \dots, \hat{S}_{m-1} \quad (84)$$

and repeating. To be more precise, the first r rows are a sequence starting with \hat{S}_3 , and the subscripts of \hat{S} increase by 4. The next $r + 1$ rows, i.e., rows $r + 1$ to $2r + 1$, are a sequence starting with \hat{S}_1 , and the subscripts increase by 4 as well. After that, the subsequent r rows are the sequence starting with a multiple of \hat{S}_3 , followed by $r + 1$ rows starting with a multiple of \hat{S}_1 , and so on and so forth. Each element in the second and higher columns maintains the same form as the elements in the first column, except that the subscripts decreasing by 1, where $\hat{S}_j \equiv 0$ for $j < 0$.

Notice that each $2r + 1$ ($= m/2$) row circulates a multiple of the sequence (84) and $N_0 \equiv N \pmod{m}$, i.e., $N = km + N_0$. Hence, we define the first $m/2$ rows of $\Phi_{N \times 4N}$ as the first block matrix, the next $m/2$ rows as the second block matrix, and so on. The first km rows consist of $2k$ blocks, and each of these blocks contains two parts. The last remaining N_0 rows are called the remaining block matrix, i.e., the $(2k + 1)$ -th block matrix.

The first round of the row operation is to use the first block to eliminate the highest power term of a_m in each subsequent block, and leaving the lower power terms of a_m . This can be achieved by multiplying each row of the first part of the first block matrix by $-a_m^2/(2n - 2)!$ and multiplying each row of the second part of the first block matrix by $-a_m^2/(2n - 1)!$ and adding them to the corresponding row of the n -th block matrix. The resulting $\Phi_{N \times 4N}$ is

$$\Phi_{N \times 4N} \sim \left[\begin{array}{ccc}
\hat{S}_3 & \hat{S}_2 & \cdots \\
\hat{S}_7 & \hat{S}_6 & \cdots \\
\vdots & \vdots & \ddots \\
\hat{S}_{m-3} & \hat{S}_{m-4} & \cdots \\
a_m \hat{S}_1 + \hat{S}_{m+1} & a_m \hat{S}_0 + \hat{S}_m & \cdots \\
a_m \hat{S}_5 + \hat{S}_{m+5} & a_m \hat{S}_4 + \hat{S}_{m+4} & \cdots \\
\vdots & \vdots & \ddots \\
a_m \hat{S}_{m-1} + \hat{S}_{2m-1} & a_m \hat{S}_{m-2} + \hat{S}_{2m-2} & \cdots \\
a_m \hat{S}_{m+3} + \hat{S}_{2m+3} & a_m \hat{S}_{m+2} + \hat{S}_{2m+2} & \cdots \\
\vdots & \vdots & \ddots \\
a_m \hat{S}_{2m-3} + \hat{S}_{3m-3} & a_m \hat{S}_{2m-4} + \hat{S}_{3m-4} & \cdots \\
\left(\frac{1}{2!} - \frac{1}{3!}\right) a_m^2 \hat{S}_{m+1} + O(a_m) & \left(\frac{1}{2!} - \frac{1}{3!}\right) a_m^2 \hat{S}_m + O(a_m) & \cdots \\
\vdots & \vdots & \ddots \\
\left(\frac{1}{2!} - \frac{1}{3!}\right) a_m^2 \hat{S}_{2m-1} + O(a_m) & \left(\frac{1}{2!} - \frac{1}{3!}\right) a_m^2 \hat{S}_{2m-2} + O(a_m) & \cdots \\
\frac{a_m^3}{3!} \hat{S}_{m+3} + \frac{a_m^2}{2!} \hat{S}_{2m+3} + O(a_m) & \frac{a_m^3}{3!} \hat{S}_{m+2} + \frac{a_m^2}{2!} \hat{S}_{2m+2} + O(a_m) & \cdots \\
\vdots & \vdots & \ddots \\
\frac{a_m^3}{3!} \hat{S}_{2m-3} + \frac{a_m^2}{2!} \hat{S}_{3m-3} + O(a_m) & \frac{a_m^3}{3!} \hat{S}_{2m-4} + \frac{a_m^2}{2!} \hat{S}_{3m-4} + O(a_m) & \cdots \\
\vdots & \vdots & \ddots
\end{array} \right]. \quad (85)$$

The second round of the row operation is to use the second block to eliminate the highest power term of a_m in each subsequent block, and leaving the lower power terms of a_m . This results in

$$\Phi_{N \times 4N} \sim \left[\begin{array}{ccc}
\hat{S}_3 & \hat{S}_2 & \cdots \\
\hat{S}_7 & \hat{S}_6 & \cdots \\
\vdots & \vdots & \ddots \\
\hat{S}_{m-3} & \hat{S}_{m-4} & \cdots \\
a_m \hat{S}_1 + \hat{S}_{m+1} & a_m \hat{S}_0 + \hat{S}_m & \cdots \\
a_m \hat{S}_5 + \hat{S}_{m+5} & a_m \hat{S}_4 + \hat{S}_{m+4} & \cdots \\
\vdots & \vdots & \ddots \\
a_m \hat{S}_{m-1} + \hat{S}_{2m-1} & a_m \hat{S}_{m-2} + \hat{S}_{2m-2} & \cdots \\
a_m \hat{S}_{m+3} + \hat{S}_{2m+3} & a_m \hat{S}_{m+2} + \hat{S}_{2m+2} & \cdots \\
\vdots & \vdots & \ddots \\
a_m \hat{S}_{2m-3} + \hat{S}_{3m-3} & a_m \hat{S}_{2m-4} + \hat{S}_{3m-4} & \cdots \\
\left(\frac{1}{2!} - \frac{1}{3!}\right) a_m^2 \hat{S}_{m+1} + O(a_m) & \left(\frac{1}{2!} - \frac{1}{3!}\right) a_m^2 \hat{S}_m + O(a_m) & \cdots \\
\vdots & \vdots & \ddots \\
\left(\frac{1}{2!} - \frac{1}{3!}\right) a_m^2 \hat{S}_{2m-1} + O(a_m) & \left(\frac{1}{2!} - \frac{1}{3!}\right) a_m^2 \hat{S}_{2m-2} + O(a_m) & \cdots \\
\left(\frac{1}{2!} - \frac{1}{3!}\right) a_m^2 \hat{S}_{2m+3} + O(a_m) & \left(\frac{1}{2!} - \frac{1}{3!}\right) a_m^2 \hat{S}_{2m+2} + O(a_m) & \cdots \\
\vdots & \vdots & \ddots \\
\left(\frac{1}{2!} - \frac{1}{3!}\right) a_m^2 \hat{S}_{3m-3} + O(a_m) & \left(\frac{1}{2!} - \frac{1}{3!}\right) a_m^2 \hat{S}_{3m-4} + O(a_m) & \cdots \\
\vdots & \vdots & \ddots
\end{array} \right]. \quad (86)$$

We can continue to perform these row operation to $\Phi_{N \times 4N}$, which have $2k$ rounds in total. Similar column operations can be applied to the matrix $\Psi_{4N \times N}$.

At the end of these operations, we arrive at the situation where the determinant (81) does not vanish

when we keep only the highest order term in a_m for each element. The difference with the previous work in [60] is that we cannot generate the lower triangular block matrix or upper triangular block matrix after keeping the highest order terms and row switchings. This indicates that the size of determinant $\tau_{\mathbf{n}}$ is unchanged. Moreover, it can be shown that $\tau_{\mathbf{n}}$ reduces to the form

$$\tau_{\mathbf{n}} = \beta_1 |a_m|^{\gamma_1} \begin{vmatrix} \mathbf{O}_{N \times N} & \hat{\Phi}_{N \times 4N} \\ -\hat{\Psi}_{4N \times N} & \mathbf{I}_{4N \times 4N} \end{vmatrix} [1 + O(a_m^{-1})], \quad (87)$$

where $\beta_1 \neq 0, \gamma_1 > 0$ are constants, and

$$\begin{aligned} \hat{\Phi} &= \begin{pmatrix} \hat{\Phi}_{N_1 \times 4N}^{(1)} \\ \hat{\Phi}_{N_3 \times 4N}^{(3)} \end{pmatrix}, \quad \hat{\Psi} = \begin{pmatrix} \hat{\Psi}_{4N \times N_1}^{(1)} & \hat{\Psi}_{4N \times N_3}^{(3)} \end{pmatrix}, \\ \hat{\Phi}_{i,j}^{(I)} &= (h_0)^{-(j-1)} S_{4i+1-I-j} [\mathbf{y}^+(\mathbf{n}) + (j-1)\mathbf{s}], \\ \hat{\Psi}_{i,j}^{(J)} &= (h_0^*)^{-(i-1)} S_{4j+1-J-i} [\mathbf{y}^-(\mathbf{n}) + (i-1)\mathbf{s}^*]. \end{aligned} \quad (88)$$

Since the rogue wave solutions are independent of the constants β_1 and γ_1 , we can rewrite (87) into a 2×2 block determinant [61]

$$\tau_{\mathbf{n}} = \det \begin{pmatrix} \tau_{\mathbf{n}}^{[1,1]} & \tau_{\mathbf{n}}^{[1,3]} \\ \tau_{\mathbf{n}}^{[3,1]} & \tau_{\mathbf{n}}^{[3,3]} \end{pmatrix} [1 + O(a_m^{-1})] \quad (89)$$

where

$$\tau_{\mathbf{n}}^{[I,J]} = \left(m_{4i-I, 4j-J}^{(\mathbf{n}, I, J)} \right)_{1 \leq i \leq N_I, 1 \leq j \leq N_J}, \quad 1 \leq I, J \leq 3, \quad (90)$$

and

$$m_{i,j}^{(\mathbf{n}, I, J)} = \sum_{v=0}^{\min(i,j)} \left[\frac{|p_1|^2}{(p_0 + p_0^*)^2} \right]^v S_{i-v}(\mathbf{y}^+(\mathbf{n}) + v\mathbf{s}) S_{j-v}(\mathbf{y}^-(\mathbf{n}) + v\mathbf{s}^*). \quad (91)$$

Note that the determinant $\tau_{\mathbf{n}}$ is still of order N , but the degree of $\tau_{\mathbf{n}}$ with respect to x or t is reduced, so this is still a lower-order rogue wave. Moreover, in this case, $\tau_{\mathbf{n}}$ in the inner region is always approximately a 2×2 block matrix regardless of the values of N and m , i.e., $N_2 = 0$ in (15). As a result of this, when $x^2 + t^2 = O(1)$ and $|a_m| \gg 1$, the determinant in (81) is approximately a $(N_1, 0, N_3)$ -th order rogue wave of the three-components NLS equation

$$[u_{1, \hat{N}_1}(x, t), \quad u_{2, \hat{N}_1}(x, t), \quad u_{3, \hat{N}_1}(x, t)]$$

where $\hat{N}_1 = (N_1, 0, N_3)$, u_{j, \hat{N}_1} ($j = 1, 2, 3$) is given in Theorem 2.2 with $N_j = N_{j,3}$, and the internal parameters

$$(\hat{a}_{1,n}, \hat{a}_{2,n}, \hat{a}_{3,n}, \hat{a}_{5,n}, \hat{a}_{6,n} \dots, \hat{a}_{4N_{n,3}-n,n}), \quad n = 1, 3,$$

are related to those in the original rogue wave as

$$\hat{a}_{j,1} = \hat{a}_{j,3} = a_j, \quad j = 1, 2, 3, 5, 6, 7 \dots, m-1, m+1, \dots$$

and

$$\hat{a}_{m,1} = \hat{a}_{m,3} = 0.$$

From (89), we deduce that the approximation error of this lower-order rogue wave is $O(|a_m|^{-1})$.

Next, we consider the case $m \equiv 1 \pmod{4}$, i.e., $m = 4r + 1$ ($r > 1$). Notice that the coefficients of the highest a_m power terms in the first column of $\Psi_{N \times 4N}$ are proportional to

$$\hat{S}_3, \hat{S}_7, \dots, \hat{S}_{4r-1}, \hat{S}_2, \hat{S}_6, \dots, \hat{S}_{4r-2}, \hat{S}_1, \hat{S}_5, \dots, \hat{S}_{4r-3}, \hat{S}_0, \hat{S}_4, \dots, \hat{S}_{4r}$$

and repeating. Similar to the previous case, we can think of the first m rows as the first block matrix of $\Phi_{N \times 4N}$, the next m rows as the second block matrix, and so on. On account of $N = km + N_0$, the remaining N_0 rows are called the remaining block matrix, i.e., the $(k+1)$ -th block matrix. Each block matrix can be divided into four parts, for example, the first column of these four parts are sequences starting with $\hat{S}_3, \hat{S}_2, \hat{S}_1$ and \hat{S}_0 respectively.

Then, using similar argument as in [59], we arrive at the situation where the determinant (81) does not vanish when we keep only the highest order term in a_m for each element. In this case, after row and column swapping, upper and lower triangular block matrices will be generated. After expanding these block matrices, $\tau_{\mathbf{n}}$ reduces to the form

$$\tau_{\mathbf{n}} = \beta_2 |a_m|^{\gamma_2} \begin{vmatrix} \mathbf{O}_{\bar{N}_3 \times \bar{N}_3} & \widehat{\Phi}_{\bar{N}_3 \times \hat{N}} \\ -\widehat{\Psi}_{\hat{N} \times \bar{N}_3} & \mathbf{I}_{\hat{N} \times \hat{N}} \end{vmatrix} [1 + O(a_m^{-1})], \quad (92)$$

where $\beta_2 \neq 0, \gamma_2 > 0$ are constants, $\bar{N}_3 = \sum_{n=1}^3 N_{n,3}$, $\hat{N} = \max_{1 \leq i \leq 3} (4N_{i,3} - i + 1)$,

$$\widehat{\Phi} = \begin{pmatrix} \widehat{\Phi}_{N_{1,3} \times \hat{N}}^{(1)} \\ \widehat{\Phi}_{N_{2,3} \times \hat{N}}^{(2)} \\ \widehat{\Phi}_{N_{3,3} \times \hat{N}}^{(3)} \end{pmatrix}, \quad \widehat{\Psi} = \begin{pmatrix} \widehat{\Psi}_{\hat{N} \times N_{1,3}}^{(1)} & \widehat{\Psi}_{\hat{N} \times N_{2,3}}^{(2)} & \widehat{\Psi}_{\hat{N} \times N_{3,3}}^{(3)} \end{pmatrix} \quad (93)$$

$$\widehat{\Phi}_{i,j}^{(I)} = (h_0)^{-(j-1)} S_{4i+1-I-j} [\mathbf{y}^+(\mathbf{n}) + (j-1 + \nu_0) \mathbf{s}]$$

$$\widehat{\Psi}_{i,j}^{(J)} = (h_0^*)^{-(i-1)} S_{4j+1-J-i} [\mathbf{y}^-(\mathbf{n}) + (i-1 + \nu_0) \mathbf{s}^*]$$

and $\nu_0 = N - \bar{N}_1$. Finally, using similar argument as in [61], we find that $\tau_{\mathbf{n}}$ can be asymptotically reduced to a $(N_{1,3}, N_{2,3}, N_{3,3})$ -th order rogue wave of the three-components NLS equation in the inner region. Notice that the internal parameters

$$(\hat{a}_{1,n}, \hat{a}_{2,n}, \hat{a}_{3,n}, \hat{a}_{5,n}, \hat{a}_{6,n} \dots, \hat{a}_{4N_{n,3}-n,n}), \quad n = 1, 2, 3,$$

are related to those in the original rogue wave as

$$\hat{a}_{j,1} = \hat{a}_{j,2} = \hat{a}_{j,3} = a_j + (N - \bar{N}_3) s_j, \quad j = 1, 2, 3, 5, 6, 7 \dots$$

As pointed before, the proofs of our 1st type and 3rd type rogue waves of the three-component NLS are very similar, so we omit the proof of 3rd type. However, there are some differences in the proof of 2nd type rogue waves in the inner region. This is explained as follows.

We rewrite the determinant $\tau_{\mathbf{n}}$ as a $5N \times 5N$ determinant as in (81). Note that $m \equiv j \pmod{4}, j = 1, 2, 3$, and the different case is still $j = 2$, i.e., $m = 4r + 2 (r \geq 0)$. In this case, we can substitute (83) into (81) to expand each element into a polynomial in a_m . Similar to the proof of 1st type, we can rewrite $\Phi_{N \times 4N}$ as follows

$$\Phi_{N \times 4N} \sim \begin{bmatrix} \hat{S}_2 & \hat{S}_1 & \cdots \\ \hat{S}_6 & \hat{S}_5 & \cdots \\ \vdots & \vdots & \ddots \\ \hat{S}_{m-4} & \hat{S}_{m-5} & \cdots \\ a_m \hat{S}_0 + \hat{S}_m & \hat{S}_{m-1} & \cdots \\ a_m \hat{S}_4 + \hat{S}_{m+4} & a_m \hat{S}_3 + \hat{S}_{m+3} & \cdots \\ \vdots & \vdots & \ddots \\ a_m \hat{S}_{m-2} + \hat{S}_{2m-2} & a_m \hat{S}_{m-3} + \hat{S}_{2m-3} & \cdots \\ \frac{a_m^2}{2!} \hat{S}_2 + a_m \hat{S}_{m+2} + \hat{S}_{2m+2} & \frac{a_m^2}{2!} \hat{S}_1 + a_m \hat{S}_{m+1} + \hat{S}_{2m+1} & \cdots \\ \vdots & \vdots & \ddots \\ \frac{a_m^2}{2!} \hat{S}_{m-4} + a_m \hat{S}_{2m-4} + \hat{S}_{3m-4} & \frac{a_m^2}{2!} \hat{S}_{m-5} + a_m \hat{S}_{2m-5} + \hat{S}_{3m-5} & \cdots \\ \frac{a_m^3}{3!} \hat{S}_0 + \frac{a_m^2}{2!} \hat{S}_m + O(a_m) & \frac{a_m^2}{2!} \hat{S}_{m-1} + O(a_m) & \cdots \\ \vdots & \vdots & \ddots \\ \frac{a_m^3}{3!} \hat{S}_{m-2} + \frac{a_m^2}{2!} \hat{S}_{2m-2} + O(a_m) & \frac{a_m^3}{3!} \hat{S}_{m-3} + \frac{a_m^2}{2!} \hat{S}_{2m-3} + O(a_m) & \cdots \\ \vdots & \vdots & \ddots \end{bmatrix}. \quad (94)$$

It can be seen that the matrix $\Phi_{N \times 4N}$ can be divided into a number of blocks. We use the same method as before, that is, we use the preceding blocks to eliminate the highest-order terms in a_m of the subsequent blocks in turn. After the above operations, we find that only the coefficient of the highest-power term in $(r+1)$ -th row is \hat{S}_0 . This inspires us to eliminate one row and one column through some operations.

We first keep only the highest remaining power of a_m in the $(r+1)$ -th row of $\Phi_{N \times 4N}$. Then, from the original determinant $\tau_{\mathbf{n}}$, we can expand it according to the $(r+1)$ -th row, and obtain

$$\Phi_{N \times 4N} \sim \begin{bmatrix} \hat{S}_1 & \hat{S}_0 & \cdots \\ \hat{S}_5 & \hat{S}_4 & \cdots \\ \vdots & \vdots & \ddots \\ \hat{S}_{m-5} & \hat{S}_{m-6} & \cdots \\ a_m \hat{S}_3 + \hat{S}_{m+3} & a_m \hat{S}_2 + \hat{S}_{m+2} & \cdots \\ \vdots & \vdots & \ddots \\ a_m \hat{S}_{m-3} + \hat{S}_{2m-2} & a_m \hat{S}_{m-4} + \hat{S}_{2m-3} & \cdots \\ a_m \hat{S}_{m+1} + \hat{S}_{2m+1} & a_m \hat{S}_m + \hat{S}_{2m} & \cdots \\ \vdots & \vdots & \ddots \\ a_m \hat{S}_{2m-5} + \hat{S}_{3m-5} & a_m \hat{S}_{2m-6} + \hat{S}_{3m-6} & \cdots \\ \left(\frac{1}{2!} - \frac{1}{3!}\right) a_m^2 \hat{S}_{m-1} + O(a_m) & \left(\frac{1}{2!} - \frac{1}{3!}\right) a_m^2 \hat{S}_{m-2} + O(a_m) & \cdots \\ \vdots & \vdots & \ddots \\ \left(\frac{1}{2!} - \frac{1}{3!}\right) a_m^2 \hat{S}_{2m-3} + O(a_m) & \left(\frac{1}{2!} - \frac{1}{3!}\right) a_m^2 \hat{S}_{2m-4} + O(a_m) & \cdots \\ \vdots & \vdots & \ddots \end{bmatrix}. \quad (95)$$

Similar treatment can be applied to the matrix $\Psi_{4N \times N}$. It can be observed that we have a similar situation to the inner region of 1st type rogue wave with $m = 4r + 2$. Finally, we can rewrite (87) into a 2×2 block determinant

$$\tau_{\mathbf{n}} = \det \begin{pmatrix} \tau_{\mathbf{n}}^{[1,1]} & \tau_{\mathbf{n}}^{[1,3]} \\ \tau_{\mathbf{n}}^{[3,1]} & \tau_{\mathbf{n}}^{[3,3]} \end{pmatrix} [1 + O(a_m^{-1})] \quad (96)$$

where

$$\tau_{\mathbf{n}}^{[I,J]} = \left(m_{4i-I, 4j-J}^{(\mathbf{n}, I, J)} \right)_{1 \leq i \leq N_I, 1 \leq j \leq N_J}, \quad 1 \leq I, J \leq 3, \quad (97)$$

and

$$m_{i,j}^{(\mathbf{n}, I, J)} = \sum_{v=0}^{\min(i,j)} \left[\frac{|p_1|^2}{(p_0 + p_0^*)^2} \right]^v S_{i-v}(\mathbf{x}_I^+(\mathbf{n}) + v\mathbf{s}) S_{j-v}(\mathbf{x}_J^-(\mathbf{n}) + v\mathbf{s}^*). \quad (98)$$

Note that the determinant $\tau_{\mathbf{n}}$ is always $(N-1) \times (N-1)$ and $\tau_{\mathbf{n}}$ in the inner region is always approximately a 2×2 block matrix regardless of the values of N and m , i.e., $N_2 = 0$ in (15). Moreover, we remark that the internal parameters

$$(\hat{a}_{1,n}, \hat{a}_{2,n}, \hat{a}_{3,n}, \hat{a}_{5,n}, \hat{a}_{6,n} \dots, \hat{a}_{4N_n, 2-n, n}), \quad n = 1, 3,$$

are related to those in the original rogue wave as

$$\hat{a}_{j,1} = \hat{a}_{j,3} = a_j + s_j, \quad j = 1, 2, 3, 5, 6, 7 \dots, m-1, m+1, \dots$$

and

$$\hat{a}_{m,1} = \hat{a}_{m,3} = s_m.$$

This completes the proof of Theorem 3.1 for the inner region.

Proof of Theorem 3.2. Since the proofs are similar for different $i \in \{1, 2, 3, 4\}$, it suffices to present the proof for $i = 1$.

Assume $|a_m|$ is large and other parameters are $O(1)$. We first consider the situation when (x, t) is

located in the outer region, i.e., $\sqrt{x^2 + t^2} = O(|a_m|^{1/m})$. Since the proof is very similar to Theorem 3.1, we only show the differences.

To begin with, we have

$$S_j(\mathbf{x}^+(\mathbf{n}) + \nu \mathbf{s}) = S_j(x_1^+, x_2^+, x_3^+, x_4^+, \nu s_5, x_6^+, x_7^+, x_8^+, x_9^+, \nu s_{10}, \dots, x_m^+ + \nu s_m, \dots) \sim S_j(\mathbf{v}), \quad (99)$$

where

$$\mathbf{v} = (p_0 x + 2p_0 p_1 i t, 0, \dots, 0, a_m, 0, \dots). \quad (100)$$

This relation is the same as (62), but the values of p_0 and p_1 are different from the three-component NLS equation. Then, after some calculations similar to the proof of Theorem 3.1, we find that the highest order term in a_m for $\tau_{\mathbf{n}}$ is

$$\tau_{\mathbf{n}} \sim |\alpha|^2 |a_m|^{4N(N+1)/m} \left| W_N^{[m,5,4]}(z) \right|^2, \quad (101)$$

where

$$\alpha = h_0^{N(N-1)/2} (c_N^{[m,5,4]})^{-1}, \quad h_0 = p_1 / (p_0 + p_0^*), \quad z = a_m^{-1/m} (p_0 x + 2p_0 p_1 i t).$$

Note that the order of a_m is changed from $3N(N+1)/m$ in the three-component case to $4N(N+1)/m$. Thus, the solutions

$$u_{1, \mathcal{N}_1}(x, t), \quad u_{2, \mathcal{N}_1}(x, t), \quad u_{3, \mathcal{N}_1}(x, t), \quad u_{4, \mathcal{N}_1}(x, t)$$

are the plane-wave backgrounds, except at or near $(\tilde{x}_0, \tilde{t}_0)$, where

$$z_0 = a_m^{-1/m} (p_0 \tilde{x}_0 + 2p_0 p_1 i \tilde{t}_0) \quad (102)$$

is a root of $W_N^{[m,5,4]}(z)$.

In what follows, we show that, when (x, t) is contained in a small neighborhood of $(\tilde{x}_0, \tilde{t}_0)$ given by (102), the underlying rogue wave is approximately a fundamental rogue wave. Denote by

$$\hat{x}_2^+(x, t) = p_2 x + (2p_0 p_2 + p_1^2)(it),$$

which contains the dominant terms of $x_2^+(x, t)$ in (11) with the index 'I' removed. Then, for (x, t) in the neighborhood of $(\tilde{x}_0, \tilde{t}_0)$, we have a more refined asymptotics for $S_j(\mathbf{x}^+(\mathbf{n}) + \nu \mathbf{s})$

$$S_j(\mathbf{x}^+(\mathbf{n}) + \nu \mathbf{s}) = [S_j(\hat{\mathbf{v}}) + \hat{x}_2^+(\tilde{x}_0, \tilde{t}_0) S_{j-2}(\hat{\mathbf{v}})] \left[1 + O\left(a_m^{-2/m}\right) \right], \quad |a_m| \gg 1, \quad (103)$$

where

$$\hat{\mathbf{v}} = (p_0 x + 2p_0 p_1 i t + n_1 \theta_{11} + n_2 \theta_{12} + n_3 \theta_{13} + n_4 \theta_{14}, 0, \dots, 0, a_m, 0, \dots). \quad (104)$$

Here, the normalization of $a_1 = 0$ has been utilized. Next, we rewrite $\tau_{\mathbf{n}}$ in a similar form as (67) by means of Laplace expansion. Further, the contribution from the first index choice of $\nu_j = j - 1$ can be expressed as

$$\alpha a_m^{\frac{2N(N+1)-1}{m}} \left[p_0 (x - \tilde{x}_0) + 2p_0 p_1 i (t - \tilde{t}_0) + \sum_{k=1}^4 n_k \theta_{1k} + \bar{\Delta}_1 \right] \left[W_N^{[m,5,4]}'(z_0) \left[1 + O\left(a_m^{-1/m}\right) \right] \right] \quad (105)$$

where

$$\bar{\Delta}_1 = \frac{\hat{x}_2^+(\tilde{x}_0, \tilde{t}_0) \sum_{j=1}^N \det_{1 \leq i \leq N} \left[p_{5i-1}^{[m]}(z_0), \dots, p_{5i-j-2}^{[m]}(z_0), \dots, p_{5i-N}^{[m]}(z_0) \right]}{a_m^{1/m} \left[W_N^{[m,5,4]}'(z_0) \right]} \quad (106)$$

and $\bar{\Delta}_1 = O(1)$ as $\hat{x}_2^+(\tilde{x}_0, \tilde{t}_0) = O\left(|a_m^{1/m}\right|$. By absorbing $\bar{\Delta}_1$ into $(\tilde{x}_0, \tilde{t}_0)$ [28], we obtain

$$\alpha a_m^{\frac{2N(N+1)-1}{m}} \left[p_0 (x - \bar{x}_0) + 2p_0 p_1 i (t - \bar{t}_0) + \sum_{k=1}^4 n_k \theta_{1k} \right] \left[W_N^{[m,5,4]}'(z_0) \left[1 + O\left(a_m^{-1/m}\right) \right] \right]. \quad (107)$$

where \bar{x}_0 and \bar{t}_0 are given in Theorem 3.2.

For the second index choice, i.e., $\nu = (0, 1, \dots, N-2, N)$, the dominant terms in a_m can be calculated

in a similar way as (76), that is,

$$h_0^{\frac{N(N-1)+2}{2}} a_m^{\frac{2N(N+1)-1}{m}} \det_{1 \leq i \leq N} \left[p_{5i-1}^{[m]}(z_0), p_{5i-2}^{[m]}(z_0), \dots, p_{5i-(N-1)}^{[m]}(z_0), p_{5i-N-1}^{[m]}(z_0) \right] \left[1 + O\left(a_m^{-1/m}\right) \right]. \quad (108)$$

Since $p_{j-1}^{[m]}(z) = \left[p_j^{[m]} \right]'(z)$, the above term can be expressed as

$$h_0 \alpha a_m^{\frac{2N(N+1)-1}{m}} \left[W_N^{[m,5,4]} \right]'(z_0) \left[1 + O\left(a_m^{-1/m}\right) \right]. \quad (109)$$

Summarizing the above two contributions, we conclude that

$$\tau_{\mathbf{n}}(x, t) \quad (110)$$

$$= |\alpha|^2 \left| \left[W_N^{[m,5,4]} \right]'(z_0) \right|^2 |a_m|^{\frac{2N(N+1)-1}{m}} \times \left([p_1(x - \bar{x}_0) + 2ip_0 p_1(t - \bar{t}_0) + n_1 \theta_{11} + n_2 \theta_{12} + n_3 \theta_{13} + n_4 \theta_{14}] \right. \\ \left. [p_1^*(x - \bar{x}_0) - 2ip_0^* p_1^*(t - \bar{t}_0) - n_1 \theta_{11}^* - n_2 \theta_{12}^* - n_3 \theta_{13}^* - n_4 \theta_{14}^*] + |h_0|^2 \right) \times \left[1 + O\left(a_m^{-1/m}\right) \right]. \quad (111)$$

Thus, the proof for outer region is completed.

In order to study the patterns of the 1st type rogue waves of the four-component NLS rogue waves under the condition $|a_m| \gg 1$ in the inner region with $x^2 + t^2 = O(1)$, we first rewrite the determinant $\tau_{\mathbf{n}}$ as a $6N \times 6N$ determinant

$$\tau_{\mathbf{n}} = \begin{vmatrix} \mathbf{O}_{N \times N} & \Phi_{N \times 5N} \\ -\Psi_{5N \times N} & \mathbf{I}_{5N \times 5N} \end{vmatrix}, \quad (112)$$

where

$$\Phi_{i,j} = \left(\frac{p_1}{p_0 + p_0^*} \right)^{j-1} S_{5i-j} [\mathbf{x}^+(\mathbf{n}) + (j-1)\mathbf{s}], \quad \Psi_{i,j} = \left(\frac{p_1^*}{p_0 + p_0^*} \right)^{i-1} S_{5j-i} [\mathbf{x}^-(\mathbf{n}) + (i-1)\mathbf{s}^*].$$

Then, we can apply (82) and (83) to express each element in (112) into a polynomial in a_m explicitly. Notice that have totally four cases to consider, i.e., $m \equiv j \pmod{5}$, $j = 1, 2, 3, 4$. Since the proofs for all cases are similar, it suffices to provide the proof for $j = 1$. To determine the highest order term in a_m of $\tau_{\mathbf{n}}$, we can use similar argument as that in [60, 62] to perform row and column operations. After these operations, $\tau_{\mathbf{n}}$ can be reduced to the form

$$\tau_{\mathbf{n}} = \beta |a_m|^\gamma \begin{vmatrix} \mathbf{O}_{\bar{N}_4 \times \bar{N}_4} & \hat{\Phi}_{\bar{N}_4 \times \hat{N}} \\ -\hat{\Psi}_{\hat{N} \times \bar{N}_4} & \mathbf{I}_{\hat{N} \times \hat{N}} \end{vmatrix} \left[1 + O\left(a_m^{-1}\right) \right], \quad (113)$$

where $\beta \neq 0, \gamma > 0$ are constants, $\bar{N}_4 = \sum_{n=1}^4 N_{n,4}$, $\hat{N} = \max_{1 \leq i \leq 4} (5N_{i,4} - i + 1)$,

$$\hat{\Phi} = \begin{pmatrix} \hat{\Phi}_{N_{1,4} \times \hat{N}}^{(1)} \\ \hat{\Phi}_{N_{2,4} \times \hat{N}}^{(2)} \\ \hat{\Phi}_{N_{3,4} \times \hat{N}}^{(3)} \\ \hat{\Phi}_{N_{4,4} \times \hat{N}}^{(4)} \end{pmatrix}, \quad \hat{\Psi} = \begin{pmatrix} \hat{\Psi}_{\hat{N} \times N_{1,4}}^{(1)} & \hat{\Psi}_{\hat{N} \times N_{2,4}}^{(2)} & \hat{\Psi}_{\hat{N} \times N_{3,4}}^{(3)} & \hat{\Psi}_{\hat{N} \times N_{4,4}}^{(4)} \end{pmatrix} \quad (114)$$

$$\hat{\Phi}_{i,j}^{(I)} = (h_0)^{-(j-1)} S_{5i-I} [\mathbf{y}^+(\mathbf{n}) + (j-1 + \nu_0)\mathbf{s}]$$

$$\hat{\Psi}_{i,j}^{(J)} = (h_0^*)^{-(i-1)} S_{5j-J} [\mathbf{y}^-(\mathbf{n}) + (i-1 + \nu_0)\mathbf{s}^*]$$

and $\nu_0 = N - \bar{N}_4$. Since the rogue wave solutions are independent of the constants β and γ , we can rewrite (113) into a 4×4 block determinant

$$\tau_{\mathbf{n}} = \det \begin{pmatrix} \tau_{\mathbf{n}}^{[1,1]} & \tau_{\mathbf{n}}^{[1,2]} & \tau_{\mathbf{n}}^{[1,3]} & \tau_{\mathbf{n}}^{[1,4]} \\ \tau_{\mathbf{n}}^{[2,1]} & \tau_{\mathbf{n}}^{[2,2]} & \tau_{\mathbf{n}}^{[2,3]} & \tau_{\mathbf{n}}^{[2,4]} \\ \tau_{\mathbf{n}}^{[3,1]} & \tau_{\mathbf{n}}^{[3,2]} & \tau_{\mathbf{n}}^{[3,3]} & \tau_{\mathbf{n}}^{[3,4]} \\ \tau_{\mathbf{n}}^{[4,1]} & \tau_{\mathbf{n}}^{[4,2]} & \tau_{\mathbf{n}}^{[4,3]} & \tau_{\mathbf{n}}^{[4,4]} \end{pmatrix} \left[1 + O\left(a_m^{-1}\right) \right] \quad (115)$$

where

$$\tau_{\mathbf{n}}^{[I,J]} = \left(m_{5i-I, 5j-J}^{(\mathbf{n}, I, J)} \right)_{1 \leq i \leq N_{I,4}, 1 \leq j \leq N_{J,4}} \quad (116)$$

and

$$m_{i,j}^{(\mathbf{n}, I, J)} = \sum_{\nu=0}^{\min(i,j)} \left[\frac{|p_1|^2}{(p_0 + p_0^*)^2} \right]^{\nu} S_{i-\nu}(\mathbf{y}^+(\mathbf{n}) + \nu_0 \mathbf{s} + \nu \mathbf{s}) S_{j-\nu}(\mathbf{y}^-(\mathbf{n}) + \nu_0 \mathbf{s}^* + \nu \mathbf{s}^*). \quad (117)$$

Finally, the determinant in (115) becomes a $(N_{1,4}, N_{2,4}, N_{3,4}, N_{4,4})$ -th order rogue wave of the four-components NLS equation, and the internal parameters

$$(\bar{a}_{1,n}, \bar{a}_{2,n}, \bar{a}_{3,n}, \bar{a}_{4,n}, \bar{a}_{6,n} \dots, \bar{a}_{5N_{n,4}-n,n}), \quad n = 1, 2, 3, 4,$$

are related to those in the original rogue wave as

$$\bar{a}_{j,1} = \bar{a}_{j,2} = \bar{a}_{j,3} = \bar{a}_{j,4} = a_j + (N - \bar{N}_4) s_j, \quad j = 1, 2, 3, 4, 6, 7 \dots$$

From (115), we deduce that the approximation error of this lower-order rogue wave is $O(|a_m|^{-1})$. This completes the proof of Theorem 3.2 for the inner region.

6 Conclusion

In summary, we have constructed rogue waves of the vector (or M -component) NLS equation (1) and analyzed their patterns for $M = 3, 4$. These solutions are expressed in terms of Gram-type determinants of $K \times K$ block matrices ($K = 1, 2, \dots, M$) with index jumps of $M + 1$ via Kadomtsev-Petviashvili hierarchy reduction technique. One crucial step in this process is solving a system of algebraic equations (see Lemma 2.1 and its proof). The rogue wave patterns corresponding to $M = 3, 4$ and $K = 1$ have been investigated comprehensively. We find that when specific internal parameters are large enough, these patterns are described by new polynomial hierarchies, i.e., the generalized Wronskian-Hermite polynomials, in contrast with the scalar NLS equation and the Manakov system. Since the Yablonskii-Vorob'ev polynomial hierarchy and Okamoto polynomial hierarchies are special cases of the generalized Wronskian-Hermite polynomials, our results have unified rogue wave patterns of the scalar NLS equation and the vector NLS equation for $M = 2, 3, 4$. It is worth noting that the case $M = 3$ presents a unique feature as, in certain cases, the sizes of the Gram-type determinants cannot be reduced in the approximation of inner regions.

The rogue wave patterns for $M = 3, 4$ exhibit very rich structures similar to the Manakov system [62], these patterns are, in general, distorted from root structures of the generalized Wronskian-Hermite polynomials. The predicted rogue wave patterns have been compared with true solutions, and excellent agreement is achieved. As pointed out in [58, 62], universal rogue wave patterns, which depend on the index jumps, exist in integrable systems. We expect that the patterns uncovered in the present paper will appear in many other systems and thus are universal, as long as the corresponding Schur polynomials have index jumps of 4 or 5.

Acknowledgements

B.F. Feng was partially supported by National Science Foundation (NSF) under Grant No. DMS-1715991 and U.S. Department of Defense (DoD), Air Force for Scientific Research (AFOSR) under grant No. W911NF2010276. C.F. Wu was supported by the National Natural Science Foundation of China (Grant Nos. 11701382 and 11971288) and Guangdong Basic and Applied Basic Research Foundation, China (Grant No. 2021A1515010054). We would like to thank Mr. Yuke Wang for drawing some of the figures.

Appendix A

In this appendix, we provide the proof of Lemma 2.1. Assume ξ is a root of $\mathcal{R}_M(z) = 0$ of multiplicity M with $\Im(\xi) \neq 0$, then we have

$$\mathcal{R}_M^{(n)}(\xi) = 0, \quad n = 0, 1, 2, \dots, M - 1, \quad (118)$$

where

$$\mathcal{R}_M^{(m)}(\xi) = (-1)^m (m+1)! \sum_{j=1}^M \frac{r_j}{(\xi + k_j)^{m+2}}, \quad m \geq 1.$$

The system of equations (118) is linear in r_j , $j = 1, 2, \dots, M$, so we can solve for them and obtain

$$(\xi + k_j)^{M+1} = -\frac{1}{2} \prod_{\substack{i=1 \\ i \neq j}}^M (k_j - k_i) r_j. \quad (119)$$

Denote by

$$\xi = x + iy, \quad -\frac{1}{2} \prod_{\substack{i=1 \\ i \neq j}}^M (k_j - k_i) r_j = \lambda_j^{M+1} \exp(i\theta_j \pi), \quad j = 1, 2, \dots, M, \quad (120)$$

where $\lambda_j > 0$, x, y are real, $y \neq 0$ and

$$\theta_j = \begin{cases} 0, & \text{if } -\frac{1}{2} \prod_{\substack{i=1 \\ i \neq j}}^M (k_j - k_i) r_j > 0, \\ 1, & \text{if } -\frac{1}{2} \prod_{\substack{i=1 \\ i \neq j}}^M (k_j - k_i) r_j < 0, \end{cases} \quad (121)$$

then we deduce from (119) that, for each k_j , there exists $l_j \in \{0, 1, \dots, M\}$ such that

$$x + k_j + iy = \begin{cases} \lambda_j \exp[2l_j \pi i / (M+1)], & \text{if } \theta_j = 0, \\ \lambda_j \exp[(2l_j + 1) \pi i / (M+1)], & \text{if } \theta_j = 1, \end{cases} \quad (122)$$

Comparing both sides of (122) gives

$$y = \begin{cases} \lambda_j \sin[2l_j \pi / (M+1)], & \text{if } \theta_j = 0, \\ \lambda_j \sin[(2l_j + 1) \pi / (M+1)], & \text{if } \theta_j = 1. \end{cases} \quad (123)$$

This implies that all the corresponding $\sin[2l_j \pi / (M+1)]$ or $\sin[(2l_j + 1) \pi / (M+1)]$, $j = 1, 2, \dots, M$, should have the same sign. Without loss of generality, we may assume $y > 0$. Note that the set

$$\{1, \exp[\pi i / (M+1)], \exp[2\pi i / (M+1)], \dots, \exp[2M\pi i / (M+1)], \exp[(2M+1)\pi i / (M+1)]\} \quad (124)$$

contains exactly M elements with positive imaginary parts, which are

$$\exp[\pi i / (M+1)], \quad \exp[2\pi i / (M+1)], \dots, \quad \exp[M\pi i / (M+1)]. \quad (125)$$

Since the k_j 's are distinct, it then follows that

$$x + k_j + iy = \lambda_j \exp[\sigma_j \pi i / (M+1)] \quad (126)$$

where $(\sigma_1, \sigma_2, \dots, \sigma_M)$ can be any permutation of the set $\{1, 2, \dots, M\}$. Without loss of generality, we may take

$$\sigma_j = j, \quad (127)$$

where $j = 1, 2, \dots, M$. In this circumstance, we have $\theta_j = [1 + (-1)^{j+1}] / 2$ and

$$x = \lambda_j \cos[j\pi / (M+1)] - k_j, \quad (128)$$

$$y = \lambda_j \sin[j\pi / (M+1)], \quad (129)$$

and hence

$$\lambda_j = \lambda_1 \frac{\sin[\pi / (M+1)]}{\sin[j\pi / (M+1)]}, \quad (130)$$

$$k_j = k_1 + \lambda_j \cos[j\pi / (M+1)] - \lambda_1 \cos[\pi / (M+1)], \quad (131)$$

$$= k_1 + \lambda_1 (\sin[\pi / (M+1)] \cot[j\pi / (M+1)] - \cos[\pi / (M+1)]) \quad (132)$$

where $j = 1, 2, \dots, M$. Further, we find from (120) and (130) that

$$r_j = 2(-1)^{j+1} \prod_{\substack{i=1 \\ i \neq j}}^M (k_j - k_i)^{-1} \left(\lambda_1 \frac{\sin[\pi/(M+1)]}{\sin[j\pi/(M+1)]} \right)^{M+1}. \quad (133)$$

As $\mathcal{R}_M(z)$ is a rational function with real coefficients, it is clear that ξ^* is a root of $\mathcal{R}_M(z) = 0$ of multiplicity M as well. This completes the proof.

Appendix B

In this appendix, we apply Hirota's bilinear method to derive rogue wave solutions of the vector NLS equation (1) presented in Theorem 2.2 based on the KP reduction technique. For convenience, we only consider the case when $\tau_{\mathbf{n}}$ given in (17) consists of $M \times M$ block matrices, i.e., $K = M$, as other cases can be treated in a similar manner. In such case, we have $I_j = j$ ($j = 1, 2, \dots, M$) in (17).

We first transform the vector NLS equation (1) into a set of bilinear equations

$$\begin{aligned} \left(D_x^2 + \sum_{j=1}^M \sigma_j \rho_j^2 \right) f \cdot f &= \sum_{j=1}^M \sigma_j \rho_j^2 g_j g_j^*, \\ (\mathrm{i}D_t + D_x^2 + 2\mathrm{i}k_j D_x) g_j \cdot f &= 0, \quad j = 1, 2, \dots, M, \end{aligned} \quad (134)$$

under the non-zero boundary condition at $\pm\infty$ by the variable transformation

$$u_j = \rho_j \frac{g_j}{f} e^{\mathrm{i}(k_j x + w_j t)}, \quad j = 1, 2, \dots, M, \quad (135)$$

where $w_j = \sum_{j=1}^M \sigma_j \rho_j^2 - k_j^2$, f is a real-valued function, g_j is a complex-valued function, and D is the Hirota's bilinear operator [33] defined by

$$D_x^m D_t^n f \cdot g = \left(\frac{\partial}{\partial x} - \frac{\partial}{\partial x'} \right)^m \left(\frac{\partial}{\partial t} - \frac{\partial}{\partial t'} \right)^n [f(x, t) g(x', t')] \Big|_{x'=x, t'=t}.$$

Next we define

$$\begin{aligned} m^{\mathbf{n}} &= \frac{1}{p+q} \sum_{j=1}^M \left(-\frac{p - \mathrm{i}k_j}{q + \mathrm{i}k_j} \right)^{n_j} e^{\xi + \eta}, \\ \xi &= px + p^2 y + \sum_{j=1}^M \frac{1}{p - \mathrm{i}k_j} v_j + \xi_0(p), \\ \eta &= qx - q^2 y + \sum_{j=1}^M \frac{1}{q + \mathrm{i}k_j} v_j + \eta_0(q), \end{aligned}$$

where $\mathbf{n} = (n_1, n_2, \dots, n_M)$ with n_j being integers, p, q, v_j are arbitrary complex constants, $j = 1, 2, \dots, M$, and $\xi_0(p), \eta_0(q)$ are arbitrary functions of p and q respectively. Let \mathcal{A}_i and \mathcal{B}_j be differential operators of order i and j , respectively, defined by

$$\mathcal{A}_i(p) = \frac{1}{i!} [f_1(p) \partial_p]^i, \quad \mathcal{B}_j(q) = \frac{1}{j!} [f_2(q) \partial_q]^j,$$

where $f_1(p), f_2(q)$ are arbitrary functions of p and q respectively. Then it can be calculated that [45] the determinant

$$\tau_{\mathbf{n}} = \det_{1 \leq \nu, \mu \leq N} \left(m_{i_\nu, j_\mu}^{\mathbf{n}} \right)$$

where (i_1, i_2, \dots, i_N) and (j_1, j_2, \dots, j_N) are arbitrary sequences of indices, and the matrix element $m_{ij}^{\mathbf{n}}$ is defined as

$$m_{ij}^{\mathbf{n}} = \mathcal{A}_i \mathcal{B}_j m^{\mathbf{n}}, \quad (136)$$

would satisfy the bilinear equations

$$\begin{aligned} \left(\frac{1}{2}D_x D_{v_j} - 1\right) \tau_{\mathbf{n}} \cdot \tau_{\mathbf{n}} &= -\tau_{\mathbf{n}_{j,1}} \tau_{\mathbf{n}_{j,-1}}, \quad j = 1, 2, \dots, M, \\ (D_x^2 - D_y + 2ik_j D_x) \tau_{\mathbf{n}_{j,1}} \cdot \tau_{\mathbf{n}} &= 0, \quad j = 1, 2, \dots, M, \end{aligned} \quad (137)$$

where

$$\mathbf{n}_{j,i} = \mathbf{n} + i \times \mathbf{n}_j, \quad \mathbf{n}_j = \sum_{l=1}^M \delta_{jl} \mathbf{e}_l,$$

\mathbf{e}_l is the standard unit vector in \mathbb{R}^M and δ_{jl} is the Kronecker delta.

In what follows, we will establish the reductions from the bilinear equations (137) in the KP hierarchy to the bilinear equations (134), thereby obtaining rogue wave solutions of the vector NLS equation (1). This procedure consists of several steps.

i) *Dimension reduction*

Note that

$$\left(2\partial_x + \sum_{k=1}^M \sigma_k \rho_k^2 \partial_{v_k}\right) m_{ij}^{\mathbf{n}} = \mathcal{A}_i \mathcal{B}_j [\mathcal{G}_M(p) + \mathcal{H}_M(q)] m^{\mathbf{n}}, \quad (138)$$

where

$$\mathcal{G}_M(p) = \sum_{j=1}^M \frac{\sigma_j \rho_j^2}{p - ik_j} + 2p, \quad \mathcal{H}_M(q) = \sum_{j=1}^M \frac{\sigma_j \rho_j^2}{q + ik_j} + 2q. \quad (139)$$

This implies that

$$\left(2\partial_x + \sum_{k=1}^M \sigma_k \rho_k^2 \partial_{v_k}\right) m_{ij}^{\mathbf{n}} = \sum_{\mu=0}^i \frac{1}{\mu!} [(f_1 \partial_p)^\mu \mathcal{G}_M(p)] m_{i-\mu,j}^{\mathbf{n}} + \sum_{l=0}^j \frac{1}{l!} [(f_2 \partial_q)^l \mathcal{H}_M(q)] m_{i,j-l}^{\mathbf{n}}. \quad (140)$$

Then we can use the method introduced in [59] to find $f_1(p)$ and $f_2(q)$ such that

$$(f_1 \partial_p)^{M+1} \mathcal{G}_M(p) = \mathcal{G}_M(p), \quad (f_2 \partial_q)^{M+1} \mathcal{H}_M(q) = \mathcal{H}_M(q). \quad (141)$$

Choosing $q_0 = p_0^*$ and using (141) and the assumption that p_0 is a root of $\mathcal{G}'_M(p) = 0$ of multiplicity M , the equation (140) reduces to

$$\begin{aligned} & \left(2\partial_x + \sum_{k=1}^M \sigma_k \rho_k^2 \partial_{v_k}\right) m_{ij}^{\mathbf{n}} \Big|_{p=p_0, q=q_0} \\ &= \mathcal{G}_M(p_0) \sum_{\substack{\mu=0 \\ \mu \equiv 0 \pmod{M+1}}}^i \frac{1}{\mu!} m_{i-\mu,j}^{\mathbf{n}} + \mathcal{H}_M(q_0) \sum_{\substack{l=0 \\ l \equiv 0 \pmod{M+1}}}^j \frac{1}{l!} m_{i,j-l}^{\mathbf{n}} \Big|_{p=p_0, q=q_0}. \end{aligned} \quad (142)$$

Let $N = N_1 + N_2 + \dots + N_M$, where $N_j, j = 1, 2, \dots, M$, are positive integers, and define the determinant $\tau_{\mathbf{n}}$ by

$$\tau_{\mathbf{n}} = \det \begin{pmatrix} \tau_{\mathbf{n}}^{[1,1]} & \tau_{\mathbf{n}}^{[1,2]} & \dots & \tau_{\mathbf{n}}^{[1,M]} \\ \tau_{\mathbf{n}}^{[2,1]} & \tau_{\mathbf{n}}^{[2,2]} & \dots & \tau_{\mathbf{n}}^{[2,M]} \\ \vdots & \vdots & \ddots & \vdots \\ \tau_{\mathbf{n}}^{[M,1]} & \tau_{\mathbf{n}}^{[M,2]} & \dots & \tau_{\mathbf{n}}^{[M,M]} \end{pmatrix}, \quad (143)$$

where

$$\tau_{\mathbf{n}}^{[I,J]} = \text{mat}_{1 \leq i \leq N_I, 1 \leq j \leq N_J} \left(m_{(M+1)i-I, (M+1)j-J}^{\mathbf{n}} \Big|_{p=p_0, q=q_0, \xi_0=\xi_{0,I}, \eta_0=\eta_{0,J}} \right), \quad 1 \leq I, J \leq M, \quad (144)$$

and $m_{i,j}^{\mathbf{n}}$ is given by (136).

With (142), we can use similar argument as in [45] to show that the determinant $\tau_{\mathbf{n}}$ satisfies the

dimensional reduction condition

$$\left(2\partial_x + \sum_{k=1}^M \sigma_k \rho_k^2 \partial_{v_k}\right) \tau_{\mathbf{n}} = N [\mathcal{G}_M(p_0) + \mathcal{H}_M(q_0)] \tau_{\mathbf{n}}. \quad (145)$$

Therefore, we can use (145) to eliminate the variables $v_j, j = 1, 2, \dots, M$, from the higher dimensional bilinear system (137). As a result of this, we have

$$\begin{aligned} \left(D_x^2 + \sum_{j=1}^M \sigma_j \rho_j^2\right) \tau_{\mathbf{n}} \cdot \tau_{\mathbf{n}} &= \sum_{j=1}^M \sigma_j \rho_j^2 \tau_{\mathbf{n}_{j,1}} \tau_{\mathbf{n}_{j,-1}} \\ (iD_t + D_x^2 + 2ik_j D_x) \tau_{\mathbf{n}_{j,1}} \cdot \tau_{\mathbf{n}} &= 0, \quad j = 1, 2, \dots, M, \end{aligned} \quad (146)$$

where $t = -iy$.

ii) *Complex conjugate reduction*

Impose the parameter constraint

$$\xi_{0,I} = \eta_{0,I}^*,$$

and in view of $p_0 = q_0^*$, we have $[f_1(p_0)]^* = f_2(q_0)$. It then follows that

$$\tau_{\mathbf{n}} = \tau_{-\mathbf{n}}^*. \quad (147)$$

Define

$$f = \tau_{\mathbf{n}_0}, \quad g_j = \tau_{\mathbf{n}_j}, \quad j = 1, 2, \dots, M, \quad (148)$$

then the complex conjugacy condition (147) implies that f is real. Therefore, from (146) and (147), we conclude that the functions f and g_j satisfy the bilinear system (134), thereby yielding rational solutions to the vector NLS equation (1) via the transformation (135).

iii) *Introduction of free parameters*

We apply the method proposed in [59] to introduce free parameters in the following form

$$\xi_{0,I} = \sum_{n=1}^{\infty} a_{n,I} \ln^n \mathcal{U}(p), \quad (149)$$

where $\mathcal{U}(p)$ is defined by the relation

$$f_1(p) = \frac{\mathcal{U}(p)}{\mathcal{U}'(p)},$$

and the $a_{n,I}$'s are free complex constants.

iv) *Simplification of solutions*

With the aid of the generator \mathcal{D} of the differential operators $(p\partial_p)^k (q\partial_q)^l$ given as

$$\mathcal{D} = \sum_{k=0}^{\infty} \sum_{l=0}^{\infty} \frac{\kappa^k}{k!} \frac{\lambda^l}{l!} (p\partial_p)^k (q\partial_q)^l = \exp(\kappa p\partial_p + \lambda q\partial_q) = \exp(\kappa \partial_{\ln p} + \lambda \partial_{\ln q}), \quad (150)$$

we are able to simplify the solutions expressed by (148) using differential operators into the form of Schur polynomials as presented in Theorem 2.2. Since the computations are very similar to those in the three-wave system by Yang and Yang [59], we omit the details.

Thus the proof of Theorem 2.2 is completed.

Appendix C

In the first part of this appendix, we provide the values of N_1, N_2, N_3, N_4 that appear in Theorem 2.4 in the following lemma.

Lemma 6.1. The values of N_1, N_2, N_3, N_4 involved in Theorem 2.4 are characterized as follows.

$m \equiv 1, 2, 3, 4 \pmod{5}$, as other cases can be proved in a similar manner.

Firstly, we define a new class of special Schur polynomials $S_j^{[m]}(z; a)$ and the polynomials $\widehat{W}_N^{[m,5,4]}(z; a)$ as

$$\sum_{j=0}^{\infty} S_j^{[m]}(z; a) \epsilon^j = \exp[z\epsilon + a\epsilon^m], \quad (151)$$

$$\widehat{W}_N^{[m,5,4]}(z; a) = c_N^{[m,5,4]} \begin{vmatrix} S_4^{[m]}(z; a) & S_3^{[m]}(z; a) & \cdots & S_{5-N}^{[m]}(z; a) \\ S_9^{[m]}(z; a) & S_8^{[m]}(z; a) & \cdots & S_{10-N}^{[m]}(z; a) \\ \vdots & \vdots & \vdots & \vdots \\ S_{5N-1}^{[m]}(z; a) & S_{5N-2}^{[m]}(z; a) & \cdots & S_{4N}^{[m]}(z; a) \end{vmatrix}, \quad (152)$$

where a is a parameter, $c_N^{[m,5,4]}$ is a constant defined in (34), and $S_j^{[m]}(z; a) \equiv 0$ when $j < 0$. Compared with the generalized Wronskian-Hermite polynomials $W_N^{[m,k,l]}$, the polynomials $\widehat{W}_N^{[m,5,4]}(z; a)$ have a new parameter a . Note that the polynomials $S_j^{[m]}(z; a)$ are related to $p_j^{[m]}(z)$ by

$$S_j^{[m]}(z; a) = a^{j/m} p_j^{[m]}(\hat{z}), \quad \hat{z} = a^{-1/m} z. \quad (153)$$

In addition, we have

$$\widehat{W}_N^{[m,5,4]}(z; a) = a^{2N(N+1)/m} W_N^{[m,5,4]}(\hat{z}). \quad (154)$$

From (153) and (154), we find that each term in the polynomial $\widehat{W}_N^{[m]}(z; a)$ is a constant multiple of $a^s z^k$ and $k + ms = 2N(N+1)$. This indicates that when the power of a is larger, the power of z is lower. Thus, to find the lowest order of z , it suffices to find the highest order of a . To this end, we rewrite the polynomials $S_j^{[m]}(z; a)$ as

$$S_j^{[m]}(z; a) = \sum_{n=0}^{[j/m]} \frac{a^n}{n!(j-nm)!} z^{j-nm} \quad (155)$$

and substitute (155) into the determinant (152). Note that coefficients of each $a^s z^k$ in each row are proportional to each other, thus we can ignore them. In particular, for $m = 5r + 1$, where r is positive integer, we get

$$\widehat{W}_N^{[m,5,4]}(z; a) \sim c_N \begin{vmatrix} z^4 & z^3 & \cdots \\ \vdots & \vdots & \ddots \\ z^{5r-1} & z^{5r-2} & \cdots \\ az^3 + \cdots & az^2 + \cdots & \cdots \\ \vdots & \vdots & \ddots \\ az^{5r-2} + z^{5r-2+m} & az^{5r-3} + z^{5r-3+m} & \cdots \\ a^2 z^2 + a z^{2+m} + \cdots & a^2 z^1 + a z^{1+m} + \cdots & \cdots \\ \vdots & \vdots & \ddots \\ a^2 z^{5r-3} + a z^{5r-3+m} + \cdots & a^2 z^{5r-4} + a z^{5r-4+m} + \cdots & \cdots \\ a^3 z^1 + a^2 z^{1+m} + \cdots & a^3 z^0 + a^2 z^m + \cdots & \cdots \\ \vdots & \vdots & \ddots \\ a^3 z^{5r-4} + a^2 z^{5r-4+m} + \cdots & a^3 z^{5r-5} + a^2 z^{5r-5+m} + \cdots & \cdots \\ a^4 z^0 + a^3 z^m + \cdots & a^3 z^{5r} + \cdots & \cdots \\ \vdots & \vdots & \ddots \\ a^4 z^{5r} + a^3 z^{5r+m} + \cdots & a^4 z^{5r-1} + a^3 z^{5r-1+m} + \cdots & \cdots \\ \vdots & \vdots & \ddots \end{vmatrix}. \quad (156)$$

Next, we perform row operations to (156), which consist of several steps.

1. Note that the coefficients of the highest order terms in a in the first column of (156) are periodic

and one period is given by

$$z^4 \dots z^{5r-1}; \quad z^3 \dots z^{5r-2}; \quad z^2 \dots z^{5r-3}; \quad z^1 \dots z^{5r-4}; \quad z^0 \dots z^{5r}. \quad (157)$$

According to this periodicity, we divide the determinants (156) into $[N/m]$ block matrices of size $m \times N$ and one $N_0 \times N$ block matrix, where $N_0 \equiv N \pmod{m}$. In addition, we divide the first column in each block into five parts, which have distinct initial powers in z , and the difference of the powers in z of consecutive terms in each part is 5. We denote the number of parts starting with power j by $N_{5-j}, j = 1, \dots, 4$.

2. We are only concerned with the first column of (156), since other columns have similar structures. According to the above discussions, we may use each part of the first block to cancel the highest order terms in a of the corresponding parts for the subsequent blocks. After the first round row operations, the coefficients of the highest order terms in a in the first column of the second block become

$$z^{4+m} \dots z^{5r-1+m}; z^{3+m} \dots z^{5r-2+m}; z^{2+m} \dots z^{5r-3+m}; z^{1+m} \dots z^{5r-4+m}; z^m \dots z^{5r+m}, \quad (158)$$

and from the third to the last blocks, the corresponding coefficients change to z^{i+m} from z^i . In the second round, we can use the second block to cancel the highest order terms in a of the blocks below. Then we continue this process until the last block. At the end of these operations, we can exchange the rows in each block such that the highest order terms in a of the first column are

$$z^0, z^1, z^2, \dots, z^{5r}; z^m, z^{m+1}, z^{m+2}, \dots, z^{m+5r}; \dots; z^{km}, z^{km+1}, z^{km+2}, \dots, z^{km+5r}; \dots.$$

and the determinant (156) becomes

$$\widehat{W}_{N \times N}^{[m,5,4]} \sim \begin{pmatrix} \mathbf{L}_{(N-N_0) \times (N-N_0)} & \mathbf{0}_{(N-N_0) \times N_0} \\ \mathbf{M}_{N_0 \times (N-N_0)} & \widehat{W}_{N_0 \times N_0} \end{pmatrix}$$

where $\mathbf{L}_{(N-N_0) \times (N-N_0)}$ is a lower triangular matrix whose diagonal entries are all 1.

3. Therefore, to calculate the lowest power of z of $\widehat{W}_N^{[m,5,4]}(z; a)$, it suffices to compute the power of the reduced $N_0 \times N_0$ determinant $\widehat{W}_{N_0 \times N_0}$ and the final result is Γ as given in (40).

Next, we derive the factorization of $W_N^{[m,5,4]}(z)$ provided in Theorem 2.4. Since the multiplicity of the zero root of $W_N^{[m,5,4]}(z)$ is Γ , we can write

$$W_N^{[m,5,4]}(z) = z^\Gamma q_N^{[m]}(z). \quad (159)$$

Note that

$$p_j^{[m]}(\omega z) = \omega^j p_j^{[m]}(z), \quad (160)$$

where ω is any of the m -th root of 1, i.e., $\omega^m = 1$. From (159) and (160), we immediately have

$$W_N^{[m,5,4]}(\omega z) = \omega^{2N(N+1)} W_N^{[m,5,4]}(z)$$

and

$$q_N^{[m]}(\omega z) = \omega^{2N(N+1)-\Gamma} q_N^{[m]}(z).$$

Since $2N(N+1) - \Gamma$ is a multiple of m , we have $\omega^{2N(N+1)-\Gamma} = 1$, and hence

$$q_N^{[m]}(\omega z) = q_N^{[m]}(z).$$

This completes the proof.

Remark 8. We note that the row operations performed above are similar to those in the proof of rogue patterns in the inner region. For some special cases, such as $m = 4r + 2$ in the three-components NLS equation, the proof needs some modifications similar to the proof of Theorem 2.3.

References

- [1] M. J. ABLOWITZ, M. ABLOWITZ, AND P. A. CLARKSON, *Solitons, nonlinear evolution equations and inverse scattering*, vol. 149, Cambridge University Press, 1991.
- [2] N. AKHMEDIEV, A. ANKIEWICZ, AND J. M. SOTO-CRESPO, *Rogue waves and rational solutions of the nonlinear Schrödinger equation*, Phys. Rev. E, 80 (2009), p. 026601.
- [3] N. N. AKHMEDIEV AND A. ANKIEWICZ, *Nonlinear pulses and beams*, Springer, 1997.
- [4] H. BAILUNG, S. SHARMA, AND Y. NAKAMURA, *Observation of Peregrine solitons in a multicomponent plasma with negative ions*, Phys. Rev. Lett., 107 (2011), p. 255005.
- [5] F. BALOGH, M. BERTOLA, AND T. BOTHNER, *Hankel determinant approach to generalized Vorob'ev–Yablonski polynomials and their roots*, Constr. Approx., 44 (2016), pp. 417–453.
- [6] F. BARONIO, M. CONFORTI, A. DEGASPERIS, S. LOMBARDO, M. ONORATO, AND S. WABNITZ, *Vector rogue waves and baseband modulation instability in the defocusing regime*, Phys. Rev. Lett., 113 (2014), p. 034101.
- [7] F. BARONIO, A. DEGASPERIS, M. CONFORTI, AND S. WABNITZ, *Solutions of the vector nonlinear Schrödinger equations: evidence for deterministic rogue waves*, Phys. Rev. Lett., 109 (2012), p. 044102.
- [8] C. BESSE, B. BIDÉGARAY, AND S. DESCOMBES, *Order estimates in time of splitting methods for the nonlinear schrödinger equation*, SIAM Journal on Numerical Analysis, 40 (2002), pp. 26–40.
- [9] D. BILMAN AND R. BUCKINGHAM, *Large-order asymptotics for multiple-pole solitons of the focusing nonlinear Schrödinger equation*, J. Nonlinear Sci., 29 (2019), pp. 2185–2229.
- [10] D. BILMAN, L. LING, AND P. D. MILLER, *Extreme superposition: rogue waves of infinite order and the Painlevé-III hierarchy*, Duke Math. J., 169 (2020), pp. 671–760.
- [11] D. BILMAN AND P. D. MILLER, *A robust inverse scattering transform for the focusing nonlinear Schrödinger equation*, Comm. Pure Appl. Math., 72 (2019), pp. 1722–1805.
- [12] ———, *Broader universality of rogue waves of infinite order*, Physica D, 435 (2022), p. 133289.
- [13] Y. V. BLUDOV, V. KONOTOP, AND N. AKHMEDIEV, *Matter rogue waves*, Phys. Rev. A, 80 (2009), p. 033610.
- [14] R. J. BUCKINGHAM AND P. D. MILLER, *Large-degree asymptotics of rational Painlevé-II functions: noncritical behaviour*, Nonlinearity, 27 (2014), p. 2489.
- [15] J. CHEN, Y. CHEN, B.-F. FENG, AND K.-I. MARUNO, *Rational solutions to two-and one-dimensional multicomponent Yajima–Oikawa systems*, Phys. Lett. A, 379 (2015), pp. 1510–1519.
- [16] J. CHEN, Y. CHEN, B.-F. FENG, K.-I. MARUNO, AND Y. OHTA, *General high-order rogue waves of the $(1+1)$ -dimensional Yajima–Oikawa system*, J. Phys. Soc. Japan, 87 (2018), p. 094007.
- [17] J. CHEN AND D. E. PELINOVSKY, *Rogue periodic waves of the focusing nonlinear Schrödinger equation*, Proc. R. Soc. A: Math. Phys. Eng. Sci., 474 (2018), p. 20170814.
- [18] J. CHEN, D. E. PELINOVSKY, AND R. E. WHITE, *Rogue waves on the double-periodic background in the focusing nonlinear Schrödinger equation*, Phys. Rev. E, 100 (2019), p. 052219.
- [19] S. CHEN AND D. MIHALACHE, *Vector rogue waves in the Manakov system: diversity and compossibility*, J. Phys. A Math. Theor., 48 (2015), p. 215202.
- [20] P. A. CLARKSON, *The fourth Painlevé equation and associated special polynomials*, J. Math. Phys., 44 (2003), pp. 5350–5374.
- [21] P. A. CLARKSON AND E. L. MANSFIELD, *The second Painlevé equation, its hierarchy and associated special polynomials*, Nonlinearity, 16 (2003), p. R1.

- [22] P. DUBARD, P. GAILLARD, C. KLEIN, AND V. MATVEEV, *On multi-rogue wave solutions of the NLS equation and positon solutions of the KdV equation*, Eur. Phys. J.: Spec. Top., 185 (2010), pp. 247–258.
- [23] J. M. DUDLEY, G. GENTY, A. MUSSOT, A. CHABCHOUB, AND F. DIAS, *Rogue waves and analogies in optics and oceanography*, Nat. Rev. Phys, 1 (2019), pp. 675–689.
- [24] K. DYSTHE, H. E. KROGSTAD, AND P. MÜLLER, *Oceanic rogue waves*, Annu. Rev. Fluid Mech., 40 (2008), pp. 287–310.
- [25] L. H. ELIASSON AND S. B. KUKSIN, *Kam for the nonlinear schrödinger equation*, Annals of mathematics, (2010), pp. 371–435.
- [26] B.-F. FENG, L. LING, AND D. A. TAKAHASHI, *Multi-breather and high-order rogue waves for the nonlinear Schrödinger equation on the elliptic function background*, Stud. Appl. Math., 144 (2020), pp. 46–101.
- [27] B.-F. FENG, C. SHI, G. ZHANG, AND C. WU, *Higher-order rogue wave solutions of the Sasa–Satsuma equation*, J. Phys. A Math. Theor., 55 (2022), p. 235701.
- [28] S. FUKUTANI, K. OKAMOTO, AND H. UMEMURA, *Special polynomials and the Hirota bilinear relations of the second and the fourth Painlevé equations*, Nagoya Math. J., 159 (2000), pp. 179–200.
- [29] A. GANSHIN, V. EFIMOV, G. KOLMAKOV, L. MEZHOV-DEGLIN, AND P. V. MCCLINTOCK, *Observation of an inverse energy cascade in developed acoustic turbulence in superfluid helium*, Phys. Rev. Lett., 101 (2008), p. 065303.
- [30] B. GUO, L. LING, AND Q. LIU, *Nonlinear Schrödinger equation: generalized Darboux transformation and rogue wave solutions*, Phys. Rev. E, 85 (2012), p. 026607.
- [31] S. HAVER, *A possible freak wave event measured at the Draupner jacket January 1 1995*, in Rogue waves, vol. 2004, 2004, pp. 1–8.
- [32] J. HE, H. ZHANG, L. WANG, K. PORSEZIAN, AND A. FOKAS, *Generating mechanism for higher-order rogue waves*, Phys. Rev. E, 87 (2013), p. 052914.
- [33] R. HIROTA, *The direct method in soliton theory*, no. 155, Cambridge University Press, 2004.
- [34] Y. KAMETAKA, *On poles of the rational solution of the Toda equation of Painlevé-II type*, Proc. Jpn. Acad. A: Math., 59 (1983), pp. 358–360.
- [35] J. KANG, G. STEGEMAN, J. AITCHISON, AND N. AKHMEDIEV, *Observation of Manakov spatial solitons in AlGaAs planar waveguides*, Phys. Rev. Lett., 76 (1996), p. 3699.
- [36] T. KANNA AND M. LAKSHMANAN, *Exact soliton solutions, shape changing collisions, and partially coherent solitons in coupled nonlinear Schrödinger equations*, Phys. Rev. Lett., 86 (2001), p. 5043.
- [37] T. KATO, *On nonlinear schrödinger equations*, in Annales de l’IHP Physique théorique, vol. 46, 1987, pp. 113–129.
- [38] D. J. KEDZIORA, A. ANKIEWICZ, AND N. AKHMEDIEV, *Circular rogue wave clusters*, Phys. Rev. E, 84 (2011), p. 056611.
- [39] D. J. KEDZIORA, A. ANKIEWICZ, AND N. AKHMEDIEV, *Classifying the hierarchy of nonlinear-Schrödinger-equation rogue-wave solutions*, Phys. Rev. E, 88 (2013), p. 013207.
- [40] Y. KODAMA AND A. MIKHAILOV, *Symmetry and perturbation of the vector nonlinear Schrödinger equation*, Physica D, 152 (2001), pp. 171–177.
- [41] L. LING, B. GUO, AND L.-C. ZHAO, *High-order rogue waves in vector nonlinear Schrödinger equations*, Phys. Rev. E, 89 (2014), p. 041201.
- [42] S. V. MANAKOV, *On the theory of two-dimensional stationary self-focusing of electromagnetic waves*, Sov. phys. JETP, 38 (1974), pp. 248–253.
- [43] G. MU, Z. QIN, AND R. GRIMSHAW, *Dynamics of rogue waves on a multisoliton background in a vector nonlinear Schrödinger equation*, SIAM J. Appl. Math., 75 (2015), pp. 1–20.

- [44] A. A. OBLOMKOV, *Monodromy-free Schrödinger operators with quadratically increasing potentials*, Theor. Math. Phys., 121 (1999), pp. 1574–1584.
- [45] Y. OHTA AND J. YANG, *General high-order rogue waves and their dynamics in the nonlinear Schrödinger equation*, Proc. R. Soc. A: Math. Phys. Eng. Sci., 468 (2012), pp. 1716–1740.
- [46] K. OKAMOTO, *Studies on the Painlevé equations. III: Second and fourth Painlevé equations, P_{II} and P_{IV}* , Math. Ann., 275 (1986), pp. 221–255.
- [47] D. E. PELINOVSKY AND J. YANG, *Parametric resonance and radiative decay of dispersion-managed solitons*, SIAM J. Appl. Math., 64 (2004), pp. 1360–1382.
- [48] D. H. PEREGRINE, *Water waves, nonlinear Schrödinger equations and their solutions*, ANZIAM J., 25 (1983), pp. 16–43.
- [49] J. RAO, K. PORSEZIAN, T. KANNA, Y. CHENG, AND J. HE, *Vector rogue waves in integrable M -coupled nonlinear Schrödinger equations*, Phys. Scr., 94 (2019), p. 075205.
- [50] M. SHATS, H. PUNZMANN, AND H. XIA, *Capillary rogue waves*, Phys. Rev. Lett., 104 (2010), p. 104503.
- [51] D. R. SOLLI, C. ROPERS, P. KOONATH, AND B. JALALI, *Optical rogue waves*, Nature, 450 (2007), pp. 1054–1057.
- [52] M. TANEDA, *Remarks on the Yablonskii–Vorob’ev polynomials*, Nagoya Math. J., 159 (2000), pp. 87–111.
- [53] A. VOROB’EV, *On the rational solutions of the second Painlevé equation*, Diff. Eqns., 1 (1965), pp. 79–81.
- [54] M. I. WEINSTEIN, *Nonlinear schrödinger equations and sharp interpolation estimates*, Communications in Mathematical Physics, 87 (1982), pp. 567–576.
- [55] C. WU, G. ZHANG, C. SHI, AND B.-F. FENG, *General rogue wave solutions to the Sasa–Satsuma equation*, arXiv preprint arXiv:2206.02210, (2022).
- [56] A. YABLONSKII, *On rational solutions of the second Painlevé equation*, Vesti AN BSSR, ser. fiz-tekhn, Nauk, 3 (1959), pp. 30–35.
- [57] B. YANG, J. CHEN, AND J. YANG, *Rogue waves in the generalized derivative nonlinear Schrödinger equations*, J. Nonlinear Sci., 30 (2020), pp. 3027–3056.
- [58] B. YANG AND J. YANG, *Universal rogue wave patterns associated with the Yablonskii–Vorob’ev polynomial hierarchy*, Physica D, 425 (2021), p. 132958.
- [59] B. YANG AND J. YANG, *General rogue waves in the three-wave resonant interaction systems*, IMA J. Appl. Math., 86 (2021), pp. 378–425.
- [60] B. YANG AND J. YANG, *Rogue wave patterns in the nonlinear Schrödinger equation*, Physica D, 419 (2021), p. 132850.
- [61] B. YANG AND J. YANG, *Pattern transformation in higher-order lumps of the Kadomtsev–Petviashvili I equation*, J. Nonlinear Sci., 32 (2022), pp. 1–45.
- [62] B. YANG AND J. YANG, *Rogue wave patterns associated with Okamoto polynomial hierarchies*, arXiv preprint arXiv:2208.03214, (2022).
- [63] J. YANG, *Nonlinear waves in integrable and nonintegrable systems*, SIAM, Philadelphia, 2010.
- [64] ———, *A normal form for Hamiltonian–Hopf bifurcations in nonlinear Schrödinger Equations with general external potentials*, SIAM J. Appl. Math., 76 (2016), pp. 598–617.
- [65] G. ZHANG, L. LING, AND Z. YAN, *Multi-component nonlinear Schrödinger equations with nonzero boundary conditions: higher-order vector peregrine solitons and asymptotic estimates*, J. Nonlinear Sci., 31 (2021), pp. 1–52.